

**A Design Study for a Multivariable Feedback Control
System for Controlling the Air Gap of Maglev Train
Suspension System**

دراسة في تصميم نظم السيطرة متعددة المتغيرات للتحكم في الفجوة الهوائية
لنظام التعليق في القطارات المغناطيسية

by

IBRAHIM AHMED AI-NASSIR

**A dissertation submitted in fulfilment
of the requirements for the degree of
SYSTEMS ENGINEERING**

at

The British University in Dubai

Supervisor's Name

Professor Robert Whalley

February 2017

DECLARATION

I warrant that the content of this research is the direct result of my own work and that any use made in it of published or unpublished copyright material falls within the limits permitted by international copyright conventions.

I understand that a copy of my research will be deposited in the University Library for permanent retention.

I hereby agree that the material mentioned above for which I am author and copyright holder may be copied and distributed by The British University in Dubai for the purposes of research, private study or education and that The British University in Dubai may recover from purchasers the costs incurred in such copying and distribution, where appropriate.

I understand that The British University in Dubai may make a digital copy available in the institutional repository.

I understand that I may apply to the University to retain the right to withhold or to restrict access to my thesis for a period which shall not normally exceed four calendar years from the congregation at which the degree is conferred, the length of the period to be specified in the application, together with the precise reasons for making that application.

Signature of the student

COPYRIGHT AND INFORMATION TO USERS

The author whose copyright is declared on the title page of the work has granted to the British University in Dubai the right to lend his/her research work to users of its library and to make partial or single copies for educational and research use.

The author has also granted permission to the University to keep or make a digital copy for similar use and for the purpose of preservation of the work digitally.

Multiple copying of this work for scholarly purposes may be granted by either the author, the Registrar or the Dean of Education only.

Copying for financial gain shall only be allowed with the author's express permission.

Any use of this work in whole or in part shall respect the moral rights of the author to be acknowledged and to reflect in good faith and without detriment the meaning of the content, and the original authorship.

Abstract

This research presents a study of the control of multivariable systems which are subjected to variable input and external load change. The topic of research is to design a controller to control the air gap of the suspension system of a Maglev Train. The design is conducted by implementing a recent research methodology called **Least Effort Technique**. This methodology was introduced by R. Whalley and M. Ebrahimi in 2006. The significant advantages of the Least effort technique is to reduce the energy consumption in the controller, reducing actuator activity, wear, heat, heat generation, operational and maintenance cost. This research emphasizes this technique enabling comparable transient and disturbance rejection characteristics against results obtained by classical control theories, such as Inverse Nyquist Array and H_{∞} control theory.

The research is focusing on the control problems of the vertical clearance in the suspension system. Initially, the mathematical model of the system is compensated the effect of double integrator which appears in the characteristic equation

Simulation of the system is presented to evaluate the effectiveness of the controller to maintain the air gap within the allowable limits, MATLAB-SIMILINK software will be used for simulation purposes and design validation.

خلاصة البحث

يقدم هذا البحث دراسة في تصميم أنظمة التحكم في المنظومات متعددة المدخلات والمتغيرات التي تخضع الى احمال خارجية متغيرة ، ويتناول هذا البحث تصميم وحدة تحكم باستخدام نظرية تقنية حديثة تعمل على استراتيجية تقليل استهلاك الجهد او الطاقة (Least Effort), للتحكم في قيمة الفجوة الهوائية في نظام التعليق للقطارات المغناطيسية والمحافظة عليها ضمن ضمن الحد المسموح به. وتعتبر هذه النظرية من النظريات الحديثة جدا والتي تم تطويرها من قبل البروفيسور روبيرت والى و إبراهيمي في سنة 2006، وتركز على تقليل الطاقة المستهلكة في نظام التحكم نفسه مما له من تأثير مباشر على توفير الطاقة والجهد وكذلك التقليل من الانهك والبلى الذي يتعرض له القطار المغناطيسي بصورة عامة, وبالنتيجة يؤدي الى تقليل استهلاك الطاقة وتكاليف الصيانة.

و يقوم هذا البحث على تأكيد هذه التقنية وذلك من خلال مقارنة النتائج الخاصة بأداء وسرعة استجابة نظام التحكم مع النتائج المستحصلة من النظريات التقليدية مثل **Inverse Nyquist Array and H-Infinity Control Theory**،

وتناول البحث أيضا النموذج الرياضي او المعادلة الرياضية الاساسية لنموذج القطار المغناطيسي وبعض الاضافات التي تمكن من تطبيق النظرية الحديثة والتي يتم على اساسها اجراء التحليل الرياضي والمحاكاة المطلوبة , وهذه الاضافات لا تؤثر على المعادلات الاساسية للقطار المغناطيسي.

تم اجراء المحاكاة لنموذج النظام النهائي باستخدام برنامج الماتلاب ودراسة النتائج من اجل تقييم فعالية نظام التحكم الذي تم تصميمه, وبمقارنة النتائج التي تم الحصول عليها عن طريق النظرية الحديثة مع النتائج المستحصلة من النظريات الاخرى بان هذه التقنية هي الاقل استهلاكا للطاقة وتبين استجابة اسرع وكفاءة عالية للتحكم في تعديل الاضطرابات التي يتعرض القطار المغناطيسي من اجل المحافظة على الفجوة الهوائية ضمن الحدود المسموحة. وكذلك يتميز نظام التحكم بانه اقل تعقيدا من النظم الاخرى ويستهلك اقل طاقة مما يؤوله للاستخدام في صناعة القطارات وتطبيقات الانظمة متعددة المتغيرات.

Acknowledgements

I am pleased to extend my sincere thanks and gratitude to my supervisor Professor Robert Whalley who gave me all the support for the completion of this research, His office was always open whenever I expected trouble or had questions about my research. It has also been a great opportunity to learn new theory and obtaining information about it from the theorist himself and the benefits from this. I would also like to extend my thanks and gratitude to Dr. Alaa Abdul Ameer for support and valuable guidance in completing this work.

Dedication

To my Parents, who put their trust on me, and who's Avni their old for our
Upbringing and our Education

To my Wife, who gave me the great support, patience, sacrifice warmest in
order to complete my studies.

To my lovely Children

I Dedicate my work

List of Notation and Abbreviations

$a_{i,j}$	Element of $A(s)$, $1 \leq i, j \leq m$
$a_{i,j}, b_{i,j}, \dots, \gamma_{ij}$	Coefficients of $a_{i,j}(s)$
$A(s)$	Numerator of $G(s)$
A	State Space Matrix
$b(s)$	Polynomial
b_0	Leading coefficient of $b(s)$
b_0, b_1, \dots, b_{m-1}	Coefficient of $b(s)$
B	State Space Matrix
C	State Space Matrix
$C(s)$	Compensator transfer function
d	Demanded value
$d(s)$	Denominator of $G(s)$
D	State space Matrix
$e(s)$	Error signal comparing the reference input and the output
EMS	Electro-Magnetic Suspension
EDS	Electro-Dynamic Suspension
f, f_1, f_2, \dots, f_m	Output loop feedback gains
$g_{i,j}$	Elements of $G(s)$, $1 \leq i, j \leq m$
$G(s)$	Transfer Function Array (input /output)
h	Feed-back path gain
h_1, h_2, \dots, h_m	Gains of $h_j(s)$, $1 \leq i, j \leq m$
$h(s)$	Feed-back path function

$H(s)$	Feed-back path compensator
$H(s)$	Closed loop transfer function
$\hat{H}(s)$	Inverted Closed Loop Transfer Function Matrix
$\hat{h}_{i,i}$	Diagonal terms of inverted closed loop transfer function matrix
I	Identity matrix
J	Performance index
k	Forward path gain
k_1, k_2, \dots, k_m	Gains of $k_j(s)$, $1 \leq i, j \leq m$
$k(s)$	Forward Path Function
$k \succ h$	Outer Product of k and h
$\langle k, h \rangle$	Inner product of k and h
$K(s)$	Forward path controller model (pre-compensator)
L	Observer gain matrix
$L(s)$	Left (row) Factor
L	Laplace Transformation
MS	Maglev System
n_1, n_2, \dots, n_{m-1}	Gain ratios
\hat{N}_{qi}	Number of origin encirclements by mapping D-contour for \hat{q}_{ii}
\hat{N}_{hi}	Number of origin encirclements by mapping D-contour for \hat{h}_{ii}
$P(s)$	Pre- compensator
Q	Coefficient array
Q	States weighting matrix
$Q(s)$	Open loop transfer function matrix
$\hat{Q}(s)$	Inversion of open loop transfer matrix

\hat{q}_{ii}	Diagonal terms within the inverted open loop transfer function matrix
\hat{q}_{ij}	Off Diagonal terms within the inverted open loop transfer function matrix
$r_1(s), r_2(s)$	Transformed reference inputs
$\bar{r}(s)$	Transferred inner loop reference input
$R(s)$	Right (column) factors
R	Input weighting matrix
$S(s)$	Sensitivity array
$u(s)$	Transformed input
$u(t)$	Input vectors
$x(t)$	State vector
$\bar{x}(t)$	Estimated state vector
$y(s)$	Transformed output
$y(t)$	Outputs vector
z_0	Number of right-half complex plane zeroes for open-loop system
z_c	Number of right-half complex plane zeroes for closed-loop system
$\Gamma(s)$	Finite time array
$\delta(s)$	Transformed disturbance signal
$\delta_1(s)$	The Air gap 1
$\delta_2(s)$	The air gap 2
λ	Eigen value
λ_j	Singular values $1 \ll j \ll m$
$\underline{\lambda}(S(s))$	Smallest singular value of $S(i\omega)$
$\bar{\lambda}(S(s))$	Largest singular value of $S(i\omega)$
$\phi_i(s)$	Ostrawski shrinking factors of Gershgorin circles for column i

$\Phi(t)$	State transition matrix
θ	Observability test matrix
CARDIAD	Complex acceptability region for diagonal Dominance
IFAC	International federation of automatic
INA	Inverse Nyquist Array
LEC	Least Effort Control
LQG	Linear quadratic Gaussian
LQE	Linear Quadratic Estimator
LQR	Linear Quadratic regulator
LMI	Linear Matrix Inequalities
MVCS	Multivariable control Synthesis
PID	Proportional, Integral and derivative controller

Contents

Abstract	I
خلاصة البحث	II
Acknowledgements	III
Dedication	IV
List of Notation and Abbreviations	V
Contents	IX
List of Figures	XII
Chapter 1 Introduction	1
1.1. Research Background	1
1.2. Electro-Magnetic Suspension (EMS) System Description	3
1.3. Maglev Train Development History	4
1.3.1. German Maglev System (Trans-Rapid)	5
1.3.2. Japanese Maglev System	6
1.4. Korean UTM	8
1.5. China Low and High Speed Maglev Train	8
1.6. Research problem statement.	9
1.6.1. Air Gap Control	9
1.6.2. Maglev Train Control System.....	10
1.7. Research Aims and Objectives.	11
1.8. Research Dissertation Organization.....	12
Chapter 2 Literature Review	13
2.1. Introduction	13
2.2. The Control History	14
2.3. Definition of Control Systems	15
2.4. Feedback Control Theory.....	16
2.5. Control Theory Review.....	19
2.5.1. Early Control- Before 1900	20
2.5.2. The Pre-classical period of control (1900-1935)	23
2.5.3. The Classical Control Period 1935 -1950s	23

2.5.4.	Modern Control History	25
2.5.5.	Stability Theory	26
2.6.	Schools of Multivariable Control.....	27
2.6.1.	The British School for Multivariable Control.....	28
2.6.2.	Inverse Nyquist Array (INA)	29
2.6.3.	Characteristic Locus Method	31
2.6.4.	The Recent Control Theory – Least Effort Regulation.....	32
2.7.	American School of Control	33
2.7.1.	State space representation	33
2.7.2.	Optimal Control Theory.....	35
2.7.3.	H_{∞} -Infinity Control Theory	35
2.8.	Maglev Train Modeling and Control Review	36
Chapter 3 Research Methodology		45
3.1.	Maglev Train Mathematical Model	45
3.2.	Open Loop Response and Control Objective.....	50
3.3.	Least Effort Control Methodology.....	54
3.3.1.	Inner-loop Design	57
3.3.2.	Optimization	60
3.3.3.	Disturbance rejection	61
3.3.4.	Stability of control system	61
3.4.	The Inverse Nyquist Array (INA) Method	61
3.4.1.	Diagonally Dominance	65
3.4.2.	System Stability	67
3.4.3.	Graphical Criteria for Stability	67
3.5.	H_{∞} - Robust Optimal Control Method.....	68
3.5.1.	H_{∞} -Infinity Control.....	69
3.5.2.	The Over-All Control Problem Formation,	69
3.5.3.	The General Case of Controller Design.....	71
Chapter 4 Controller Design and Simulation Results Discussions		74
4.1.	least Effort Controller	74
4.1.1.	Mathematical -Least Effort Controller Design	74
4.1.2.	Inner loop design:	75

4.1.3.	Outer Loop Design.....	79
4.1.4.	Simulation Results	81
4.1.5.	Disturbance Rejection:	90
4.1.6.	Control Energy Dissipation.....	93
4.2.	Inverse Nyquist Array Controller Design	94
4.2.1.	Dynamic Controller	98
4.3.	H^∞ -Controller Design	100
4.4.	Comparison study	104
4.4.1.	Closed Loop Responses Comparisons	105
4.4.2.	Disturbance Rejection Results	109
4.4.3.	Energy Consumption	111
Chapter 5 Conclusions and Recommendations.....		113
5.1.	Conclusions	113
5.2.	Recommendations	115
Chapter 6 References and Appendix.....		116
6.1.	References	116
Appendix-A.....		122
Open loop system		122
Least Effort system model:		123
Inverse Nyquist Array (INA) Model:		124
H-Infinity:		125
Appendix-B		127
M-files Commands		127

List of Figures

Figure 1.1 , EMS Suspension with Linear Motor (Zhigang et al., 2015).....	2
Figure 1.2 , Layout of German Maglev system TR (Zhigang et al., 2015).....	5
Figure 1.3 , Guidance Principle of German Style Maglev system (Zhigang et al., 2015). ...	5
Figure 1.4 , General Concept of German Maglev system(Hyung-Woo Lee et al., 2006).....	6
Figure 1.5 , Section of Japanese MLX High speed Maglev Train (Zhigang et al., 2015). ...	7
Figure 1.6 , Concept of Japanese HSST maglev system, (Zhigang et al., 2015).	8
Figure 1.7 , General View of Vehicle on Guideway (General Atomics, 2002)	11
Figure 2.1 , Arrangement of Suspension Control system, (Zhiqiang et al., 2007).....	13
Figure 2.2 , Process to be controlled (Dorf and Bishop, 2008).....	15
Figure 2.3 , System without feedback (Dorf and Bishop, 2008).....	16
Figure 2.4 , Closed Loop System with feedback (Dorf and Bishop, 2008)	17
Figure 2.5 , Closed Loop System With External Disturbances (Dorf and Bishop, 2008)...	17
Figure 2.6 , Double Loop Feedback System (Dorf and Bishop, 2008).....	18
Figure 2.7 , Multivariable Control System Representation (Dorf and Bishop, 2008).....	18
Figure 2.8 , Boulton & Watt governed steam engine (Bissell, 2009)	21
Figure 2.9 , Example of Recent Watt Governor Application (Allwright J., 1970)	22
Figure 2.10 , Sequence of International Maglev Train Development	37
Figure 3.1 , Lateral view of the CMS04 low speed maglev vehicle(He and Cui, 2015)....	45
Figure 3.2 , Diagram of the module suspension control system (He and Cui, 2015).....	46
Figure 3.3 , force analysis of one levitation unit in lateral (He and Cui, 2015).	47
Figure 3.4 , Block Diagram Representation of the general Open Loop System	50
Figure 3.5 , System responses following step change on $r_1(s)$, and $r_2s = 0$	51
Figure 3.6 , System responses following step change on r_2s , and $r_1s = 0$	51
Figure 3.7 , Block Diagram Representation for Open Loop System Includes the Filters...	52

Figure 3.8, Open loop response following step change at magnetically lifting force $r_1(s)$	53
Figure 3.9, Open loop response following step change at magnetically lifting force $r_2(s)$	54
Figure 3.10, Common Representation of Multivariable control system	62
Figure 3.11, General Form of Multivariable Closed Loop Transfer Function With feedback	64
Figure 3.12, Sketch to define the Dominance of a rational matrix $Q(s)$	66
Figure 3.13, Inverse Nyquist Diagram of q_{iis} (Hawkins and McMorran, 1973).....	66
Figure 3.14, General Description of the system	69
Figure 3.15, Feedback Control Structures	69
Figure 3.16, Feedback with Weighing Functions.....	72
Figure 4.1, Block Diagram Representation For Open Loop System.....	74
Figure 4.2, Root Locus Diagram	77
Figure 4.3, The performance Index J against Gain ration n	79
Figure 4.4, Closed loop response with $f=0.1$, following unit step input at $r_1(s)$	81
Figure 4.5, Closed Loop Response with $f=0.1$, Following Unit Step Input at $r_2(s)$	82
Figure 4.6, Closed Loop Response With $f=0.3$, Following Unit Step Input at $r_1(s)$	83
Figure 4.7, Closed Loop Response With $f=0.3$, Following Unit Step Input at $r_2(s)$	84
Figure 4.8, Closed Loop Response With $f=0.5$, Following Unit Step Input at $r_1(s)$	85
Figure 4.9, Closed Loop Response With $f=0.5$, Following Unit Step Input at $r_2(s)$	86
Figure 4.10, Closed Loop Response With $f=0.8$, Following Unit Step Input at r_1	87
Figure 4.11, Closed Loop Response With $f=0.8$, Following Unit Step Input at $r_2(s)$	88
Figure 4.12, Closed Loop Response Following Unit step input at $r_1(s)$, $r_2(s) = 0$	89
Figure 4.13, Closed Loop Response Following Unit step input at r_2 , $r_1 = 0$	90
Figure 4.14, Disturbance Rejection With Input at d_1 , and $r_1 = r_2 = d_2 = 0$	91
Figure 4.15, Disturbance rejection with unit step input at d_2 , and $r_1 = r_2 = d_1 = 0$	92

Figure 4.16, Energy Consumed Compared Between, Least Effort, INA and H-infinity ...	93
Figure 4.17, Nyquist diagram of g_{11} with Gershgorin bands.....	95
Figure 4.18, Nyquist diagram of g_{22} with Gershgorin bands.....	95
Figure 4.19, Overview Of Nyquist Plot With Gershgorin Circles For Element q_{11}	96
Figure 4.20, Nyquist diagram of q_{11} with Gershgorin circles	97
Figure 4.21, Nyquist Diagram of q_{22} with Gershgorin Circles.....	98
Figure 4.22, INA -Closed Loop Response Following Unit Step Input at $r_1(s)$	99
Figure 4.23, INA -Closed Loop Response Following Unit Step Input at $r_2(s)$	100
Figure 4.24, System Response Following Unit Step Change On r_1	103
Figure 4.25, System Response Following Unit Step Change On r_2	104
Figure 4.26, System response following step change at r_1 for all three controllers	106
Figure 4.27, Comparison responses following step change at r_2 for all three methods ..	107
Figure 4.28, Closed-loop Responses following unit step disturbance on d_1 comparing between Least Effort, Invers Nyquist Array and H-Infinity	109
Figure 4.29, Closed-loop responses following unit step disturbance on d_2 comparing between Least Effort, Invers Nyquist Array and H-Infinity	110
Figure 4.30, Energy Consumed Compared between, least effort, INA and H-infinity....	111

Chapter 1

Introduction

The research reviews the history of control theory, and review the development of maglev train systems and it is applications, also focusing on the control problems of the vertical clearance in the suspension system. Initially, the mathematical model of the system is compensated the effect of double integrator which appears in the characteristic equation.

Simulation of the system is presented to evaluate the effectiveness of the controller to maintain the air gap within the allowable limits, the research presents evaluation of system performance, and the energy dissipated by the proposed controller in comparisons with the classical designs. The results illustrate that the presented design results in a better dynamic performance, particularly regarding the reliability of the suspension control system. and practical engineering aspects.

1.1. Research Background

Maglev (Magnetic + Levitation) is a driving force technique depending on the use of magnetic force of the linear motor to lift and propel the train vehicles. The magnet field force rather than traditional wheels and axles and pivot bearings are used. The linear motor is a conventional motor, un rolled. However as explained in the Figure 1.1, the electro magnets or super conductors are mounted in the vehicle, it the same way as the rotter of the Motor. The stator coil is mounted along the guideway. In the maglev trains, the magnetic field works to raise a vehicle with small distance (air gap) over guide truck depending on magnetic force, which also push the vehicle at the same time. Generally maglev trains move more smoothly than traditional trains equipped with wheels, and do not depend on traction.

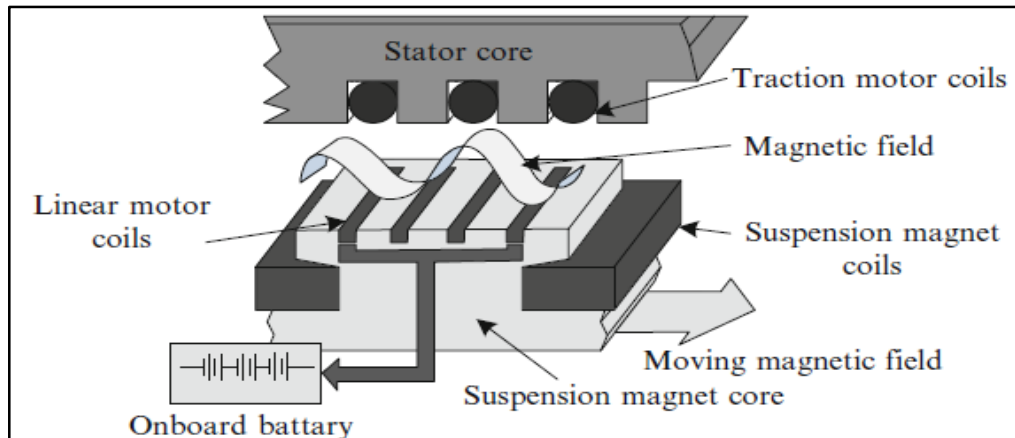


Figure 1.1, EMS Suspension with Linear Motor
(Zhigang et al., 2015)

Therefore the acceleration and deceleration is faster than trains moving on wheels. Trains running on wheels experience wear owing to friction caused by the interface between wheels and track, and the hammer effect from the wheels, leads to the weakening of the mechanical properties and higher speed.

Historically the construction and manufacturing of maglev trains is more costly than the trains running on railway tracks. However, less maintenance is required leading to reduce operational costs. The Maglev Trains can be used for passengers transportation, and goods transfer across long distances at high speeds up to hundreds of kilometers per hour. Maglev train can be considered important ways of transportation in the twenty-first century. It is probably more suitable than the other modes of transport such as automobiles, trucks and aircraft.

The operational of maglev technology have minimum overlap with wheeled railways, and it could not be compatible with the rail tracks. Also it could not be used for the same infrastructure, since the maglev train systems must be designed as an independent and integrated transport system. In addition to this, projected vacuum tube train systems would

allow trains to run at very high speeds. While this kind of system is not yet established commercially, research and efforts to study and develop these high-speed trains is underway.

In practical Electromagnetic Levitation Systems(Maglev Technology) could be divided in to two significant kinds based on suspension and operational concepts. The first type is called (Electro-Magnetic Suspension EMS). This concept describes the system functions as generates attractive electromagnetic force between the electromagnets at the car body and the ferromagnetic rail on the guideway. (Zhigang et al., 2015).

An example of this type is (Japanese HSST) and German Trans-Rapid Systems, China, Korea and Sweden. This kind of levitation system is controlled by an Electronic Controller to maintain the air gap at the designed limit about 8-10 mm.

The second kind (named for the Electro-Dynamic Suspension (EDS)), was developed based on the concept of generating repulsive electromagnetic force between the superconducting magnets on the car body and the non-ferromagnetic rail at the guideway (Zhigang et al., 2015).An example of this type is the “Japanese c using EDS-type Maglev System”. This kind of levitation system depends on the magnetic field generated by the superconductors, an induced current will be generated in the nearby conductors, resulting a magnetic force pushing and pulling the train to stay in the designed levitation position on the (Zhigang et al., 2015). The EDS technique is concentrating on super-conducting since the permanent magnets cannot deliver adequate field power (General Atomics, 2002).

1.2.Electro-Magnetic Suspension (EMS) System Description

In general Electromagnetic suspension (EMS) for maglev train is a group of subsystems designed and constructed in an integrated manner to allow the vehicle to be lifted over guideway with a limited air gap, guided and moved according to the design conditions. The main parts of maglev train are the Vehicle / Car Body, the Magnets, and the Guideway

Assembly. The vehicle / Car body, is the part allocated to carry passengers and goods. It is designed to meet the standards of Safety, Quality, Environment and ride comfort. Each car body has a structure (Chassis) which is equipped with devices and components for lift, thrust, guidance, breaking and a secondary suspension system (General Atomics, 2002).

The levitated car body is equipped with three kind of braking systems, the dynamic LSM brake, which is works to reduce the speed of the train by generating opposite magnetic field in the linear motor, and the electromechanical friction service brake or called position brake works to stop the train in the desired position, and the permanent magnet emergency brake. Each brake system provide deceleration of 0.2 g. (General Atomics, 2002).

The Magnet system could be electromagnetic or permanent magnets. It is the important component for levitation vehicles, which is located in the lowest part of vehicle below the guideway. It is responsible for generating the magnetic force required to lift over the guideway, guide, and thrust the train, with no direct contact between the moving and stationed parts, so that there is no friction forces affects to ride comfort and the smoothness of operation. Also frictionless operation reduces the wear resulting in low maintenance cost in comparison with wheeled trains. The guideway assembly, is the third part of the levitation system located beneath the car body. It is consists of the levitation truck coil and second set of thrust coils opposite the first set of vehicle magnets.

1.3.Maglev Train Development History

The concept of Maglev Train operation is similar to electric motors, but the motion is linear, The linear motor is a conventional motor, un rolled. However, the super-conductor or permanent magnet are mounted in the vehicles in the same manner as the rotating part in the motor, and the coil mounted along the guideway, is equivalent to the stator (General Atomics, 2002).

1.3.1. German Maglev System (Trans-Rapid)

The maglev train system in Germany started in 1969. The technology implemented in the design is based on electromagnet suspension EMS for lifting, and using LMS for thrust action as displayed in the figure 1.2.

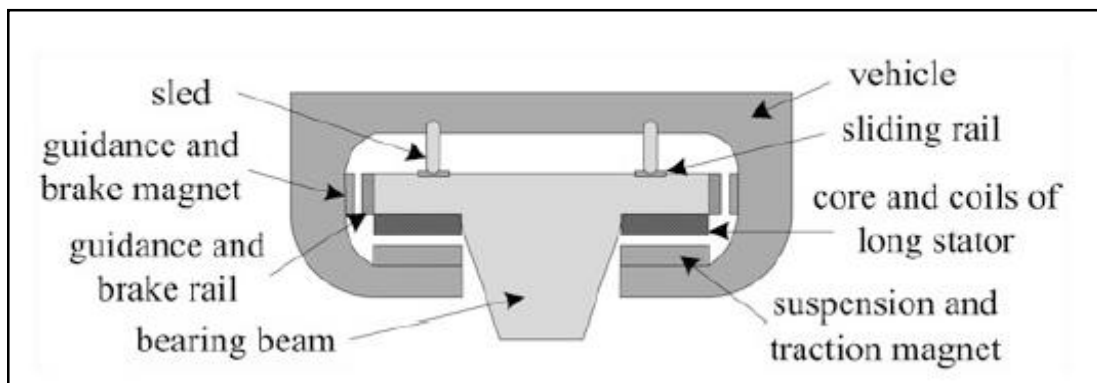


Figure 1.2, Layout of German Maglev system TR

(Zhigang et al., 2015).

The system is designed for a speed about 450 km/hr.. In 1979 TR05 system entered revenue services. This system was presented in the “International Transportation Fair” (ITF), in Hamburg, and the first high speed test was conducted in 1987 on a test track of 1.3km. Figure 1.2 and Figure 1.4, show the general layout and guidance principle of the German EMS, maglev system. There were three types of test trains, the TR06, TR07 and TR08, the highest speed was achieved with TR07 which was approx. 450km/hr. (Zhigang et al., 2015).

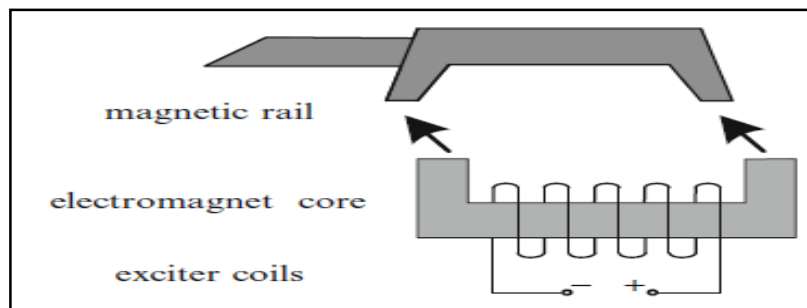


Figure 1.3, Guidance Principle of German Style Maglev system

(Zhigang et al., 2015).

Further studies arise conducted to develop a route of (300km) to link Berlin and Munich. However this was not approved by the government (Zhigang et al., 2015).

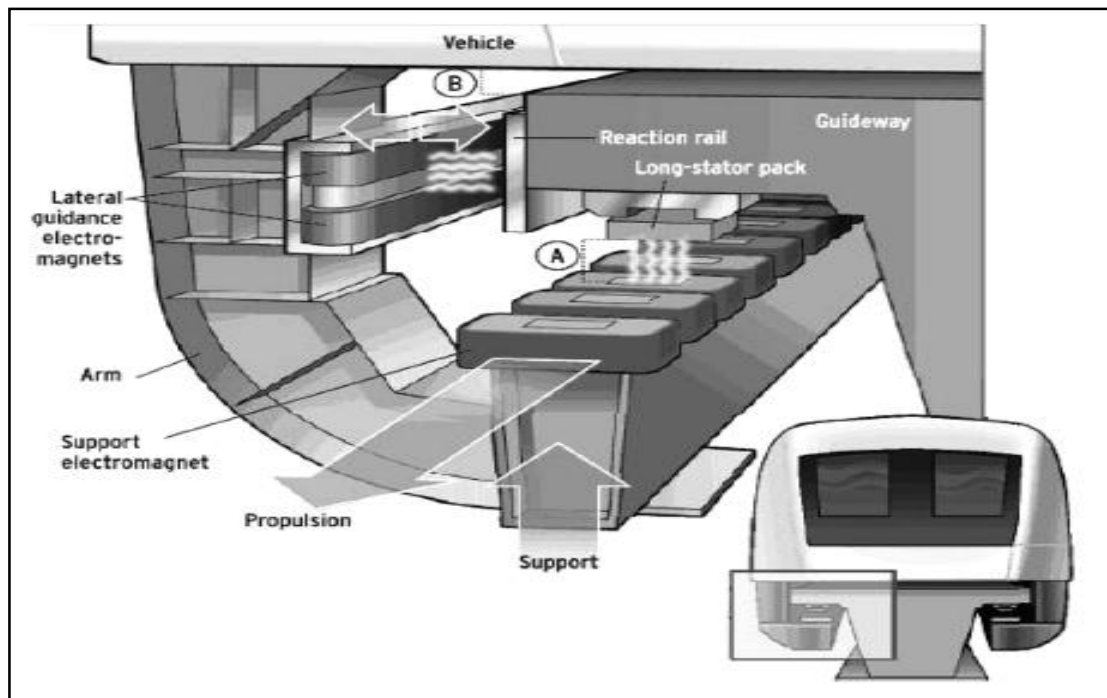


Figure 1.4, General Concept of German Maglev system

(Hyung-Woo Lee et al., 2006)

1.3.2. Japanese Maglev System

1.3.2.1. Japanese Superconducting Maglev

During the period of 1960s to 1970s the technical institute in Japan began working on improvements in the linear propulsion system, called Electro-Dynamic ED Super-Conducting system. The train works by using the superconducting magnets in the vehicle or car body as shown in Figure 1.5. A metal coil was installed along the guideway, to generate the magnetic field force to lift the train over the guideways. The idea of superconductor required that cooling to very low temperature reduce the resistance to zero, resulting in Superconducting. In 1972, the first super-conductor maglev vehicle implementing Super-Conducting Magnets, was used for both lifting and thrust (General Atomics, 2002).

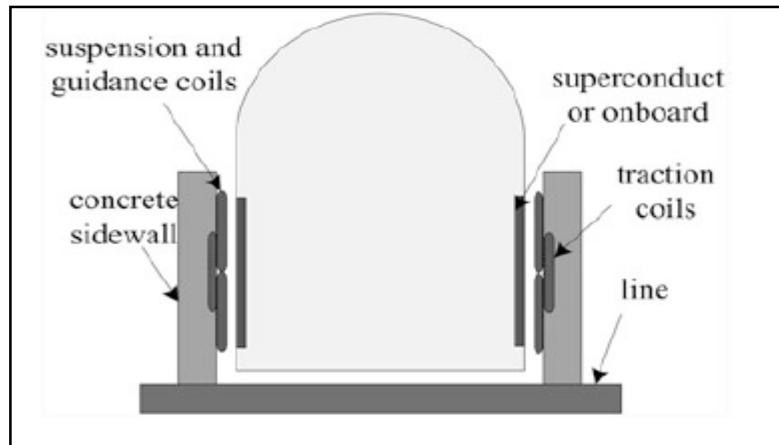


Figure 1.5, Section of Japanese MLX High speed Maglev Train
(Zhigang et al., 2015).

In 1972 the first test was conducted on vehicle LSM200 at RTRI, based on an “air-cored linear synchronous propulsion system” (Rote, and Coffey, 1994).

In 1974, the first test on Super-conductive ML was conducted on vehicle ML-100A on a test track of 500 m achieved a speed of only 60 Km/hr. because of the limited length of the test track. In 1977, a new vehicle ML-500 supported by wheels was developed and tested on a longer test track around 7 km. After 2 years, in 1979, the system succeeded in moving at higher speed of 517km/ hr.. In 1980, this system was inverted from T shape guideway to U shaped for stability purposes.

In period of 1980 to 1987, a new vehicle MLU001 was developed and tested and achieved speed was 400.8 km/hr.. In 1995 a new vehicle MLU002N was produced and the max test speed achieved was 411km/hr. In 1999, the same vehicle was tested on a longer test track, and succeeded in reaching 552km/hr. In 2013 a new series LO model was developed, 2 years later it was tested and recorded the higher speed of 603km/hr. (Rote, and Coffey, 1994).

1.3.2.2. Japanese HSST

During the period 1990 to 1991, Japan built the HSST (High Speed Surface Transportation) which is an Electromagnetic (EMS) system for testing. The first train was the HSST-100, and in 1995 the system was investigated and studied for safety and reliability by the HSST Feasibility Committee. They agreed that the system could be accepted for commercial use for 2004. Figure 1.6 show the concept of HSST maglev train (General Atomics, 2002).

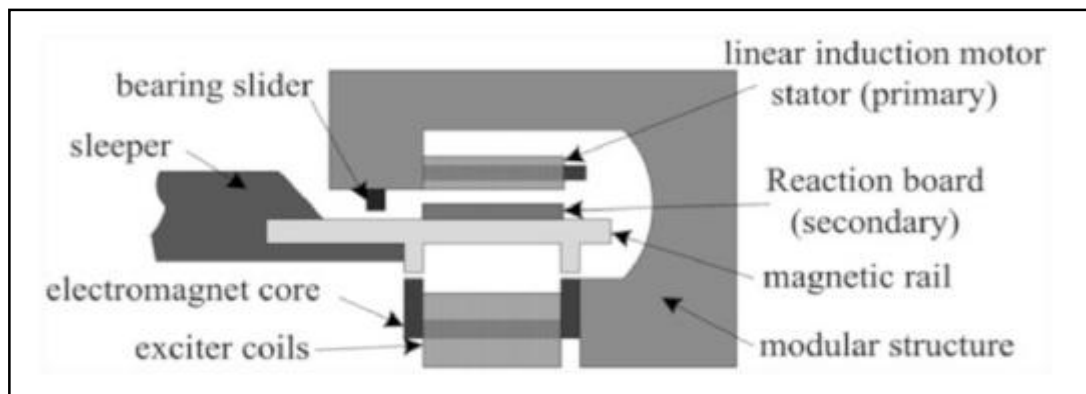


Figure 1.6, Concept of Japanese HSST maglev system

(Zhang et al., 2015).

1.4.Korean UTM

The maglev train systems in Korea are managed by “Korean Urban Transit Maglev” UTM. The system is designed for medium speed using EMS technology for lifting, and LIM for thrust. In 1997 the first test run was conducted on UTM01 over distance of 1.3 km. This system is still not used for passenger services (General Atomics, 2002).

1.5.Low and High Speed of China Maglev Train

The EMS technology of maglev train was widely developed in China during the 20th century. The development were for both low speed trains which can move in 100-130km/hr., and the high speed maglev trains, for speeds of 400-500km/hr.. The suspension system for these two

kind of trains was designed using similar concepts to the German EMS, to control the train levitation with an air gap of approx. 10mm.

The research and studies of maglev trains systems was started in 1980s by different Institutes and Universities, and more than one working group contributed in this task. In 2005 the first group worked and constructed the first maglev train model. The practical test of a train of two vehicles was conducted in 2009 using a test line of 1.54 km. The highest speed achieved during the test was 105 km/hr.

In 2012, another group succeeded in develop a new system called the “Hybrid Magnet Maglev Train”, for physical operation tests. At the same period, in 1998, one more working group in “Southwest Jiaotong University” constructed a longer test track of 425m, in order to test the new EMS-LS maglev train. The model was manufactured during 2001 and delivered for test in 2006. Another low speed test track was constructed in” Zhuzhou Railway Vehicle Factory” which was used to test the speed of the EMS, maglev train, In 2000, the high speed maglev train was constructed for Shanghai operations and entered to service in 2003. There were several problems and issues to be solved. For examples the air gap (suspension) control, vibration control, coupling between the car body and the guideway, dynamic modeling, and a suspension fault detection, (Zhigang et al., 2015).

1.6. Research problem statement.

1.6.1. Air Gap Control

Maglev train concepts are similar in operation to electric motors. However, the motion is linear. Linear motors are the conventional motors, that are found in trains and are unrolled. The super-conductor or permanent magnets (EMS) are mounted in the vehicles, in the same manner as the rotary part of the Motor, and the coil mounted along the guideway, in equivalent to the stator,

The air gap is the space (clearance) splits the fixed guideway or track from the moving part which consist the lifting Magnets or Electromagnets (EMS). This must be controlled at a certain limit, usually about (8-10 mm). The dynamic stability of the levitation system can be achieved by controlling the lifting force of the lifting magnets. Controlling the air gap presents a significant design problem, requiring a controller to maintain the air gap limit (General Atomics, 2002).

Theoretically the gap should be very small to avoid electrical and magnetically loses. However in practical this gap cannot be zero preventing direct physical contact between the electric coils in the train car body and the guide truck. So the air gap limit should be maintained allowing free movement of the train with acceptable loses. The control unit of the levitation system consist of electromagnetics, a gap sensing device (sensors), and a separate controlling system, as outlined in figure 2.1.

1.6.2. Maglev Train Control System

The (EMS) Maglev train contains a car-body, levitation bogies, suspensions systems, guidance magnetics and the levitation system. Figure 1.7 shows a general view of a low speed maglev train. Each car body in the maglev train consist of five bogies to support the car body. Each bogie includes two levitation modules, and each model consists of two electromagnets which are controlled by a decartelized single input-single outputs (SISO) controller and a central controller is proposed, so that there will be four levitation units in each bogie. The system is modeled as a single mass moving over a rigid guide-way with certain air gaps and space clearance between static guide-way and the lifting magnets. This gap must be controlled within an allowable limit of (10 mm).

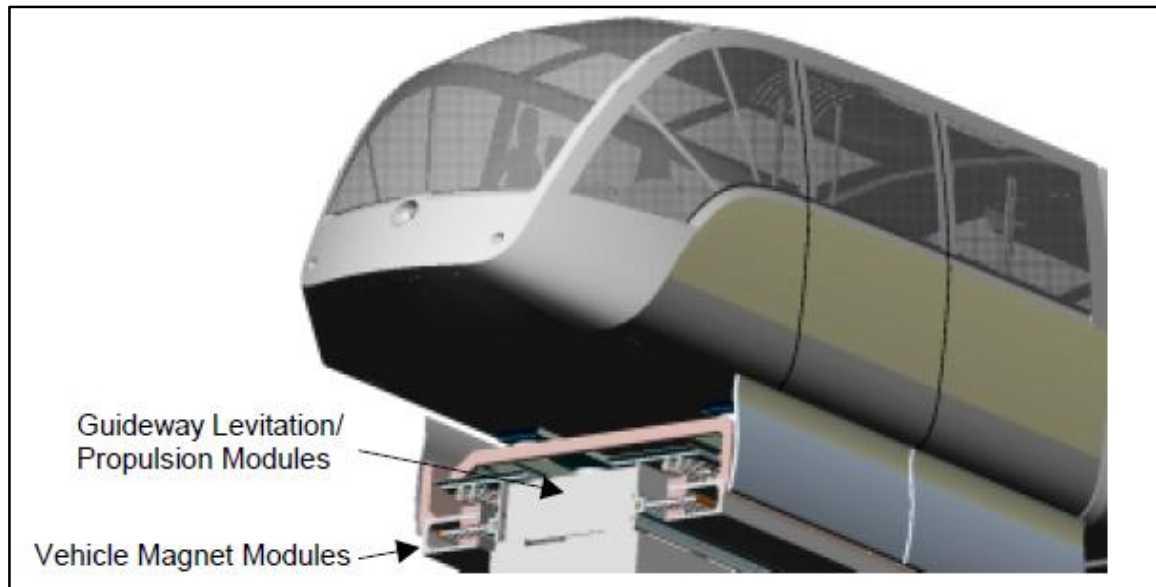


Figure 1.7, General View of Vehicle on Guideway

(General Atomics, 2002)

1.7. Research Aims and Objectives.

This research was conducted to emphasize the capability of (Least Effort Regulation) to be applicable and valid for controller design for multivariable systems. The new area of application is to design a controller for a maglev train suspension system by implementing the Least effort technique. It is a recent technique introduced by (R. Whalley, and M Ebrahimi , 2006), enabling controller design for multivariable systems with minimum control energy consumption. The main steps in the design procedure uses an inner and outer loop control strategy, and an optimization, disturbance rejection procedure.

The main objectives of this research is to design a least effort controller to control the air gap of the electromagnetic suspension system, of a maglev train. Also to Investigate the effectiveness of the controller designed for controlling the clearance, alignment and stability of a maglev train. And to guarantee the capability of the controller to solve the classical control problem of closed loop stability. To maintain the output interaction within a certain limits. The capability of the controller to reject external disturbances will be assessed. Finally

investigate and compare the results of closed loop responses, disturbances rejection, energy consumption obtained by Least effort technique with the results obtained from the classical control methodologies, such as inverse Nyquist array and H-infinity optimal control.

1.8.9 Research Dissertation Organization.

This research dissertation will be organized in five chapters. The first Chapter summary the introduction of the research, which is formed from the background, and problem statement which describes the idea and the objectives of this research.

The second chapter is comprise literature review, to crosscheck the conducted work on similar subjects for modeling and controlling maglev trains, and the levitation gap. This chapter explain the history of general control systems and the classification of multivariable control from the British and American schools.

The third chapter focuses on the methodology's which include the mathematical model of Maglev train. TITO transfer function. The control techniques and theories that will be implemented in the design of a TITO controller for a maglev train. Attention will be paid to the application of the new control technique (Least Effort Technique) in comparison with classical control methodologies such as INA and H-infinity,

Chapter four deals with implementation and simulation of the system model. Discussions of the responses of closed loop systems, disturbance rejection and energy dissipation for each controller with comparisons with the results from other design techniques.

Finally, Chapter five outlines the outcomes and advantages, of the Least effort technique in comparison with the other control theories. Recommendations are provided in this chapter for ongoing and future multivariable control applications.

Chapter 2

Literature Review

2.1.Introduction

The research reviews the history of control theory and the published work on MIMO control systems, and review the development of maglev train systems and its applications, and summarize the presented researches, also focusing on the control problems of the vertical clearance in the suspension system. It is also review Modeling, Control, Simulation of Maglev Train Suspension Systems. Maglev Train concepts are similar to the operation of electric motors, but the motion is linear. The linear motors are conventional motor, that are unrolled. However super-conductors or permanent magnet are mounted in the vehicle to act as the rotor, and the coil mounted along the guide-way, is equivalent to the stator (General Atomics, 2002).

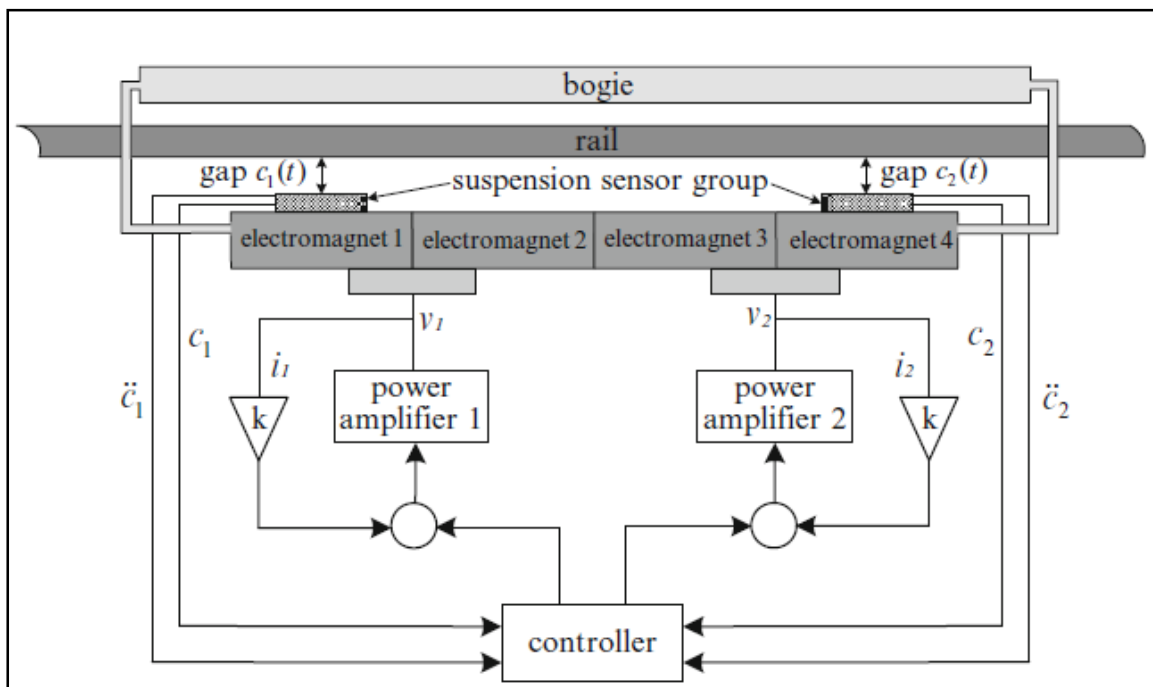


Figure 2.1, Arrangement of Suspension Control system

(Zhiqiang et al., 2007)

Maglev train modeled with consideration the vehicle as single mass moves over the stationary guideway, and the vehicle movement will be controlled to avoid the instability of the EM levitation. The clearance between the vehicle and the guideway should be controlled to maintain the desired gap. Figure 2.1 shows the arrangement of the suspension control unit.

2.2.The Control History

This field has ancient begins. The first known example of a Control System was in 1400 BC. The ancient Egyptians used a bucket shape vessel to make a water clock. The size of the hole in the bucket and the shape of the container controlled the flow of water to make accurate time indicator. Until then, the ancient civilization in Baghdad invented the water level regulator.

Another major step forward in 1850s, was ship steering rudder which was controlled by a series of mechanical connections from the helm. Since ship increased in size, the hydrodynamic forces on the rudder and gears became so great, that the vessel were difficult to steer. French and British design engineers worked to help steering the ship, via an automatic “Servomotor” control of the rudder using a specialized power engine.

The need for control systems increased greatly with the use of electrical power and urban lights in the streets in New-York were introduced in 1880s, requiring a constant regulated flow of electricity. A signal fed back to an amplifier circuit helped to produce uniform power transmission even with extreme outside temperature variations. During of the World War II, most of the traditional control principles were created.

The need to improve military gun systems, aircraft, vessels, and due to massive manufacturing experiences and educational progress, facilitated the creation of control

theories, the concepts of the feedback control, and system stability using “differential equations and Laplace transformation” (El-Hassan , 2012).

2.3. Definition of Control Systems

Control system are devices that manage, command, and regulate the behavior of systems. Industrial control system are used for controlling equipment. Control system theory extended to various fields like economy, sociality, biology and mechanical system and played a significant measure in advancing of engineering and science technology (Bissell, 2009).

Automatic control became an important concept in recent engineering, and for example the electronic control of equipment, tools and industrial operations, cooling, speed, viscosity, pressure, temperature, humidity and more of industries. When a group of components are controlled in a sequences to complete a defined activity, this group forms a system. The system become controlled, if the varying in the input quantity affect the output quantity. The output quantity variables, and the input quantity command signals are employed in the control action (Bissell, 2009).

Engineering can be defined as allocating the forces and the materials as a means to serve humanity. Proper design includes significant features to control materials and the force involved engineers, in this kind of activity become control system engineers. They focus on understanding the surrounding objects, and the materials (Named Systems) in a controlled manner.

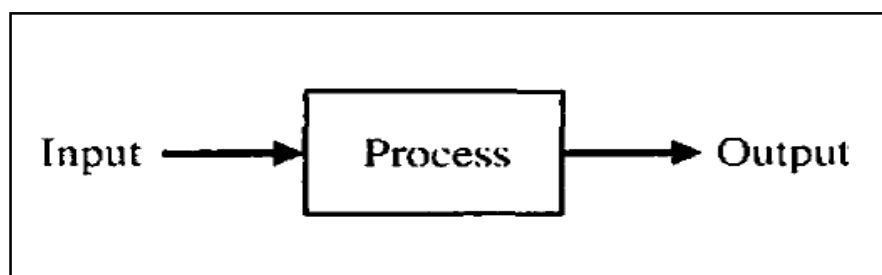


Figure 2.2, Process to be controlled
(Dorf and Bishop, 2008)

The main consideration the control engineering found was the beneficial and cost-effective product, and understanding of the system regulation. In control engineering the system itself may be not be fully understood, because in some cases chemical process are involved. The control technique depends on linear systems and feedback methods, linked to network and communication methods. The basic system block diagram of Figure 2.2 showing an uncontrolled process with its input and output in simple form (Dorf and Bishop, 2008).

Control systems are simply made of components linked together to form the system structure. System analysis for linear system depends on the cause–effect concept which relates system functions. By adding a controller and actuator to the process enables the required responses, for the open-loop control system, as shown in the Figure 2.3 (Dorf and Bishop, 2008).

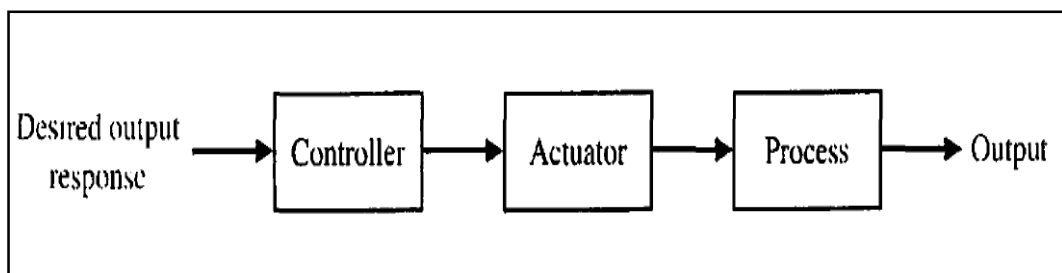


Figure 2.3, System without feedback
(Dorf and Bishop, 2008)

2.4.Feedback Control Theory

The closed loop system can be defined as system is using the output to regulating the system input, by feedback the output signal to link with the reference input. In order to obtain further accuracy, adding sensor to the feedback signals to compare the output results with the input reference as shown in the Figure 2.4,(Dorf and Bishop, 2008).

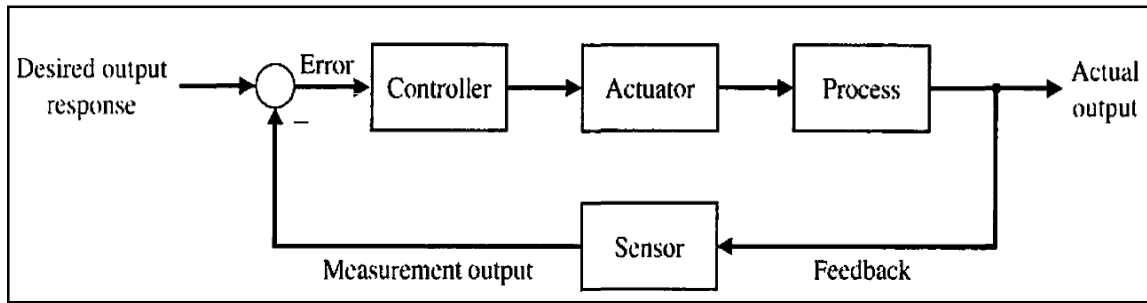


Figure 2.4, Closed Loop System with feedback
(Dorf and Bishop, 2008)

The advantages offered by the closed-loop system improve the system's capability to suppress disturbances and expand suppress Measurement noise. Figure 2.5 shows the system with external disturbances. (Dorf and Bishop, 2008)

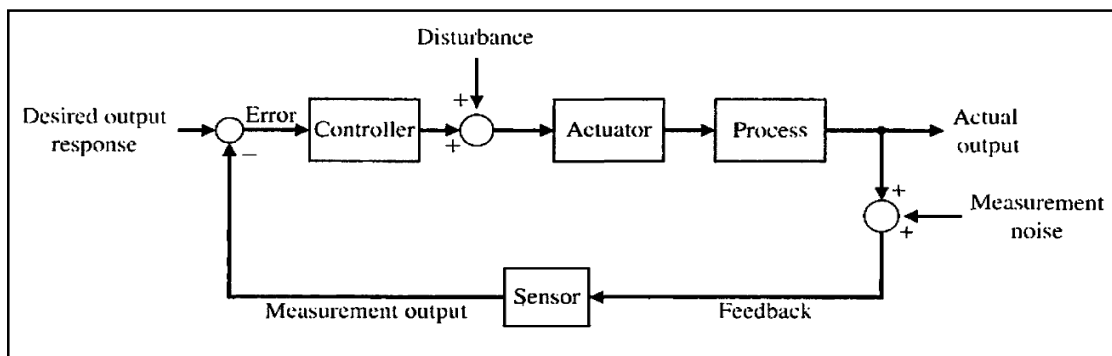


Figure 2.5, Closed Loop System With External Disturbances
(Dorf and Bishop, 2008)

Practically, feedback control systems for various applications, the system could have two or further controllers. Figure 2.6 shows system with two controllers and feedback to the inner and outer loops(Dorf and Bishop, 2008).

For more complex systems for multi inputs and multi outputs, several controlled variables should be included in the system structures. The system is then called a multivariable system. The general representation of the system structure is shown in the Figure 2.7 (Dorf and Bishop, 2008).

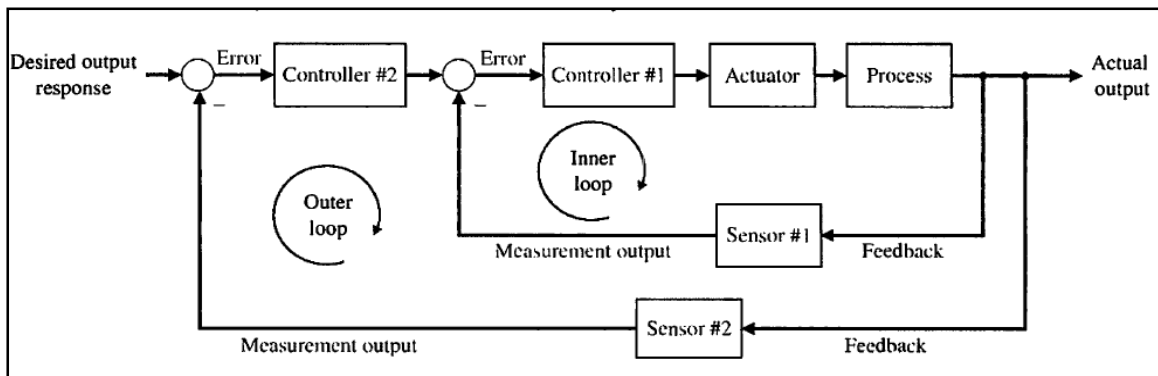


Figure 2.6, Double Loop Feedback System
(Dorf and Bishop, 2008)

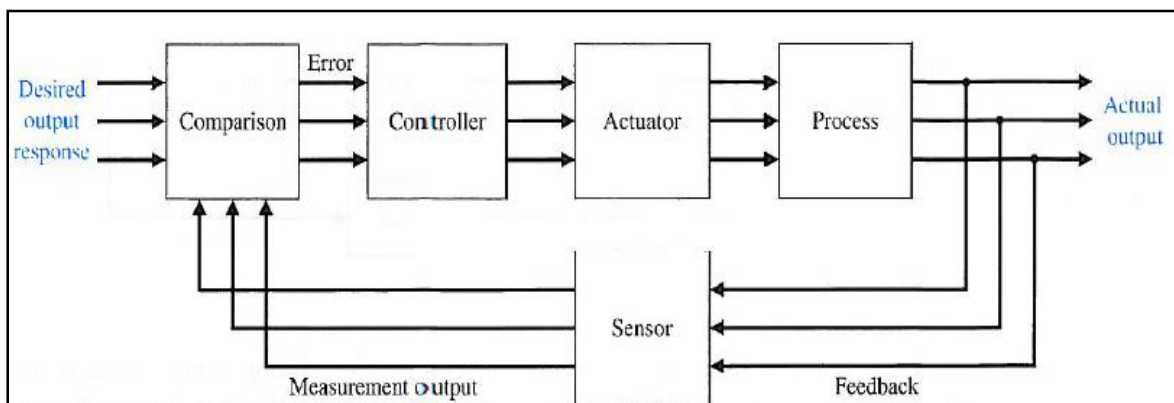


Figure 2.7, Multivariable Control System Representation
(Dorf and Bishop, 2008)

For more understanding of the meaning to control, it can be recognized in the human body through practical activity, For example, while deriving cars, using both eyes and hands and other body parts in a coordinated mode to achieve smooth and safe operation. The reaction of all these parts is in fact in responses to signals following our senses. However this difficult to study and measure since it is related to human body physics, encouraging engineers to implement the same concept for industrial controls. System control can be achieved with the main two elements. The first obtaining a system model through physical and mathematical analysis, and the second is to design a controller by implements an appropriate design strategy to obtain the required operation conditions (Warwick, 1996).

2.5. Control Theory Review

Automatic Control philosophy utilizes the use of electromechanical and energy resources in several applications to replace human energy. Similarly automatic controlled machines / equipment systems reduce the need for human intervention. In general automatic control is considered to be more efficient, consistent, and precise (Hazen, 1934).

Automatic control could be divided in principle in to two kinds, the first control is time depended control, which is depends on the some quantity to activate the control for some time, and based on the operation result time can be set. For example “Time-operated traffic-signal control” (Hazen, 1934). While the second control is depends on the operation results to regulate the input quantity, so that it may called closed loop control. The example of the second kind is the temperature thermostat, and “automatic ship steering” (Hazen, 1934).

The Control system engineering is the kind of engineering which is focusing on control principles to design the systems to achieve the required results. The control specialized persons are analyze, design, and optimize complicated systems which may consist of mechanical, hydraulic, electrical power supplies.

Automatic Control exercises feed-back techniques, to obtain basic automation. It can be turned to the 17th century through innovation of the level regulator, water clock, pneumatic and hydraulic systems. After developments in system design and control, for example the steam engine regulator, temperature control and controlling mechanisms, in the 19th century with stability principles was developed in UK by Routh and in Switzerland by Hurwitz. Moreover the servomechanism techniques originated in the same period, which includes ship-steering and autopilots. During W.W II, the need to control gun systems with high performance, and the progress of the communications engineering and servomechanisms, led to the developed of “classical control methods” in the United States and England. On the

other hand dynamic modeling developed in parallel in USSR by “Poincare and Lyapunov” (Bissell, 2009).

Automatic control in the past can be divided in to four periods of improvement. The period prior 1900 called the “ early control”, and the second period called “pre-classical period” which extended from 1900 to 1940. The third period known as “ the Classical Period” was between 1935 and 1960 and the latest period of “ Modern Control” after 1955 (Bennett, 1996).

2.5.1. Early Control- Before 1900

The early control period in the 9th century represented by the Hellenic and the Arabs with in the “Islamic culture” were the first nations to initiate feed-back control. This was experienced by the west, with innovations and application such as the “Float valve regulator, water clock, oil lamps, and water level in the tanks” (Bissell, 2009) as stated by writings of “Al-Jazari (1230) and Ibn al- Sa-ati (1206)”. Float valve regulators for animal drinking was developed in the Arab world, also the water clock was recognized by Pseudo-Archimedes.

In the 18th century during the industrial revolution in Europe, the temperature regulator in the incubation system was developed by “Derbbel 1572-1633” (Bissell, 2009).

The major progress in control occurred during 18th century representing the controller of governed steam engines. The idea was realized by James watt (1736-1819) to solve the control problem for wind and water mills. Watt’s idea was initially designed in 1788 to regulate steam engine speed, and was practically implemented on 1789, see Figure 2.8 and Figure 2.9. The main difficulties of the **Watt governor** was it delivered only proportional control, and applicable only for specific operation condition with limited speed range, so that it was comments as "a moderator, not a controller". And then, in the 19th century further development were made in the Watt governor to avoid the offset problem.

Thereafter William Semens (1823-1883) in the period of 1846 to 1853, involved the high speed governor, developed by Charles T. Porta (1858) (Bennett, 1996).

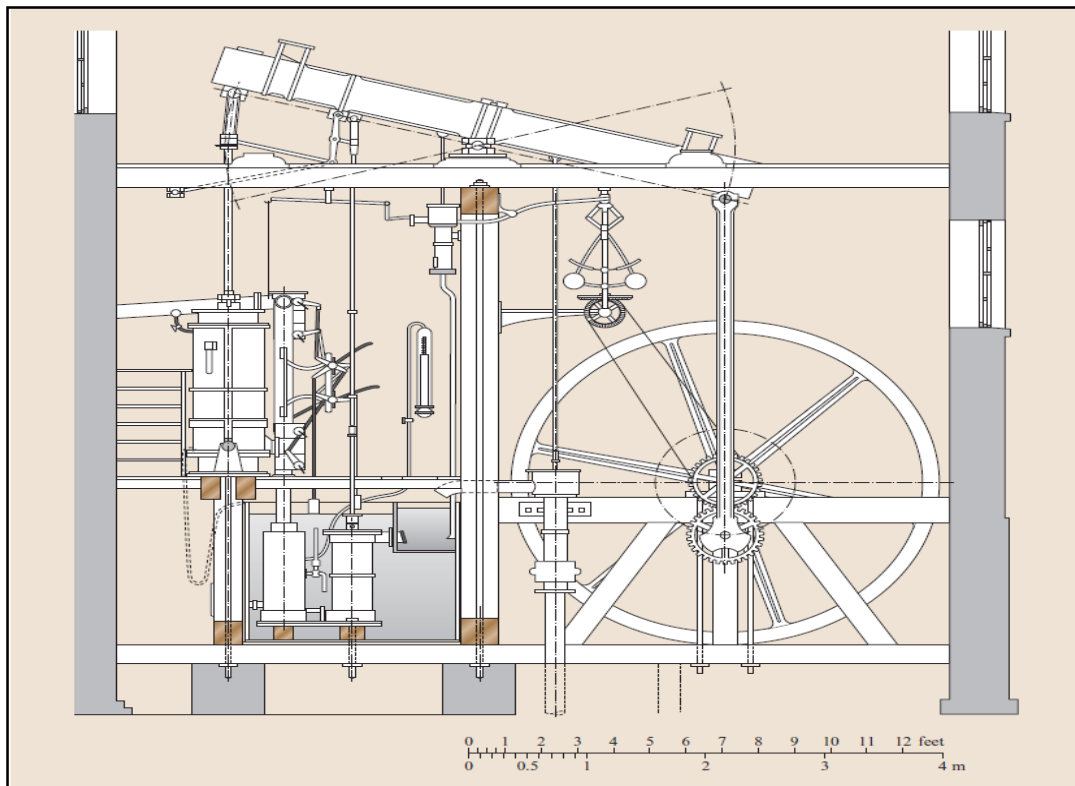


Figure 2.8, Boulton & Watt governed steam engine

(Bissell, 2009)

In the period from 1862 to 1872 both, Thomas P. and William H. respectively developed governor equipped with a spring, designed to work at speeds greater than the Watt governor. In the beginning of 19 the century attempts of Poncelet J.V in 1826 and 1836, and Airy G.B. in 1840 and 1851 to analyze the governor, to solve the reported problems of “Governor Hunting” and identify the stability conditions (Bennett, 1996).

During 1868, Maxwell J.C. published his paper entitled “On governors”. He derived the “linear differential equations” for different kind of governors, and these equations were to determine dynamical constancy. What was started by Maxwell, was followed by Routh E.J

(1831-1907) in his work on the “stability of motion” in 1877, from which the well-known “Routh-Hurwitz stability criteria” was developed (Bissell, 2009).

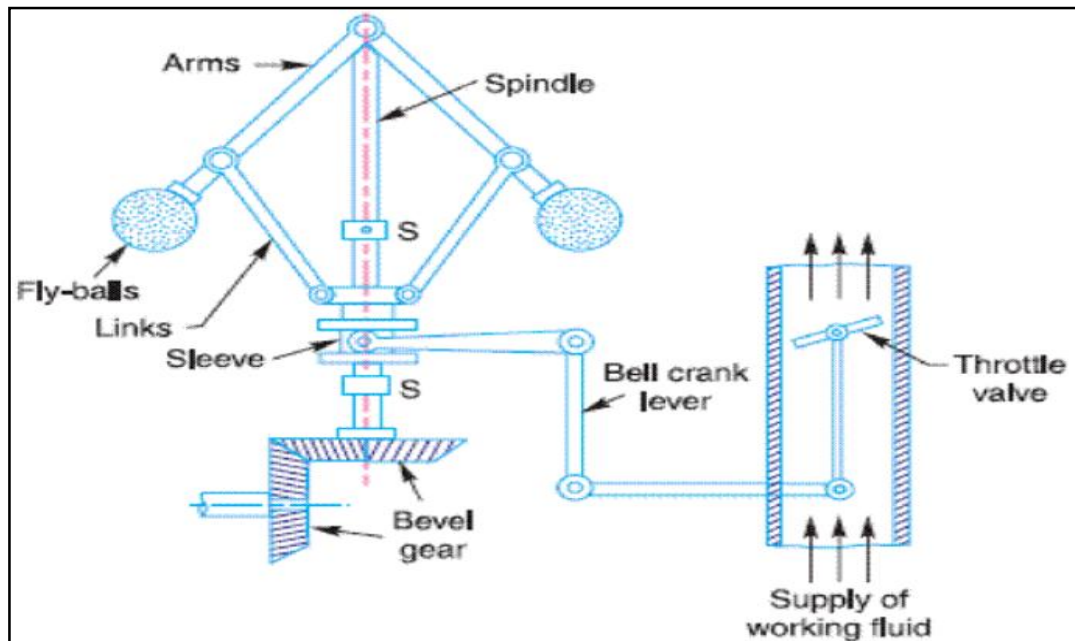


Figure 2.9, Example of Recent Watt Governor Application

(Allwright J., 1970)

Another major step forward in 1850s, was ship steering rudder where was controlled by a series of mechanical connections from the helm. Since ships became bigger, the hydrodynamic forces on the rudder and gears ratio became greats making it slow and difficult to steer a large vessels, French United States and British design engineers worked to use a power mechanism to help ships steering. The US engineer Frederick Sickels developed the first motorized steering machine in (1853), at the same period, especially in 1866, McFarlane J. designed the steering machine with feedback called “closed loop steering engine” used for steam-ships, while the French engineer “Jean Joseph Farcot” developed another wider range closed loop steering machine, which can control system based on a position. He named the machine the “ servo-moetur” now known as “servomotor” The innovation of the electricity opened the door for more control system applications. Such as Arc lamp which needs to have

a fixed clearance between the conductors, and spring type of hydraulic systems solenoid valves (Bissell, 2009).

2.5.2. The Pre-classical period of control (1900-1935)

The beginnings of 20th century noticed developments in many of closed loop applications of control, for example the electromechanical systems, to control the voltage, current, pressure, flowrate, steam generation control, also for the aerospace engineering such as aircraft steering and stabilizing control, the most of the applications were subjected to simple control due to lack of understanding, however at the same time there was complicated control law being developed (Bennett, 1996) .

During (1922), Nicholas M. (1885-1970), developed and analyze the position control system, and formulated the control law which represented the terms of the PID control. In the beginning of 1920 severe restriction of amplification made it difficult to improve long distance telecommunication, which required more development in cable design. Work was done to solve the magnification, with the use of amplifiers by AT&T in 1930. Amplifiers improved, and in 1932 Black and Harry Nyquist (1889-1976), in their research entitled “Regeneration Theory” base of frequency response and considerable progress. In 1934, a paper was presented by Hazen who conducted the initial academic study of servomechanism. This paper considered as the beginning of the expertise of control system analysis (Bennett, 1996) .

2.5.3. The Classical Control Period 1935 -1950s

There were a lot of design studies and developments made on control system in the five years from 1935- 1940s. Independent groups were working in the US, in parallel, with work conducted in Europe, including Vyschnegradsky's work in Russia, and Barkhausen's worked in Germany, The first group was working on communications field. In 1940 Bode H. studied

frequency-domain analysis finds the relationships between attenuation features and minimum phase shift. Also he identified the stability point $(-1,0)$ to be the critical point instead of $(+1,0)$, which defines the phase margin and determines the stability of the system.

In (1936) Mechanical engineers were working in the another group concerned with the process industries. In coordination with “American Society of Mechanical Engineers” major skills organization “Industrial Instruments and Regulators Committee” which deals with automatic control was formed (Bennett, 1996) .

By 1940s, PID control was developed for equipment adjustment. In 1942, Ziegler J.G. and Nichols N.B. presented the study which is called the “Ziegler-Nichols tuning rules”, to get the best setting for PI and PID control, using the critical gains at which the system is marginally stable. Also how to select the factors’ (parameters) of proportional, integral and derivative parts was identified (Bennett, 1996).

In (1948) Walter Evans introduced new graphical approach called “graphical analysis of control system”, it is a great technique to analyze transient responses. It can be used to describe quantitatively the performance of the system as various parameters are changed. Root locus techniques offer the ability to trace the characteristic equation roots. It has a significant influence are a large set of applications, enabling the location of the closed loop poles. Evans defined the rules for the create of the graph on the S-plan. This technique is applicable for the SISO systems. In order to plot values of the “poles and zeros” the transfer function will equals -1 , Root locus graphical techniques provide an effective way to understand system performance, which is important in the design of control system (Evans, 1950).

At the same time (1936) , Harold L. Hazen and Gordon, S. Brown were leading a group of the electrical engineering section of MIT. They implemented time domain methodology, and

improved block diagram usage by considering differential examination in the simulation of control systems (Bennett, 1996).

During the Second World War, the concentration was to find solution for some particular problems. The major problem was how to improve controlling anti-aircraft fire, and the difficulty of this problem was in determining the location and direction of aircraft. Then controlling the direction of gun fire. This procedure needs 14 persons complete successfully. It was very difficult to create an automatic system, servo-mechanism, gun movement.

In 1941, the manual transfer the information obtained from the radar system to the gun control system failed to deal with high speed aircraft, so an automatic system to track radar information linking it directly to the gun was required. Since the separate functioning of both frequency domain and time domain techniques, a new technique was required to adopted the greatest features of each.

In 1943, Albert C. Hall, presented in his study that of using the Laplace transformation techniques enabling the locus of the system transfer function, and then Nyquist's stability can be applied, enabling the determination of gain and phase margins, to approximate the closed loop, time domain performance (Bennett, 1996).

2.5.4. Modern Control History

After the War, understanding the lessons learned, as well as the invention of digital computers contributed to the development of new approaches to system control which is now known as Modern Control. A good example is the state variable or "state-space", and optimal control. Alistair J.G. MacFarlane (1979), introduced the main aspects of missiles and space vehicles such as launching, direction, maneuvering and chasing, and the second is development of digital computers. The term of "State Space" concepts became well known

when the aerospace engineers implements the model of Poincare, for creating “common differential equations in terms of first order equations” (Bennett, 1996).

The beginning of using digital computers on 1950s to 1960s when replacing mechanical and electrical devices with “solid –state and micro electric devices”, began in early 1970s. Digital computers used on-line information to replace the analogue systems because of complexity. Digital computers were also used to control the systems. An example in the “ICI plant at Fleetwood in the U.K. in 1962”. By the development of (digital computer), it is become useful to consider the (time-domain) formula for the equations of the control systems, this practices can be applied for the “non-linear, time varying, and multivariable systems” (Dorf and Bishop, 2008).

2.5.5. Stability Theory

The stability of systems usually depends on analyzing the system mathematically, in terms of differential equation, then to obtain the characteristic equation of the system which will give the system stability by the location of the system poles and zeros.

Dorf defined the stable system is the system with restricted responses. That is, if the system inputs and disturbances are restricted with certain references, then the system responses are restricted magnitude, in the other word, “A stable system is a dynamic system with a bounded response to a bounded input”, and the stability conditions are “ the necessary and sufficient condition for a feedback system to be stable is that all the poles of the system transfer function have negative real parts” (Dorf and Bishop, 2008).

In (1868), J.C Maxwell conducted dynamic analysis on the Watt fly-ball governor. He worked on the linearization of the motion of the differential equations to get the system Characteristics Equation. He investigated how stability can be affected by factors, and

explained that system stability can be achieved if the roots of Characteristics Equation are located in the negative region of the S-plan (Lewis, 1992).

J.C Maxwell published a paper titled On governors in 1868, he stated that the obtained equations realize the entire requirement of motion stability. However, for third order linear model and obtained the two significant stability conditions for governors were obtained , but was unable to give solutions for higher order systems.

In (1877) Routh E.J worked to solve this problem. He conducted a study of Dynamical stability and found solutions for fifth order models which was presented in his paper titled “Treatise on the Stability of a Given State of Motion” (Bissell, 2009).

In 1895, independent work conducted by Hurwitz, on dynamical stability, confirmed Routh theory, resulting the well-known Routh-Hurwitz stability methodology, (Bissell, 2009). Further definitions of Routh-Hurwitz stability as defined by Dorf and Bishop “The Routh-Hurwitz criterion states that the number of roots of $q(s)$ with positive real parts is equal to the number of changes in sign of the first column of the Routh array” (Dorf and Bishop, 2008).

2.6. Schools of Multivariable Control

Multivariable systems control can be classified based on the work of two main schools. The British schools and the American. The British school is the older, initiated in the period before and during 1960s, including a number of classical theories of control systems, The well-known British classical methods are the Inverse Nyquist Array (INA), and Characteristics locus (CL), While the American school of control began at the same period a different approach using State feedback and Observers, Optimal Control by Kalman (1960) leading to H2 and H-Infinity Control (Kimura, 1996).

The major difference between these two, was argued by Kimura that “classical design algorithms such as lead-lag compensation were not clearly formalized as a design problem to be solved, but rather as a tool largely dependent on cut-and-try processing”(Kimura, 1996).

The results of recent state space technique developed by Kalman in 1960, explained that “Design procedures were stated as the solutions of control problems formulated in terms of the state-space description of the plant, rather than cut-and-try-based practices” (Kimura, 1996).

The progress in control technique in the period of 1960s to 1970s answered the opinions and the contradictions, for examples, Modern against Classical, and (Time Domain against Frequency Domain), and (Theory against Practice).

2.6.1. The British School for Multivariable Control

The British school for control initiated during 1960s, includes a number of classical theories of control systems, for example “Routh-Hurwitz stability criterion, Nyquist stability theorem, Bode's dispersion relations, Wiener's realizability criterion and factorization theory on the one hand, and a set of design algorithms such as lead-lag compensation, Smith's prediction method, Ziegler-Nichols Sensitivity method, Evans' root locus method” (Kimura H. 1997).

Although the British school is older but still offering new designs based on frequency domain for multivariable control systems for example the philosophy offered by Horowitz with his group titled “quantitate feedback theory” (Kimura, 1996).

The single loop technique are insufficient to solve the problem of systems subject to more than one input and output (Multivariable). This concerned was answered by MacFarlane in the paper published in 1970 as the interactive effect is a significant complications in multivariable systems, the action of one feedback affects the action of the other, (Macfarlane, 1970).

The famous British classical methods are the Inverse Nyquist Array (INA), and Characteristics locus (CL), will be discussed thoroughly.

2.6.2. Inverse Nyquist Array (INA)

In 1957, Rosenbrock outlined the relationship between the transient and frequency responses for the linear and stable systems, and how it can be approximated. The responses of the system can define system dynamics and how it is performed, for any kind of input, for step or impulse, or steady change such as variable sinusoidal frequencies. Both results are identical, therefore transient response and frequency response can be obtained from each other, the advantage of frequency response is easier to calculate, while the transient response provides beneficial information for system dynamics, so that the exchange from type to other is possible with less labour, (Rosenbrock H., 1957).

Also he outlined the mathematical equation that relates the transient and frequency responses,

$$\mathbf{f}(t) = \mathbf{H}(0) + \frac{2}{\pi} \int_{\omega=0}^{\infty} \rho \mathbf{H}(j\omega) \cdot \cos \omega t \cdot d(\log \omega) \quad (2.1)$$

Based on this background, Rosenbrock extended his work to the control multivariable system based on frequency domain. For example, his “paper on reduction of system matrices transformations of linear constant system equations and on linear system theory in (1967)” (El Hassan, 2012).

During 1969 Rosenbrock presented his paper on using of the Inverse Nyquist Array (INA) to design multivariable controller, he defined INA as “a set of diagrams corresponding to the elements of the inverse of the open-loop transfer function of a control system. A number of theorems are proved which show how this array can be used to investigate the stability of multivariable control systems” (Rosenbrock, 1969). He also outlined the detailed procedure for designing multivariable controllers. The paper showed the guidance technique to enhance the decoupling of the system transfer function. The main steps for this technique were to

identify the de-coupler or the pre compensator which is required to remove or minimize the coupling or (link) between system outputs, and then to ensure the diagonally dominance of the system achieved (Zames, 1966).

The Gershgorin circles technique is one of useful graphical technique to investigate diagonalization of transfer function and system stability. This method requires generated circles on the Nyquist plot of the s-plan, (Gershgorin, 1931). Gershgorin technique stating that none of these circles should encircle the origin of S-plan. On the other hand, closed loop stability can be realized if no bands crosses the negative real axis of the s-plan (Munro, 1972). Once these conditions are achieved, the system would be considered as diagonally dominant, then classical procedures for SISO control can be implemented, such as PID technique to obtain a dynamic controller.

Practically there is difficulties for using Inverse Nyquist Array to obtain the pre-compensator, required to achieve diagonally dominance. Several attempts to realize this condition, for example (Pseudo-diagonalisation method) which was proposed by Hawkins (1972) , and the paper presented by Gary G. in 1979, states the use of new technique (called function minimization) to realize the diagonally dominance of Nyquist matrix.(Gary, 1950).

Another technique proposed by prof. Robert Whalley titled “decoupling the system using spectral factorization technique, and then relaxing the decoupling by approximation of the compensators resulting in diagonal dominance” (Whalley, 1978). In 1980s, Mees explained that the system could be close to the dominant conditions in the specific frequency by his proposed paper titled “optimal constant diagonal scaling matrix” (Mees, 1981). Limebeer continued Mees work and presented “generalized diagonal dominance approach” in 1983, (El Hassan, 2012).

2.6.3. Characteristic Locus Method

Characteristics locus is the frequency domain controller design technique, developed by Macfarlane in 1970. The main achievement of this technique produced “commutative controller” (Macfarlane, 1970).

He explained that the spectral investigation made based on decompensation of TF matrix in to Eigen-structure shape which is formed by Eigen-Vectors or (Characteristic Directions), and the diagonally decompensated matrix consisting of Eigen-values (Characteristic values). By this procedure the system decoupling was realized, then the controller can be designed by using classical control methods for SISO (Macfarlane, 1970).

In 1970 an paper on (Commutative Controllers) published by Allwright J. C. This work was an extension of Macfarlane technique. He proposed that this technique might be easier if additional general diagonalization was engaged(Allwright, 1970),.

In 1971 Macfarlane explained Characteristic Locus as “A design technique is developed which is based on the frequency-response loci associated with a set of Characteristic transfer functions for a multivariable feedback system. The method encompasses all aspects of feedback-system behavior, including integrity against transducer- and actuator-failure conditions”(Belletrutti, and MacFarlane, 1971).

In 1973, Macfarlane and Belletrutti J. J. worked together and presented another pepper titled “The Characteristic Locus Design Method”, it was indicated that Characteristic Locus can be as grouping of the classical methods of Bode-Nyquist which using of frequency responses concept to examine SISO systems, and state-space technique which utilizes “logical exploitation of the algebraic and geometric properties”(Macfarlane and Belletrutti, 1973).

This technique was build based on a number of the standard mathematics of linear operators consisting of both algebraic and geometric approaches. This method was developed based on

two significant foundations. “ it provide useful technique for the design of wide range of practical multivariable controller for industrial plants from a limited amount of experimentally data . and It provides a bridge between the recently developed state-space methods and optimal multivariable control, and optimal multivariable filtering, and the well-established classical frequency-response methods, largely restricted to single-input single-output systems” (Macfarlane and Belletrutti, 1973).

In 1997, Ken Dutton explained that The controller design based on C L method can be concluded to obtain compensators at three levels of frequency. First for high frequency compensation were at this stage the transfer function is approximately diagonal by designing suitable compensator. The second step the mid- frequency compensation, which need to have another compensator at intermediate frequency. This compensator is called the approximate Commuted Controller(ACC), to be added in the front of the system. The third stage is to design uses a compensator for the steady state low frequency in order to balance locus (loci) steady state. Usually this used as PI type (Dutton, 1997).

2.6.4. The Recent Control Theory – Least Effort Regulation

The least Effort regulation technique was introduced by (R. Whalley, and M Ebrahimi , 2006). The advantageous of Least effort technique is to reduce energy consumption in the controller, and reduces the overall effort and energy, and will reduce the maintenance cost. The main steps of this procedure are a closed loop depending on an inner and outer loop control strategy. The inner-loop analysis to demonstrate system performance and to guarantee satisfactory dynamical response. Thereafter a formal design stage, can cover the outer loop construction to realize robustness requirements with satisfactory disturbances suppressions. The optimization, disturbance rejection analysis and stability of the whole system, is determined by this technique to achieve performance and disturbance rejection characteristics, by minimizing a performance index J (Whalley and Ebrahimi, 2006).

It also result in a simple controller than presented by classical control methods, such as Inverse Nyquist Array, optimal control theory, and H_{∞} control theory. There are several research conducted and evidence that the least effort control technique is applicable for multivariable control systems, such as gas turbine, aero dynamic control surfaces, hydraulic systems, DC motors, wind tunnel control systems, Maglev trains, wind turbine, and more.

least Effort Control Technique will be used as main control technique in this research, the overall description of this technique with the controller design procedure and mathematical model will be explained in chapter 3.

2.7.American School of Control

The resent multivariable control began in USA during 1960s, which is time domain based methodology. Time domain formulations for mathematical equations of control system, where the state of system is a significant tool for time domain investigations and the design of control systems. The most famous methodology was represented by the recent techniques of control such as State feedback and Observer approach of 1960 by Kalman, and Optimal Control, H_2 and H -Infinity Control (Kimura, 1996).

2.7.1. State space representation

The State-Space is a well-known modern multivariable control methodology, developed by Kalman (1958), and presented during proceeding of the 1st IFAC Conference held in Moscow in 1960, The study was a continuation of the theory of control initiated previously by Shannon, but with different techniques. The new methodology is based on the time domain and time variant formulation for mathematical equations of control systems. The state of system is a significant tool used for time domain investigations . Kalman tried to give answer to the type and size of the information required to identify a control strategy. Kalman gave an descriptions of dynamic models, and defined the necessary expressions on models.

He defined the plant as a “physical object to be controlled”, which is subjected to specific physical measures named the (inputs), in order to control the system or the plant, a need to know the result and performance of the system. These can be obtained from the another set of variables defined as the outputs (Kalman, 1960).

Kalman gave the basic terminologies to describe the “Dynamics systems”, he defined the (state), of the plant as “the minimum group of numbers should be specified at time $t - t_0$ in order to be able to predict the behavior of the system for any time $t \geq t_0$ ”. And the state variables as “coordinates of $x_i(t)$ of the state (with respect to some fixed basis)” (Kalman, 1960). He presented the state space representation to be as two differential equations, the first equation is 1st order linked the inputs with state variable of system:

$$\dot{x}(t) = \mathbf{A}x(t) + \mathbf{B}u(t) \quad (2.2)$$

While the second equation is relates the system outputs as function of inputs,

$$y(t) = \mathbf{C}x(t) + \mathbf{D}u(t) \quad (2.3)$$

where **A**, **B**, **C** and **D** are the matristic representing the system variables,

In the same paper Kalman gave definition of the control law of the system, and provide useful tools to investigate system dynamics depending on the two important features of the system, which can advise whether the system is controllable and observable, these feature are controllability and observability, and he set the required conditions for each of them(Kalman, 1960).

Dorf and Bishop extended the study on Kalman theory, in 2008 by defining the state-space, as methodology based on the time domain and time variant formulation for mathematical equations of control systems. The state of system is a significant tool used for time domain investigation and design of control systems, with the state of system as a collection of variables, input signals, and equations clarifying system dynamics, gives the upcoming state and output of the system (Dorf and Bishop, 2008). And the time domain defined as: “the

mathematical domain that incorporates the response and description of a system in terms of time, t .” The time-varying control system defined as: “A time-varying control system is a system in which one or more of the parameters of the system may vary as a function of time” (Dorf and Bishop, 2008).

2.7.2. Optimal Control Theory

The work on optimal control theory started by Bellman in 1950s, through the calculus of variations, Another approach of dynamic programming to solve this optimization problem was suggested. In the period of 1948 to 1952, Richard Bellman worked to solve the issues of identifying of missiles targets in order to get best results, then he express the “principle of optimality” (Bennett, 1996).

In 1959, Kalman present his study “On the General Theory of Control Systems,” which explained the clear difference between problems of the multivariable control and multivariable filtering resulting a new handling of the optimal control problem, Kalman’s approach give more tolerance to handle “the linear multivariable optimal control problem with a quadratic performance index”. The thoughts of “controllability and observability” a resulted in a of further input to “state-space” techniques (Bennett, 1996).

In (1962) Bellman and Stuart Dreyfus, developed computer programs which was helped to create numerical answers, in 1956, Hamilton generalized this approach for the dynamical problems where require minimizing or maximizing a performance index with “an obvious and strong analogy with classical variational formulations of analytical mechanics, given by Lagrange and Hamilton”, (Bennett, 1996).

2.7.3. H_{∞} -Infinity Control Theory

The progress in control technique in the period of 1960s to 1970s answered the arguments and the dichotomies, for examples, Modern against Classical, and Time Domain against

Frequency Domain, and Theory against Practice. In order to reconcile these contradictions, the first successful trial to solve this problem was by Zames in 1960s (Kimura, 1996).

He discovered the “small gain theorem”, It was announced by Zames on 1976. The first was in 1976 in IEEE CDC, while the second was presented at “Allerton Conference in 1979”. In 1981 the problem was issued officially. Then during 2006, the H-infinity problem solved by Apkarian P. and Noll D. (Apkarian and Noll, 2006).

An essential developments on LQG control occurred during 1980's, The most Important improvement was the transform to H_{∞} (called H-infinity) optimization for the robust control, this change as results of the effective efforts of Zames , even though Helton (1976) realized that there were previous applications of H_{∞} optimization in the engineering industry. However, Zames thought “that the poor robustness properties of LQG could be attributed to the integral criterion in terms of the H2 norm, He also criticized the representation of uncertain disturbances by white noise processes as often unrealistic”. Equally the technique H-Infinity generated, on the other hand the two control techniques of H2 and H_{∞} found to be most linked than the original thought (Doyle et al., 1989).

The H_{∞} design method addresses the robustness case by deriving controller which is keeps all the signals, responses and errors of the system within the initially defined tolerances.

2.8. Maglev Train Modeling and Control Review

Maglev system started in European in 1911, after 11 years, in 1922 the first concept of using maglev trains in transportation was suggested by the German engineer “Hermann Kemper”, Fifteen year later, in 1934 the concept of Maglev train was entered to the Electro-Magnetic technology charters, In 1969, the first model in the world of maglev system has been established by Germany manufacturer “Krauss-Maffei”. In 1970 new plan for high speed maglev train developed in German based on the concept of the first model TR01, and two

new models, TR02, TR04 were produced. Figure 2.10, show the Classification of International Maglev system Development (Zhigang et al., 2015).

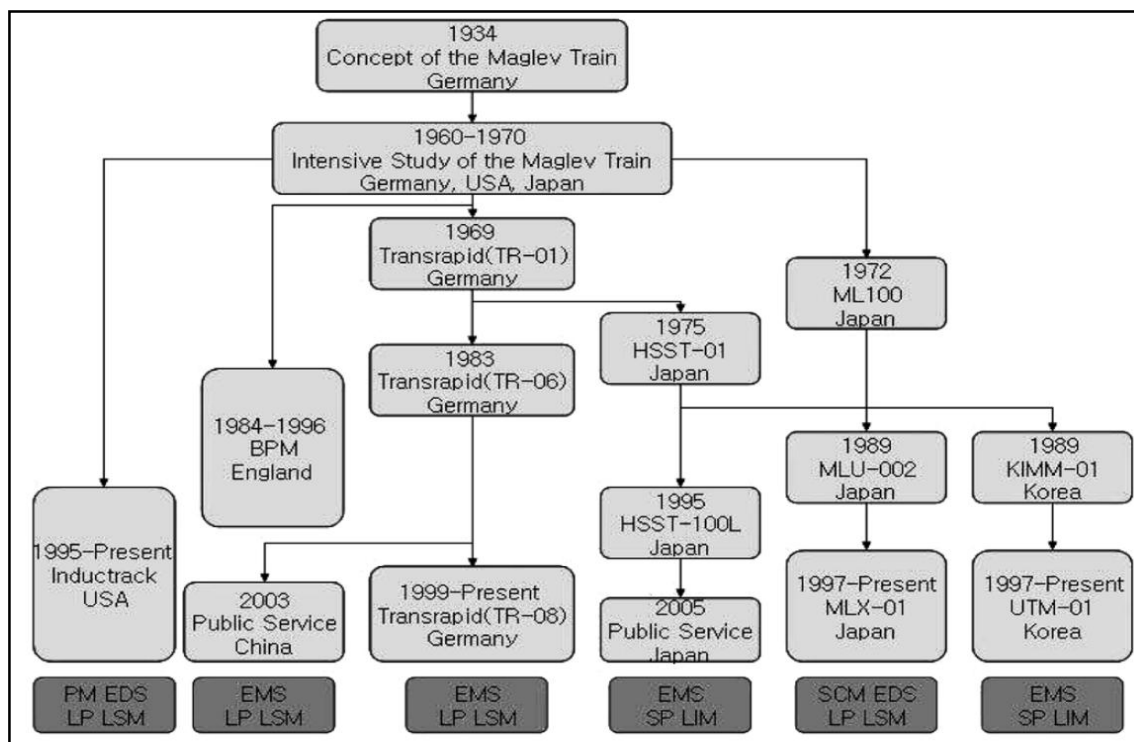


Figure 2.10, Sequence of International Maglev Train Development

(Hyung-Woo Lee et al., 2006)

In the period from 1991, new models of test trains established, such as TR06, TR07, TR08, and TR09, the highest speed achieved by TR07, and TR08 was adopted to be used as commercial maglev system. In 1974, the German company was sold to Japan-Airlines (JAL), and the model TR01 was the beginning of Japan's low speed maglev system HSST (Zhigang et al., 2015).

Since 1920s the concept of the maglev train was developed. During the 1930s this concept was entered to the Electro-Magnetic technology charters, researches on modeling of the maglev train began during 1960s in Germany and in Japan. In 1966 research on maglev train modeling was presented by Powell, Danby during ASME Winter Annual Meeting in New

York, Railway Division, In 1969, the first model in the world of maglev system was established by the German manufacturer Krauss-Maffei (Hyung-Woo Lee et al., 2006).

In 1976, Yamamura conduct a study and presented the application of maglev technology on tracked vehicles. He outlined the types of maglev systems which are utilize vehicles traveling on tracks. The main idea was an all electromagnetic levitation systems supported, steered and propelled without physical contact between the guideway and the maglev vehicles, providing solutions to the problems associated with the classical wheeled trains, such as wear, noise and vibrations, with a to reduction in maintenance cost (Yamamura, 1976).

The study explained the main concept of maglev systems, based on the generated magnetic force, the EDL (electrodynamic levitation systems) which depends on repulsive force produced between electromagnetic in the car-body, and the induced current in the guideway. The EML “electromagnetic levitation system” depends on the attractive, force between the same parts. In EML systems, the stability of levitated vehicles and controlling the air gap between moving and the stationary parts are the significant issues.

The difficulties and the technical complications of these two systems are, the EDL has low damping. However it is naturally stable, but could cause overshoots and fluctuations. The EML require small gap between the electromagnetic coils and the guideway. So that it is require accurate building of the rails to avoid the physical contact between magnets and guideway (Yamamura , 1976).

The EDL systems was initially started in Japan in 1972 by Powell and Danby. It is a repulsive force, naturally controlled so that the clearance doesn't require electronic control. While the EML systems began testing in Germany in 1971, the lifting is attractive force, which is inherently unstable, so the clearance required can be electronically controlled (Yamamura , 1976).

In 1975, a study conducted by Gottzein E. and Lange about the control system for high speed Maglev trains, discussed the difficulties in the controller design for the magnetic suspension device. The significant difficulties in modeling the moving parts comparing the car body and the magnets, and for fixed part which is the guideway. Also the disturbances generated from the physical conditions of the system and surrounding environments, such as curves and gradient in the track or guideway, air resistance, track irregularities, and the errors in the measurements. All these points were investigated, There was a lot of control techniques implemented to design a control system such as “Arbitrary dynamics and linear quadratic optimum control” (Gottzein and Lange, 1975).

The paper showed schematic of the suspension system of single vehicle with magnetic placement, system dynamic modelling and control logic were developed. Systems disturbances were considered in the modeling and simulation of the system, the paper concluded the possibility of designing control arrangement for maglev trains moving in 500km/hr. held by electric magnets (Gottzein and Lange, 1975). This paper can be considered as an important beginning of maglev train modeling and control.

In 1984 general survey performed by Rogg D. on the development and possibility of application of maglev technology. The survey outlined the beginning of magnetic levitation concepts in the Germany. The study described the types of magnetic levitation systems, and classified three types based on the magnetic levitation principle. The permanent magnet system which depends on repulsive force, and the electrodynamic system EDS which depends on repulsive force for lifting, and the electromagnetic system EMS which depends on an attractive lifting force. The paper showed the characteristic comparisons between the classical wheel/rail system and the magnetic levitation systems, for cost, performance and operation requirements and described the reasons behind the rapid development and application of maglev systems (Rogg, 1984).

In 1994 a study performed by Wang T. and Yeou-kuang T. at National Tsing Hua University, discussed the previous permanent magnet Maglev system, and addressed the repulsive type with PM was not considered for car-body and guideways. The study offered a new maglev system with zero power control. This technique emphasized the advantages of high lift/weight ratio, the magnet analyzed, and system model was developed. The controller of this system was designed for PID control with disturbance generated from the guideway irregularities. The air gap was controlled by changing the levitation force in the EMS, (Wang and Yeou-Kuang T., 1994).

In 2006, a study conducted by De-Sheng, L., Jie, L. and Kun, Z. on the Double electromagnet low speed maglev train the design for nonlinear controller, with the main objective to reduce the coupling between the two Electro-Magnet sets of the maglev train, MIMO system model was developed. Based on the mathematical analysis of the mechanical and electrical components of the system, assumptions were adopted, and multivariable decoupling matrix was developed based on feed-back linearization. The state feed-back methodology implemented the design the nonlinear controller for the electromagnetic suspension EMS (De-Sheng et al., 2006).

Again, in 2006, another paper presented by Hyung-Woo L., Ki-Chan K. and Lee J., provide a review and summary of electromagnetic levitation systems, and the information about technology aspects. Also classified the maglev train based on the levitation methods, for example Electro-magnetic Suspension (EMS), and Electro-dynamic Suspension (EDS), and the Hybrid-Electro-magnetic Suspension (HEMS). comparisons a holding, lifting, guidance, and thrust are given. Between wheeled rail system and electromagnetic systems are discussed. This provides information about the linear motor and how it is created from

rotating motors. Also it discussed the universal Maglev Train developments (Hyung-Woo et al., 2006).

In 2007, research paper introduced by Zhiqiang, L., Song, X., Zhizhou, Z. and Yunde, X which presented a new strategy of control for suspension systems. The new control strategy depends on “active fault-tolerant control methods via control law reconfiguration”, it offers the design of separate current loops for each single electromagnets, and controller designed for each current loop by implementing optimal control techniques. The mathematical model developed for all mechanical and electrical system components of electromagnetic suspension system are included . Comparisons are made between the conventional suspension system and the new model (Zhiqiang et al., 2007).

In 2007, modeling and simulation of the high speed EMS train of Shanghai conducted by Shu G., Reinhold I., Shen G.. This work discussed modeling of the mechanical and electromagnets components for both horizontal and vertical movements in the car body of the. The strategy implemented for controller design was “Optimal Linear Quadratic for minimum control energy”. The mathematical model of single car body in vertical movement presented, and optimization of the EMS suspension system was investigated. The investigation showed realistic outcomes of track Irregularities avoided coupling between EMS and its guide-way. Also it provided sensible information on the optimized suspension limitations, and acceptable results of the dynamic behavior of the Maglev system, and in 2008, another paper published by same authors, on the similar work titled “Simulation of a Maglev Train with Periodic Guide-way Deflections” (Shu et al., 2008).

In 2011, two research papers introduced by Yongzhi J. Xiao J., and Zhang K., regarding modeling of the gap sensor for the high speed maglev train, the first paper presents modeling of the gap sensor by implementing RFB neural network, which is based on “radial basis

function”. This kind of sensor model can control the air gap within the desired limit with $\pm 0.3\text{mm}$, with in heat range of $20\text{ }^{\circ}\text{C}$ to 80°C . The results obtained indicated that the “Compensated gap signal” realized the maglev system requirements (Yongzhi et al., 2011).

The second paper introduced in the same year, presented modeling of gap sensor by another technique called “Fuzzy neural network FNN”. This technique shows the capability to indicate the gap with errors of $\pm 0.4\text{mm}$ in the same range of heat within $20\text{ }^{\circ}\text{C}$ to 80°C , The obtained results indicated that the “Compensated Gap Signal” in the line of EMS requirements.(Yongzhi et al., 2011).

Another research paper presented in 2012 by Ding ZhaoHong, introduced using of optimal control technique to design control system for maglev train. The paper presents the mathematical model of the single EMS unit of suspension system. A quadratic optimal performance index was created, and weight-matrixes Q and R were studied. Discussed system stability, controllability and observability was discussed. Optimal control technique used to design the controller for suspension system, and a feedback gain matrix was developed. The results shows good system performance and disturbance rejection. The position accuracy technology of high speed maglev train, the assembly and purpose and location of the sensors was introduced. In this research a discrete-time tracking differentiator (TD) was implemented, in line of nonlinear optimal control theory. The frequency characteristics of the TD are studied and analyzed thoroughly. And due to long stator, two sensors switching technique were used to remove errors caused by the joint gaps (ZhaoHong D., 2012).

In 2012, another research paper presented by Song X., Zhiqiang L., Guang H., Ning H., the overall purpose of this paper is to use Kalman filter group to diagnosis sensor faults of the electromagnetic levitation train. The paper went to consider the closed loop system

corresponding to open loop system by making the feedback signal as external inputs, and the feedback signals are linked into the Kalman filter group. And a fault detection system was used for maglev suspension control system, to identify the fault location based on remaining error signals of the Kalman filter. The results showed effective experimental results. (Song et al., 2012).

In 2013, paper introduced by Yun Li, Guang H., and Jie L. emphasize the fault detection technique, The general objective of the paper was “to develop a nonlinear robust fault observer for the fault detection of the networked suspension control system” (Yun et al., 2013). Simulation conducted with using the real parameters of low speed CMS-04 Maglev train. The results shows the efficiency of the used technique.

In 2013, a new technique of using magnetic flux feedback was implemented to achieve decoupling EMS suspension controller of a low speed maglev train- CMS04, multivariable system model of maglev system was developed, the magnetic flux was fed-back to the suspension controller, and a MIMO system feed-back on the CMS04 system model to investigate the decouple control system was investigated, Decoupling has been achieved and the controller was designed based on classical PID control technique, (Zhang et al., 2013).

In 2014 an research conducted by Guang He, Jie Li, and Peng Cui , on low speed EMS - CMS-04 maglev train. In order to investigate the coupling problem between the outputs of the levitation component, system transfer function was obtained and improved the adjoint matrix in order to obtain the decoupler. The controller designed by different control strategies to overcome the complicated coupling between the controls loops. The adopted methods were inverse Nyquist array INA, internal model control, inverse based decoupling control.

The model reduction method was adopted by previous researchers, due to the high order and complexity of controller. For the dynamic modeling of the system, the vertical and pitch motion were considered with few assumptions as stated by the researcher (He and Cui, 2015).

The assumptions are considered by the researcher in creation of mathematical model and design procedure, and clearly presented in chapter 3.

Chapter 3

Research Methodology

3.1. Maglev Train Mathematical Model

The system selected for this case study is the CMS-04 low speed electromagnetic suspension (EMS) Maglev Train, which is the same as that referred to by “Guang He, Jie Li, and Peng Cui” in their published paper.

The maglev Train was formed from vehicle, levitation bogies, secondary suspensions, guidance and levitation magnetics. Figure 3.1 shows side view of (CMS-04) maglev train, it can be seen there is five bogies to support the care body. Each bogie includes two levitation units, and each unit consists of two electromagnets which are controlled by a decartelized single input-single outputs (SISO) controller, so that there are four levitation units in each bogie.

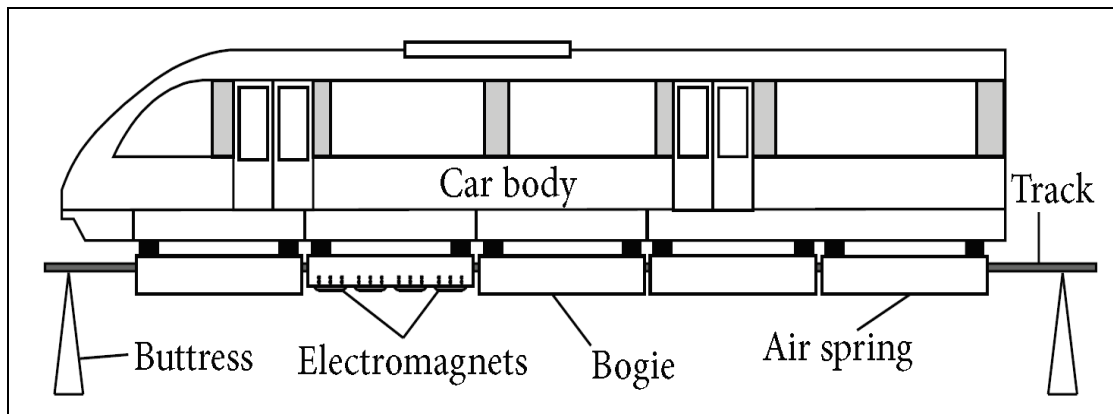


Figure 3.1, Lateral view of the CMS04 low speed maglev vehicle

(He and Cui, 2015)

The system is modeled as a single mass and a rigid guideway with an air gap which is the space (clearance) between the static guideway and the lifting magnets. This gap must be controlled within an allowable limit of about 10 mm.

The Control unit showed in the Figure 3.2, which consists of electromagnetics, a gap sensing system (sensors) and separate control system.

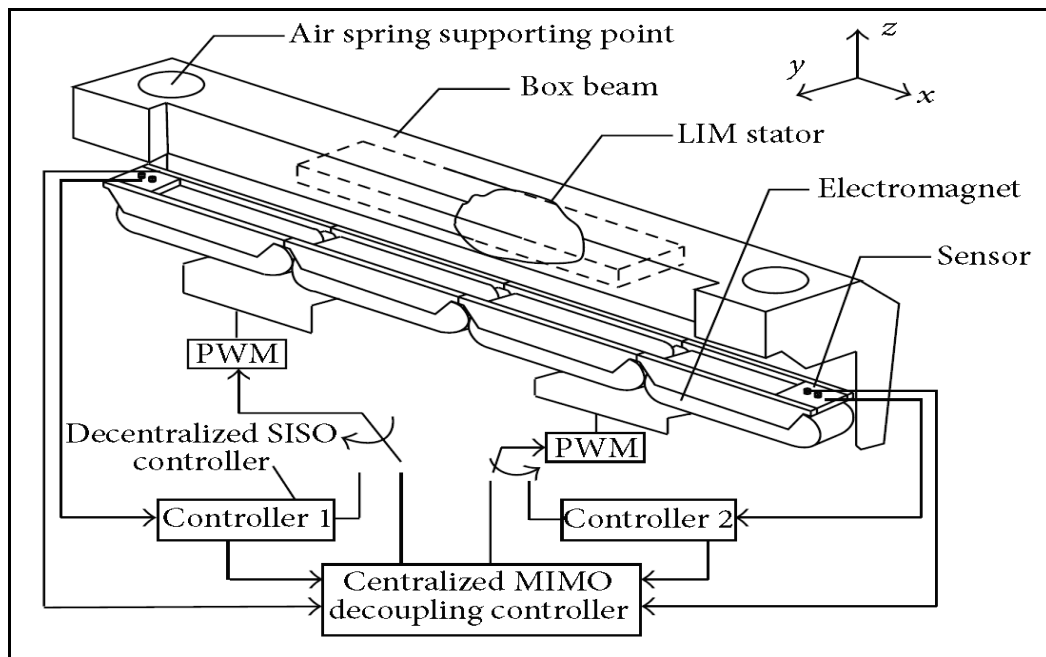


Figure 3.2, Diagram of the module suspension control system
(He and Cui, 2015)

There assumptions considered by the author during mathematically analysis of the system module, are the “The mass distribution of the levitation module is homogenous, and the gravity center of levitation module coincides with its geometrical center. The track is considered to be stiff, so the flexible distortion of the track can be neglected” (He and Cui, 2015). The second assumption is “The magnetic leakage and edge effect of the electromagnets are neglected. That is to say, the total magnetic potential during levitation is distributed evenly in the x direction” (He and Cui, 2015). And the third assumption was “The uniformly distributed electromagnet force can be equated with two concentrated forces acting on the center of levitation units in one levitation module. Essentially, the force transferred from the air spring is applied to the measuring point of the gap sensor in the y direction” (He, Li and Cui, 2015).

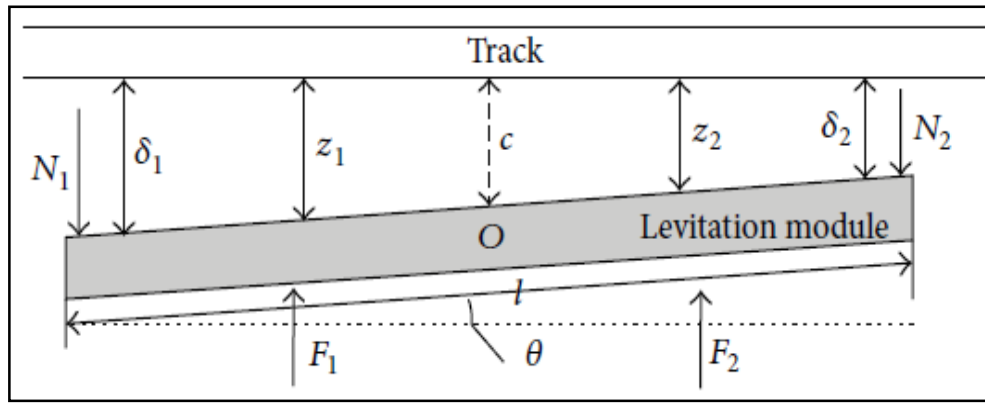


Figure 3.3, force analysis of one levitation unit in lateral
(He and Cui, 2015).

According to these assumptions, the force analysis are made as showed in the Figure 3.3, the forces diagram of the system module in lateral view with system parameters as seen in the diagram, F_1 and F_2 are forces of the electro-magnetic field at the lifting points, z_1 and z_2 are the distances between the guideway and the electromagnets of the lifting units, N_1 and N_2 are the reaction forces of the air spring against the lifting forces. δ_1 , δ_2 are the actual air gaps measured by the sensors at each end of the bogie, θ the angle of the carboy pitch with the horizontal, c the gap distance from the middle of the car body to the guideway, m the complete mass of the single levitated module (He and Cui, 2015).

The Analysis of module Geometric as made by (He and Cui, 2015) is :

$$\left\{ \begin{array}{l} c = \frac{(\delta_1 + \delta_2)}{2} \\ \theta = \frac{(\delta_1 - \delta_2)}{l} \\ z_1 = \frac{(3\delta_1 + \delta_2)}{4} \\ z_2 = \frac{(\delta_1 + 3\delta_2)}{4} \end{array} \right\} \quad (3.1)$$

It is clear from force diagram the motion in the vertical direction and rotation is around the center of gravity. By analysis the force diagram based on Newton's law, the equation of motion can be as following:

$$\left\{ \begin{array}{l} mg - F_1 - F_2 + N_1 + N_2 = m\ddot{c} \\ F_2 \frac{l}{4} \cdot \cos \theta - F_1 \frac{l}{4} \cdot \cos \theta + N_1 \frac{l}{4} \cdot \cos \theta - N_2 \frac{l}{4} \cdot \cos \theta = J\ddot{\theta} \end{array} \right\} \quad (3.2)$$

were J is the rotary inertia, of the system module,

$$F_1 = \frac{k_e I_1}{z_1}, \quad F_2 = \frac{k_e I_2}{z_2}, \quad k_e = \mu_0 N^2 A / 2, \quad I_1, I_2 \text{ are the currents on the coils of the}$$

electromagnets, N is the amount of turns of EM coil, A , is the area of levitation, and μ_0 is the vacuum coefficient, g is the gravity acceleration,

The electrical analysis of the system module can be explained by the following equations which relate the voltages and the currents,

$$\left\{ \begin{array}{l} u_1 = R_1 I_1 + \frac{2k_e}{z_1} I_1 - 2 \frac{k_e}{z_1^2} I_1 \dot{z}_1 \\ u_2 = R_2 I_2 + \frac{2k_e}{z_2} I_2 - 2 \frac{k_e}{z_2^2} I_2 \dot{z}_2 \end{array} \right\} \quad (3.3)$$

where u_1, u_2 are the voltage on the EM, R_1, R_2 are the resistances of the EM

Because of the electromagnetic levitation system is inherently unstable, so that the levitation system should be actively controlled. According to the previous assumptions, the system is considered stable, so that decoupling control technique create.

$$\left\{ \begin{array}{l} I_{e1} = k_p(\delta_1 - r_d - \delta_0) + k_d \dot{\delta}_1 \\ I_{e2} = k_p(\delta_2 - r_d - \delta_0) + k_d \dot{\delta}_2 \end{array} \right\} \quad (3.4)$$

where I_{e1}, I_{e2} are the desired currents, k_p, k_d are the proportional and derivative coefficients, δ_0 the required levitation gap, and I_{e1}, I_{e2} are the reference currents,

$$\left\{ \begin{array}{l} I_{10} = \sqrt{\frac{(mg + 1N_1 - N_2)z_0^2}{\mu_0 N^2 A}} \\ I_{20} = \sqrt{\frac{(mg + 1N_2 - N_1)z_0^2}{\mu_0 N^2 A}} \end{array} \right\} \quad (3.5)$$

The system module has been linearized, by considering $\cos \theta = 1$ because of small pitch angle,

Hence:

$$\left\{ \begin{array}{l} -2(F_1 + F_2) = m_1(\ddot{\delta}_1 + \ddot{\delta}_2) \\ \left(\frac{1}{4} F_1 - \frac{1}{4} F_2\right) l^2 = J(\ddot{\delta}_1 - \ddot{\delta}_2) \\ \dot{I}_i = \frac{z_{0i}}{2k_e} u_i - \frac{\bar{R}z_{0i}}{2k_e} I_i + \frac{I_{0i}}{z_{0i}} \dot{z}_i \\ F_i = F_z z_i - F_l I_i \\ u_i = k_p k_c (\delta_i - r_d) + k_d k_c \dot{\delta}_i \end{array} \right. \quad (3.6)$$

Where $\bar{R} = R + k_c$, $F_{li} = 2k_e I_{0i} / \delta_0^2$, and $F_{zi} = 2k_e I_{0i}^2 / \delta_0^3$

By applying Laplace transformation, the transfer function $G(s)$ with SISO control system can be expressed as follows

$$G = G_0(I + G_0)^{-1} \quad (3.7)$$

$$\text{and } G_0 = G_1 G_2 G_5 G_6 + G_1 G_2 G_4 + G_1 G_3, \quad (3.8)$$

G can be found by using the actual parameters of the low speed maglev train CMS04, Due to the complicated transfer function of the system, the author suggests the use of $G_0(s)$ as an alternative (according to system parameters) the final $G_0(s)$ is :

$$\begin{bmatrix} F_1(s) \\ F_2(s) \end{bmatrix} = \begin{bmatrix} \frac{68271.3(s + 40.15)}{s^2(s + 1135)} & \frac{553.29(s - 3285)}{s^2(s + 1135)} \\ \frac{553.29(s - 3285)}{s^2(s + 1135)} & \frac{68271.3(s + 40.15)}{s^2(s + 1135)} \end{bmatrix} \begin{bmatrix} \delta_1(s) \\ \delta_2(s) \end{bmatrix} \quad (3.9)$$

The equation (3.9) represents the open loop system, Figure 3.4 shows the block diagram representation of the general open loop system.

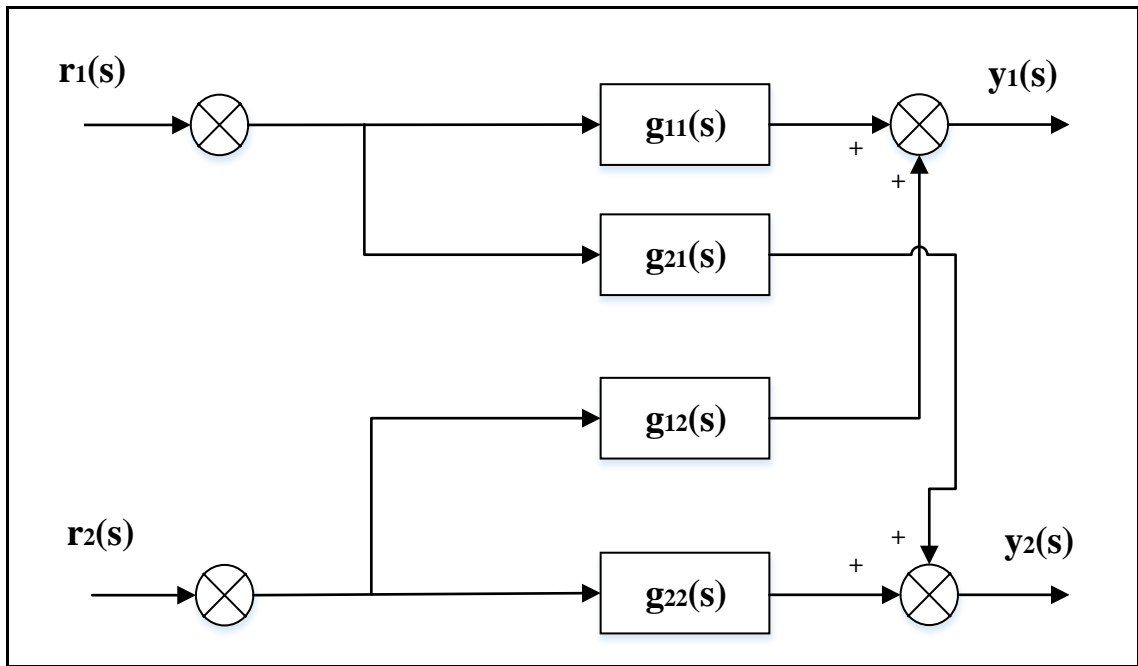


Figure 3.4, Block Diagram Representation of the general Open Loop System

3.2. Open Loop Response and Control Objective

The open loop transfer function has been identified as in the equation, in this section a direct implementation and simulation of system model. The system structure explained in the system block diagram for open loop system prior adding filters. This can be seen in Appendix A.

Direct simulation is employed on the open loop system model. A unit step is applied to the first input reference $r_1(s)$, the system response on the first output shows ramp air gap, while the second output shows declining air gap value to the negative.

In the other hand, when applying unit step on the second input reference $r_2(s)$, the output results are same as in the first input but of opposite direction, as shown in the figure 3.5 & figure 3.6 respectively.

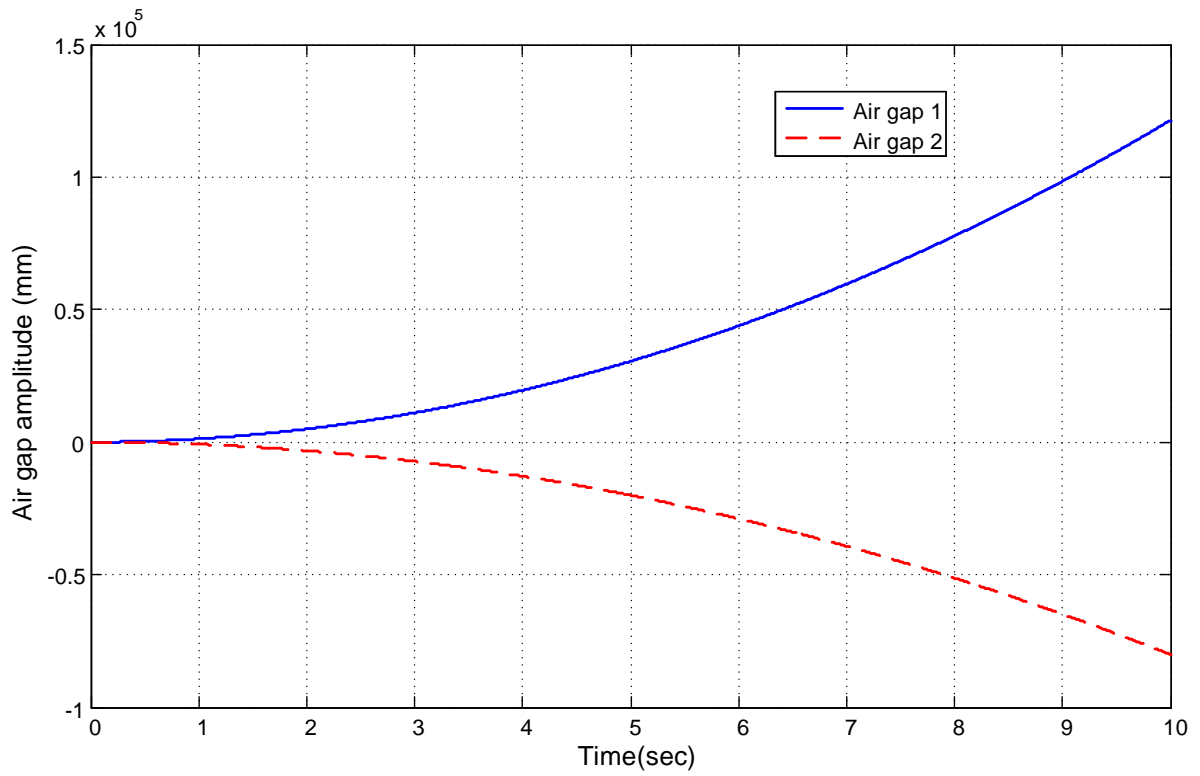


Figure 3.5, System responses following step change on $r_1(s)$, and $r_2(s) = 0$

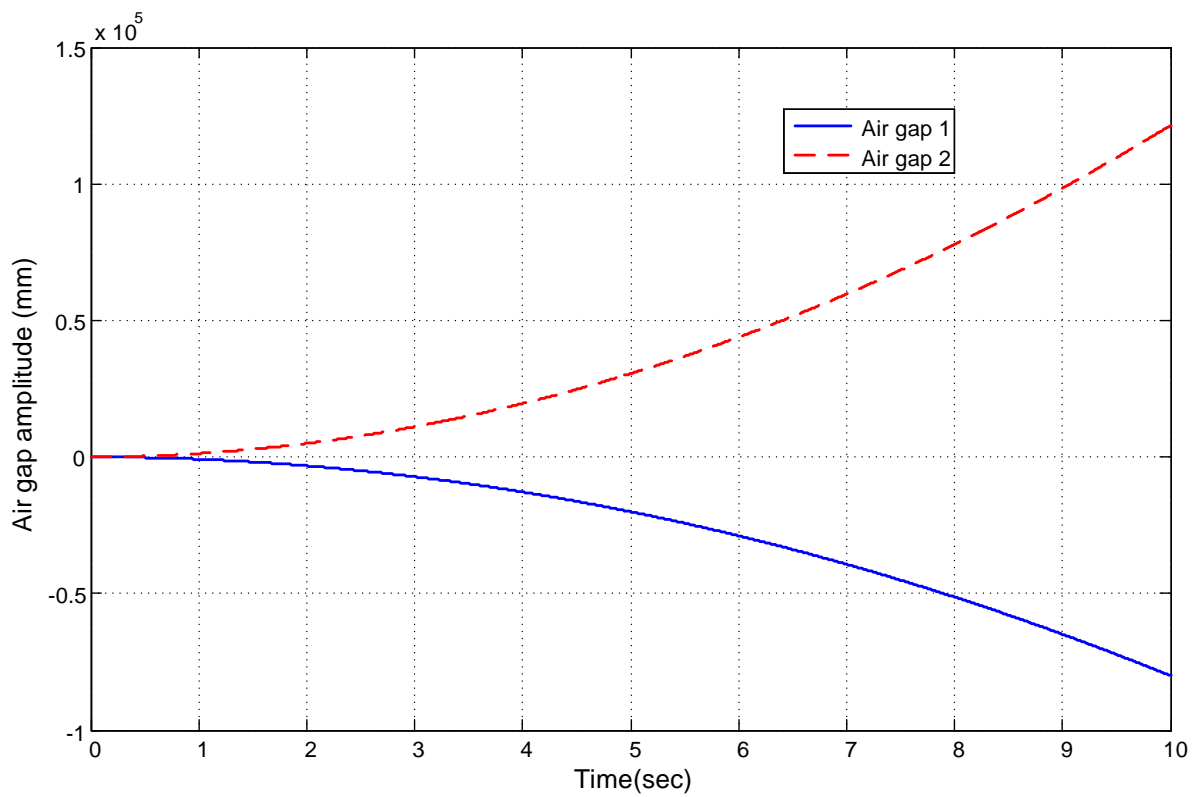


Figure 3.6, System responses following step change on $r_2(s)$, and $r_1(s) = 0$

These results are to be expected owing to of the effect of double integrator in the system transfer function. the stability of the whole system is compensated. Therefor compensators is required, by adding two filters on each input branch of the open loop system model, to eliminate the influence of the integrators. Also to meet application requirements of control strategies which were implemented in this research, such as the Least Effort techniques and the classical control methodologies, the proposed filters shown in the compensated transfer function given by equation (3.10), and the related block diagram representation explained in figure 3.7.

$$G(s) = \begin{bmatrix} \frac{68271.3s+2,741,092.695}{s^3+1135s} & \frac{553.29s-1,817,557.65}{s^3+1135s} \\ \frac{553.29s-1,817,557.65}{s^3+1135s} & \frac{68271.3s+2,741,092.695}{s^3+1135s} \end{bmatrix} \begin{bmatrix} \frac{s}{(s+10)} & 0 \\ 0 & \frac{s}{(s+10)} \end{bmatrix} \begin{bmatrix} \frac{s}{(s+100)} & 0 \\ 0 & \frac{s}{(s+100)} \end{bmatrix} \quad (3.10)$$

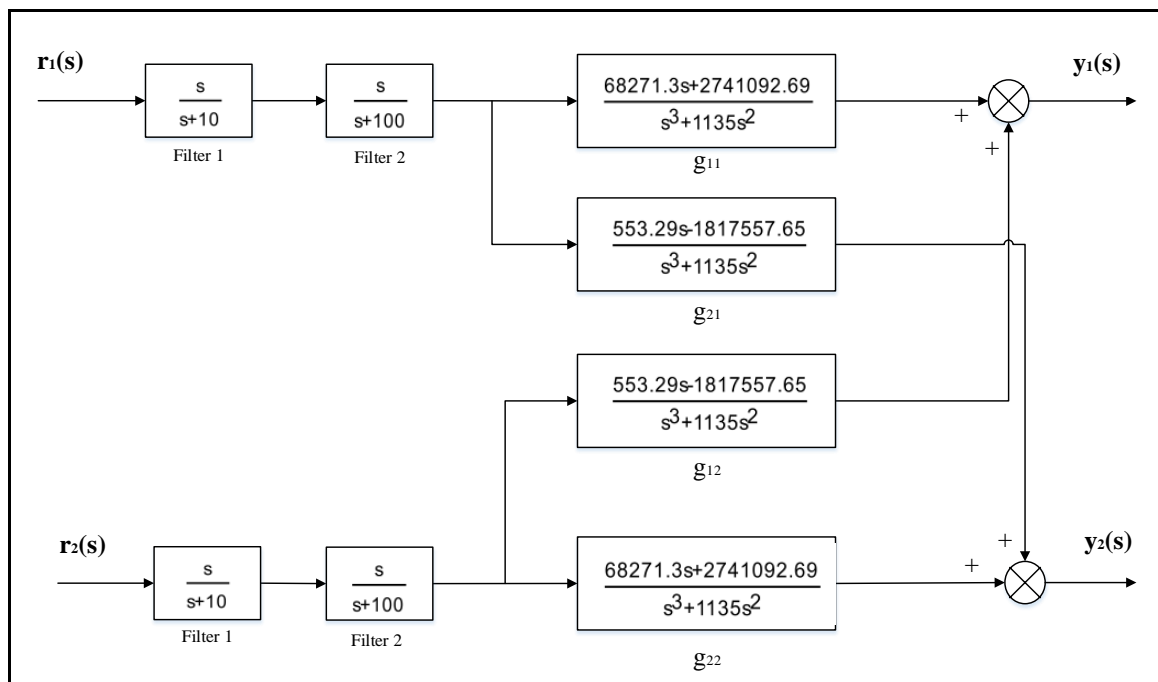


Figure 3.7, Block Diagram Representation for Open Loop System Includes the Filters

The open loop system block diagram of equation (3.10) shown Figure 3.7, the model simulated following a unit step on each input reference, the results as in the Figure 3.8 , & Figure 3.9, it can be seen from these figures that the system performance improves and the

effect of the integrators has been eliminated. For unit step change on the reference $r_1(s)$, the first output which represent air gap 1 was overdamped with settling time about 0.75sec. With steady state amplitude of 2.4 times higher than the reference, while the second output was overdamped as well, with negative value for the air gap about -1.52 times less the reference set point, which is not acceptable for train operation conditions.

The negative value means a physical contact between the car-body of the maglev train and the guideway,

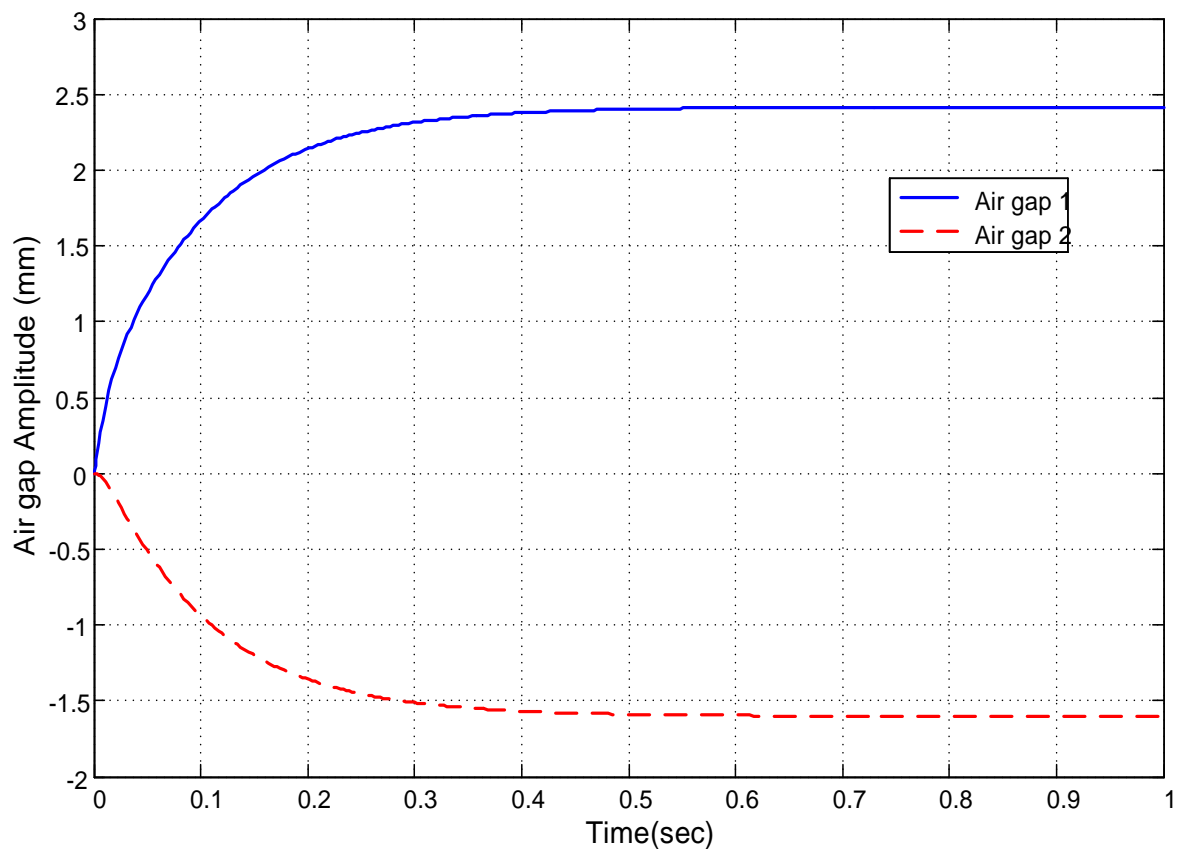


Figure 3.8, Open loop response following step change at magnetically lifting force $r_1(s)$

In the next, applying unit step change on the second system input $r_2(s)$, the responses shown in the figure 3.9, clearly the results are similar to these following $r_1(s)$, but in opposite directions, i.e. the first output goes to the same negative amplitude of (-1.52) , and same

settling time and steady state value of the 2nd output of $\mathbf{r}_1(s)$, again it is not realistic since the system operation conditions not accept zero or negative air gap value.

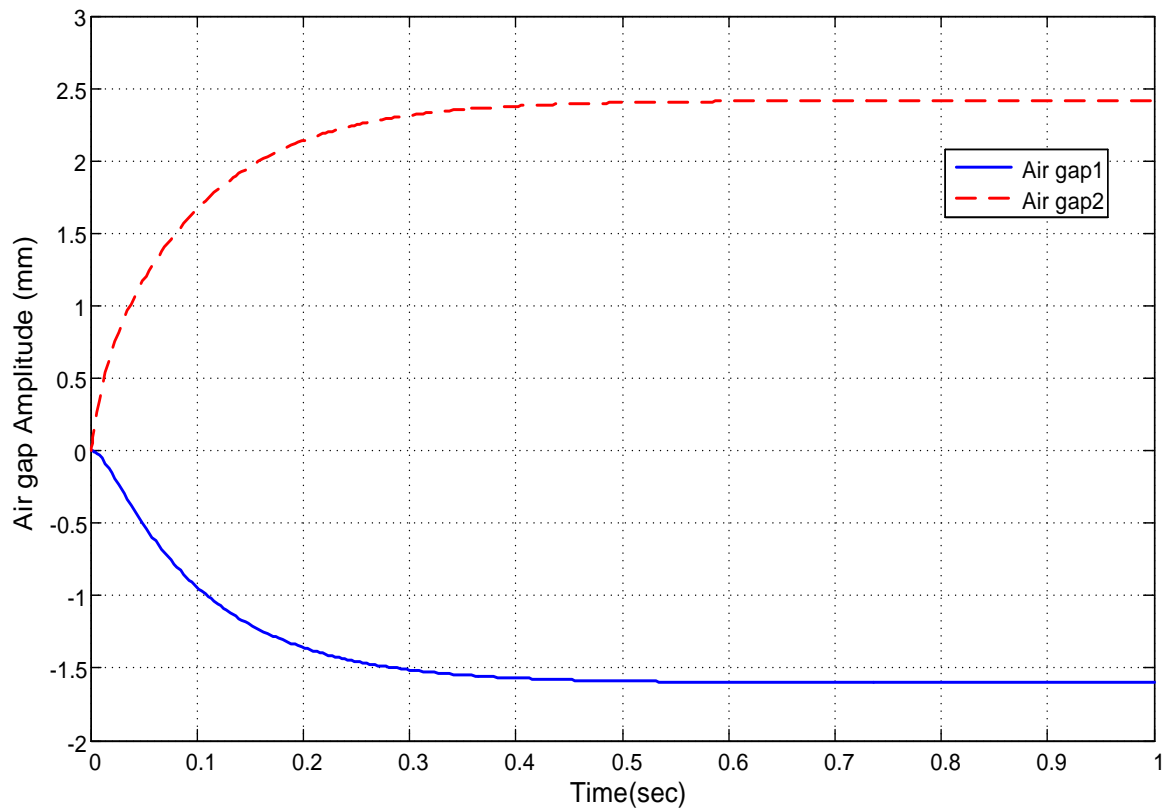


Figure 3.9, Open loop response following step change at magnetically lifting force $\mathbf{r}_2(s)$

The seconded output of $\mathbf{r}_2(s)$, show the same amplitude, and settling time and steady state of $\mathbf{r}_1(s)$ which also haggier than the required reference value. Based on the results obtained above, a suitable controller is required to be designed to bring system output response to the designed conditions. This is detailed in the controller design.

3.3. Least Effort Control Methodology

The least Effort regulation technique was introduced by Whalley R., and Ebrahimi M., in 2006. The main steps of this procedure are a closed loop depending on an inner and outer loop control strategy. The optimization, disturbance rejection analysis and stability of the whole

system, is determined by this technique to achieve performance and disturbance rejection characteristics. It also results in a simple controller than presented by classical control methods, Which minimizes a performance index J . The inner-loop analysis was calculated, to demonstrate system performance and to guarantee satisfactory dynamical response. Thereafter, a formal design stage, can cover the external-loop construction to achieve robustness requirements with acceptable disturbances suppression (Whalley and Ebrahimi, 2006). According to the design procedure introduced by the authors, the transformed open loop system equation :

$$\mathbf{y}(s) = \mathbf{G}(s)\mathbf{u}(s) + \boldsymbol{\delta}(s) \quad (3.11)$$

The control law for the proposed feedback is;

$$\mathbf{u}(s) = \mathbf{k}(s)[(\bar{\mathbf{r}}(s) - \mathbf{h}(s))\mathbf{y}(s)] + \mathbf{P}(\mathbf{r}(s) - \mathbf{F}\mathbf{y}(s)) \quad (3.12)$$

where in equation (3.11) & (3.12) there are m independent inputs, disturbance and outputs and

$$\mathbf{F} = \text{diag}(f_1, f_2, \dots, f_m), \quad 0 < f_j < 1, 1 \leq j \leq m$$

Since the inner loop controller is: $\mathbf{k}(s)[(\bar{\mathbf{r}}(s) - \mathbf{h}(s))\mathbf{y}(s)]$

This will be used to satisfy the specified dynamic behavior of the same closed loop system with the feedback law

$$\mathbf{P}(\mathbf{r}(s) - \mathbf{F}\mathbf{y}(s))$$

With $\bar{\mathbf{r}}(0) = 0$ the closed-loop equation for the complete system becomes:

$$\mathbf{y}(s) = (\mathbf{I}_m + \mathbf{G}(s)\mathbf{k}(s) >< \mathbf{h}(s) + \mathbf{P}\mathbf{F})^{-1} \times (\mathbf{G}(s)\mathbf{P}\bar{\mathbf{r}}(s) + \boldsymbol{\delta}(s)) \quad (3.13)$$

If a steady state matrix \mathbf{S}_s is now selected such that

$$\mathbf{y}(0) = \mathbf{S}_s\mathbf{r}(0)$$

then from equation (3.13) with $\mathbf{S}_s = \mathbf{I}$

$$\mathbf{P} = \{\mathbf{G}^{-1}(\mathbf{0}) + \mathbf{k}(0) \succ \mathbf{h}(0)\} \mathbf{S}_s (\mathbf{I} - \mathbf{F} \mathbf{S}_s)^{-1} \quad (3.14)$$

Consequently specifying steady state, closed loop non interaction ($S_s = I$) and substituting for P from equations (3.14) results in equation (3.13) becoming:

$$\begin{aligned} \mathbf{y}(s) = & \left\{ (\mathbf{I}_m + \mathbf{G}(s) [\mathbf{k}(s) \succ \mathbf{h}(s) + \mathbf{G}^{-1}(\mathbf{0}) + \mathbf{k}(s) \succ \mathbf{h}(s)]) (\mathbf{I}_m - \mathbf{F}) \mathbf{F}^{-1} \mathbf{F} \right\} \\ & \times \{ \mathbf{G}(s) \mathbf{P} \bar{\mathbf{r}}(s) + \boldsymbol{\delta}(s) \} \end{aligned} \quad (3.15)$$

At low frequencies, equation (3.15) becomes:

$$\mathbf{G}(s) \mathbf{P} \cong \frac{1}{1-f} (\mathbf{I}_m + \mathbf{G}(s) \mathbf{k}(0) \succ \mathbf{h}(0))$$

Consequently equation (3.15), on approaching steady state conditions becomes

$$\mathbf{y}(s) = \mathbf{I}_m \mathbf{r}(s) + \mathbf{S}_s(s) \boldsymbol{\delta}(s) \quad (3.16)$$

where the low frequency sensitivity matrix is

$$\mathbf{S}(s) = (1 - f) (\mathbf{I}_m + \mathbf{G}(s) \mathbf{k}(s) \succ \mathbf{h}(s))^{-1}, \quad 0 < f < 1.0$$

Evidently, from equation (3.16), steady state non interaction following reference input changes will be achieved. Moreover, as f is increased $0 < f < 1$, there will be increasing steady state disturbance rejection, provided stability can be maintained. For implementation purposes, a conventional multivariable regulator structures comprising a forward path $\mathbf{K}(s)$ and feedback path compensator $\mathbf{H}(s)$ are required, and these can be easily computed from the closed loop equation:

$$\mathbf{y}(s) = (\mathbf{I}_m + \mathbf{G}(s) \mathbf{K}(s) \mathbf{H}(s))^{-1} [(\mathbf{G}(s) \mathbf{P} \bar{\mathbf{r}}(s) + \boldsymbol{\delta}(s))] \quad (3.17)$$

On comparing (3.13) and (3.17), evidently

$$\mathbf{K}(s) = \mathbf{P} \quad (3.18)$$

And

$$\mathbf{K}(s)\mathbf{H}(s) = \mathbf{k}(s) \gg \mathbf{h}(s) + \mathbf{P}\mathbf{F}$$

Hence

$$\mathbf{H}(s) = \mathbf{P}^{-1}\mathbf{k}(s) \gg \mathbf{h}(s) + \mathbf{F} \quad (3.19)$$

Enabling the employment of established feedback structures

3.3.1. Inner-loop Design

The open loop system $\mathbf{G}(s)$ is assumed to be $m \times m$ linear, regular proper, or strictly proper realization, which admits a factorization

$$\mathbf{G}(s) = \mathbf{L}(s) \frac{\mathbf{A}(s)}{d(s)} \mathbf{R}(s) \mathbf{\Gamma}(s) \quad (3.20)$$

where $\mathbf{L}(s)$, $\mathbf{R}(s)$, $\mathbf{\Gamma}(s)$ and the element of $\frac{\mathbf{A}(s)}{d(s)} \in H^\infty$, $s \in \mathbb{C}$

In equation (3.20), $\mathbf{L}(s)$ contains the left (row) factors of $\mathbf{G}(s)$, while $\mathbf{R}(s)$ contains the right (column) factors, and $\mathbf{\Gamma}(s)$ contains the transformed, actuator finite time delay of $\mathbf{G}(s)$, such that be $m \times m$ matrices comprising (3.20) are:

$$\mathbf{L}(s) = \text{Diag. } (\lambda_j(s)/p_j(s))$$

$$\mathbf{R}(s) = \text{Diag. } p_j(s)/q_j(s)$$

$$\mathbf{\Gamma}(s) = \text{Diag. } (e^{-st_j}), 1 \leq j \leq m$$

and $\mathbf{A}(s)$ is nonsingular matrix, so that $\det \mathbf{A}(s) \neq 0$ with elements

$$a_{ij}s^{m-1} + b_{ij}s^{m-2} + \dots + \gamma_{ij} \quad 1 \leq i, j \leq m \quad (3.21)$$

As the transformed input-output-disturbance relationship is

$$\mathbf{y}(s) = \mathbf{G}(s)\mathbf{u}(s) + \boldsymbol{\delta}(s) \quad (3.22)$$

and if the inner control law for the internal-loop is

$$\mathbf{u}(s) = \mathbf{k}(\bar{\mathbf{r}}(s) - \mathbf{h}(s))\mathbf{y}(s) \quad (3.23)$$

Then merging equations (3.22) and (3.23) produces:

$$\mathbf{y}(s) = [\mathbf{I}_m + \mathbf{G}(s)\mathbf{k}(s) \gg \mathbf{h}(s)]^{-1} \gg \{\mathbf{G}(s)\mathbf{k}(s)\bar{\mathbf{r}}(s) + \boldsymbol{\delta}(s)\} \quad (3.24)$$

Any finite time delay in $\mathbf{L}(s)$ may be ordered with $T \geq T_j, 1 \leq j \leq m, i \neq j$, so that the forward path gain vector can be arranged as:

$$\mathbf{K}(s) = [k_1(s)e^{-s(T_i-T_1)}, k_2e^{-s(T_i-T_2)}, \dots, k_1(s), \dots, k_m e^{-s(T_i-T_m)}]^T \quad (3.25)$$

$$\text{Since } \mathbf{h}(s) = (\mathbf{h}_1(s), \mathbf{h}_2(s), \dots, \mathbf{h}_m(s)) \quad (3.26)$$

and if $k_j(s) = k_j\phi_j(s)$ and $h_j(s) = h_jx_{j(s)} \quad 1 \leq j \leq m$

where $\phi_j(s)$ and $x_{j(s)}$ are proper or strictly proper, stable, Realizable, minimum phase functions, then they may be selected such that (3.24) becomes:

$$\mathbf{y}(s) = (\mathbf{I}_m + e^{-sT_i}n(s)\mathbf{L}(s)\frac{\mathbf{A}(s)}{d(s)}\mathbf{k}(s) \gg \mathbf{h}(s))^{-1} \times (n(s)\mathbf{L}(s)\frac{\mathbf{A}(s)}{d(s)}ke^{-sT_i}\mathbf{r}(s) + \boldsymbol{\delta}(s)) \quad (3.26)$$

where

$$\mathbf{k} = (k_1, k_2, \dots, k_m)^T \quad (3.27)$$

and

$$\mathbf{h} = (h_1, h_2, \dots, h_m) \quad (3.28)$$

and $\det n(s)a_{ij}(s) < k \quad 1 \leq i, j \leq m$

The determinant required in equation (3.26) is

$$\det \left[\mathbf{I}_m + e^{-sT_i} n(s) L(s) \frac{A(s)}{d(s)} \mathbf{k}(s) \right] = 1 + e^{-sT_i} n(s) \mathbf{k}(s) \left\langle \frac{A(s)}{d(s)} \right\rangle \mathbf{h}(s) \quad (3.29)$$

The inner product in equation (3.29) could be expressed as

$$\langle \mathbf{h} A(s) \mathbf{k} \rangle = [1, s, \dots, s^{m-1}] \begin{bmatrix} \gamma_{11} & \gamma_{12} & \cdots & \gamma_{mm} \\ \vdots & \vdots & & \vdots \\ b_{11} & b_{12} & \cdots & b_{mm} \\ a_{11} & a_{12} & \cdots & a_{mm} \end{bmatrix} \times \begin{bmatrix} k_1 h_1 \\ k_2 h_1 \\ \vdots \\ k_m h_m \end{bmatrix} \quad (3.30)$$

If the gain ratio, in equation (3.30) are

$$k_2 = n_1 k_1, k_3 = n_2 k_1, \dots, k_m = n_{m-1} k_1 \quad (3.31)$$

$$\text{And } \langle \mathbf{h} A(s) \mathbf{k} \rangle = b(s) \quad (3.32)$$

Then the equation (3.32) implies that

$$k_1 [\mathbf{Q}] \mathbf{h} = (b_{m-1}, b_{m-2}, \dots, b_0)^T \quad (3.33)$$

where \mathbf{Q} matrix details as following:

$$[\mathbf{Q}] = \begin{bmatrix} \gamma_{11} + \gamma_{12} n_1 + \cdots + \gamma_{1m} n_{m-1} & \vdots & \gamma_{21} + \gamma_{22} n_1 + \cdots + \gamma_{2m} n_{m-1} & \vdots & \cdots & \gamma_{m1} + \gamma_{m2} n_1 + \cdots + \gamma_{mm} n_{m-1} \\ b_{11} + b_{12} n_1 + \cdots + b_{1m} n_{m-1} & \vdots & b_{21} + b_{22} n_1 + \cdots + b_{2m} n_{m-1} & \vdots & \cdots & b_{m1} + b_{m2} n_1 + \cdots + b_{mm} n_{m-1} \\ a_{11} + a_{12} n_1 + \cdots + a_{1m} n_{m-1} & \vdots & a_{21} + a_{22} n_1 + \cdots + a_{2m} n_{m-1} & \vdots & \cdots & a_{m1} + a_{m2} n_1 + \cdots + a_{mm} n_{m-1} \end{bmatrix} \quad (3.34)$$

Then, b_j representing the coefficient of $b(s)$, and $0 < j < m$, the value of j could be selected in the equation (3.32) as n_1, n_2, \dots, n_{m-1} for equation (3.34), so that a unique solution for $(h_1, h_2, \dots, h_m) k_1$ exists.

With selecting appropriate $b(s)$ function, and the gain ratio, n_1, n_2, \dots, n_{m-1} , the closed loop dynamics arising from the equation (3.30) would be fully defined. By solving the equation (3.33), the measurements vector \mathbf{h} can be found the selection of an arbitrary value for K_1 .

3.3.2. Optimization

To detect the absolute minimum control effort required under closed loop conditions with arbitrary disturbances entering the system, a performance index representing the energy dissipation should be defined. The control effort at time t is proportional to

$$(|k_1 h_1| + |k_2 h_2| \dots + |k_m h_1|)|y_1(t) + (|k_1 h_2| + \dots + |k_m h_2|)|y_2(t)| + \dots + (|k_1 h_m| + |k_2 h_m| = \dots + |k_m h_m|)|y_m(t)|$$

Hence, the control energy cost under these conditions are proportional to

$$E(t) = \int_0^{t=T} (\sum_{j=1}^n k_j^2 \sum_k^n h_k^2) y_k^2 d(t) \quad (3.35)$$

Then for arbitrary changes in the transformed output vector $y(t)$, following arbitrary disturbance changes

$$J = \sum_{j=1}^n k_j^2 \sum_k^n h_j^2 \quad (3.36)$$

would minimize the control energy required, given by expression (3.35).

If the relationships $k_2 = n_1 k_1$, $k_3 = n_2 k_1$,, $k_m = n_{m-1} k_1$ Are adopted, then the equation (3.36) can be written as

$$J = (k_1^2)(1 + n_1^2 + n_2^2 + \dots + n_{m-1}^2) \times (h_1^2 + h_2^2 + \dots + h_m^2) \quad (3.37)$$

and $h_1^2 + h_2^2 + \dots + h_m^2 < h, h >$. The closed loop determinant is given by the equation

(3.29) with the inner product equated to $b(s)$, as in equation (3.32) then from equation (3.33)

$$\mathbf{h} = \mathbf{k}_1^{-1} \mathbf{Q}^{-1} \mathbf{b} \quad (3.38)$$

Upon substituting for h from equation (3.38), equation (3.37) becomes

$$J = (1 + n_1^2 + n_2^2 + \dots + n_{m-1}^2) \mathbf{b}^T (\mathbf{Q}^{-1})^T \mathbf{Q}^{-1} \mathbf{b} \quad (3.39)$$

To find the minimum value for J, assuming for example, that $m=3$ gives

$$J = (1 + n_1^2 + n_2^2) \mathbf{b}^T (\mathbf{Q}^{-1})^T \mathbf{Q}^{-1} \mathbf{b}$$

3.3.3. Disturbance rejection

The employment of the minimum control effort would not in general achieve the required disturbance recovery conditions. To provide this the outer loop feedback gain f should be increased $0 < f < 1.0$ as indicated by the equation (3.16) (Whalley and Ebrahimi, 2006).

3.3.4. Stability of control system

The input output condition stability is dependent on the denominator of equation (3.15) which provides the input-output relationship for the closed loop system. The outer loop feedback gain matrix F is given by

$$\mathbf{F} = \text{diag}(f_1, f_2, \dots, f_m), \text{ and if } f_1, f_2, \dots, f_m = f$$

$$\text{Then } F = \text{Diag}(f), \quad 0 < f < 1.0$$

Then the denominator of the equation (8) can be calculated by

$$\det \{ \mathbf{I}_m + \mathbf{G}(s) \left[\frac{k(s) \gg h(s)}{1-f} + \frac{\mathbf{G}(0)^{-1}}{1-f} \right] \}$$

From this expression, it is clear that the elements of the feedback-compensator matrix

$\left[\frac{k(s) \gg h(s)}{1-f} + \frac{\mathbf{G}(0)^{-1}}{1-f} \right]$ become infinite as $f \rightarrow 1$. Practically this would always result in closed-loop system instability, so that $0 < f < 1$ is mandatory.

3.4. The Inverse Nyquist Array (INA) Method

The inverse Nyquist Array (INA) method is a famous British multivariable system control philosophy introduced by Rosenbrock H. (1969, 1974), The INA is a representation of non-eigenvalue approach depending on the input output relationship. It is a direct link between the

classical design strategy of single input-single output (SISO) frequency domain control, and multi-input multi-output (MIMO) control theory. The Nyquist array for the MIMO systems, depends on the capability of the designer to achieve diagonal dominance of the open loop system transfer function model, before going to closed loop system examination, Diagonal dominance of the transfer function should be investigated, so that the Multivariable Nyquist Array ensures closed loop system stability.

Some systems may require dynamic compensators for the feed-back controller. There were several techniques to obtain dominance, such as (Rosenbrock, 1974; Schafer and Sain, 1977), utilizing computer programs developed to present graphs to understand the system behavior avoiding theory and trial and error approaches. A summary of the mathematical foundation and design will be discussed. The main objective of this approach is to reduce output interaction, so that a diagonally dominant closed loop transfer function is achieved.

For multivariable systems (plant), it is assumed an $m \times m$ transfer function matrix $\mathbf{G}(s)$, representation is achieved and that this transfer function is controlled by interfering a compensator $\mathbf{K}(s)$ and through closing m feedback loop.

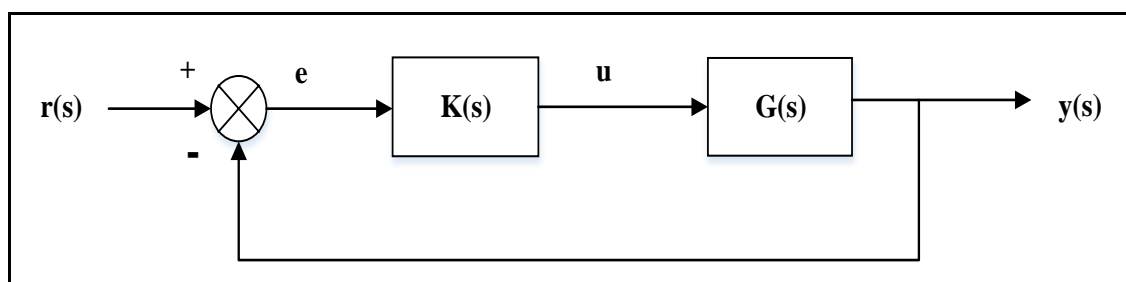


Figure 3.10, Common Representation of Multivariable control system

The open loop transfer function matrix $\mathbf{Q}(s) = \mathbf{G}(s)\mathbf{K}(s)$, Figure 3.10 shows the general form of a multivariable control system. $\mathbf{Q}(s)$ should be diagonally dominant with an appropriate selection of $\mathbf{K}(s)$ (matrix).

There are some assumptions that should be fulfilled prior to applying the INA method. Firstly, both transfer function and its compensator to be in the frequency domain. Secondly, both have to be invertible representations. Third is the important condition that the controller elements should open loop stable (all zeros and poles are in the open left half of S plan), and should satisfy diagonal dominant with minimum system output coupling. In this case the design of pre compensator for diagonally dominance can be avoided.

The diagonal dominant is also could be satisfied by plotting Gershgorin circles, As shown in Figure 3.13, ensuring none encircle the origin, and this investigation technique will be implemented in this research.

The open loop transfer function matrix is

$$\mathbf{Q}(s) = \mathbf{G}(s)\mathbf{K}(s) \quad (3.40)$$

The symbolization of the matrices inverses could be donated by

$$\mathbf{G}^{-1} = \hat{\mathbf{G}}, \quad \mathbf{k}^{-1} = \hat{\mathbf{k}}, \quad \mathbf{Q}^{-1} = \hat{\mathbf{Q}}$$

$$\text{Then, the inverse transfer function is } \hat{\mathbf{Q}}(s) = \hat{\mathbf{K}}(s)\hat{\mathbf{G}}(s) \quad (3.41)$$

And the components of inverted matrices could be offered as $q_{ij}(s)$, $\hat{q}_{ij}(s)$.

Generally, from Figure 3.10:

$$\mathbf{y} = \mathbf{G}(s)\mathbf{K}(s)\mathbf{e}(s) = \mathbf{Q}(s)(\mathbf{r}(s) - \mathbf{y}(s)) \quad (3.42)$$

Then the closed loop transfer function matrix (CLTFM) in relation of $\mathbf{y}(s)$ and $\mathbf{r}(s)$ would be

$$\mathbf{H}(s) = [\mathbf{I}_m + \mathbf{Q}(s)]^{-1}\mathbf{Q}(s) \quad (3.43)$$

$$\text{and } \hat{\mathbf{H}}(s) = \mathbf{H}(s)^{-1} = \mathbf{I}_m + \hat{\mathbf{Q}}(s) \quad (3.44)$$

For the design, a diagonal matrix of feedback gains F , to replace the basic (negative unity feedback loops). (Dutton), all of its components are zeros, excluding principal diagonal to be ones for each closed feedback path (Rosenbrock), it is could be expressed as $F = \text{diag}(f_1, f_2, f_3 \dots \dots \dots, f_n)$,

The new structure of the controller for INA methodology is shown in Figure 3.11,

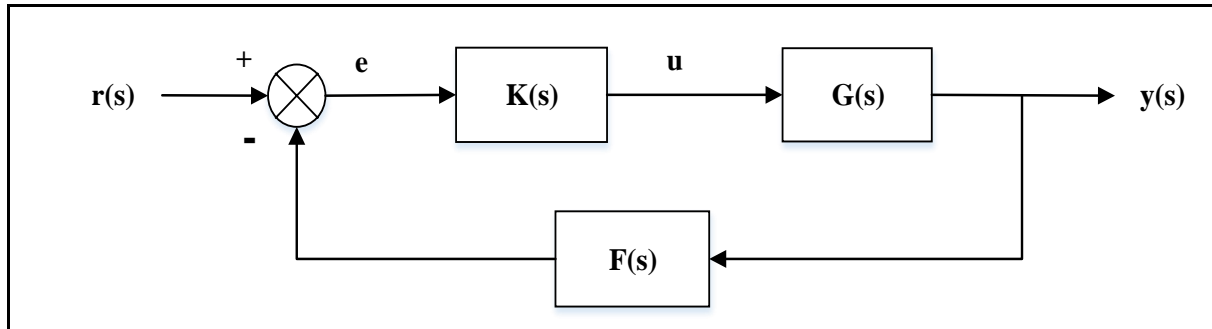


Figure 3.11, General Form of Multivariable Closed Loop Transfer Function With feedback

Hence, from the block diagram representation, the new expression relates $y(s)$ and $r(s)$ come to be

$$y(s) = [I_m + Q(s)F]^{-1}Q(s)r(s) \quad (3.45)$$

Then

$$R(s) = [I_m + Q(s)F]^{-1}Q(s) \quad (3.46)$$

With the suitable selection matrix of $K(s)$, \hat{Q} can be completed , then, by inverting the equation (3.46) results:

$$\hat{R}(s) = \hat{Q}[I_m + Q(s)F] = \hat{Q} + F \quad (3.47)$$

when $F = 0$, $\hat{R} = \hat{Q}$ while $F = I_m$, $\hat{R} = \hat{H}$

$$\text{then } \hat{H}(s) = \hat{Q}(s) + F \quad (3.48)$$

3.4.1. Diagonally Dominance

The fundamental of the INA methodology is to keep the transfer function matrix $\mathbf{Q}(s)$ ‘approximately diagonal’ for all frequencies. After that, classical design using SISO could be implemented. It was observed that there are restrictions on make the matrix $\mathbf{Q}(s)$ diagonal, such as (very complicated compensators, mathematical problems) and additional unwanted consequences (for example unstable compensators). Thus INA methodology changed this requirements with the simpler concept, that $\mathbf{Q}(s)$, should be (diagonally dominant) for all related frequencies. Once this conditions is realized, compensator for SISO will be created to satisfy the system requirements. (Dutton et al. , 1997).

“(Several methods were suggested to systematically approach diagonal dominance. For example, (Hawkins, 1972), developed Pseudo-Diagonalisation method, (Mees, 1981) developed scaling matrix, and the technique of spectral factorization was introduced by (Whalley, 1978)” (Al-Saadi, 2014).

As explained by Rosenbrock , the inverse Nyquist Array (INA) is represented by a set of \mathbf{m}^2 diagrams for the elements $\hat{\mathbf{q}}_{ij}(\mathbf{j}\omega)$ of $\hat{\mathbf{Q}}_{ij}(\mathbf{j}\omega)$). The Inverse Nyquist Array permits the components of $\hat{\mathbf{R}}_{ij}(\mathbf{j}\omega)$ could be found using elementary technique. Since $\hat{r}_{ij} = \hat{q}_{ij}$ if $i \neq j$, $\hat{r}_{ii} = \hat{q}_{ii}$ if loop of i th is open, and $\hat{r}_{jj} = I + \hat{q}_{jj}$ if loop of j th is closed. These graphs help to examine diagonally dominance of the open-loop transfer function matrix $\mathbf{Q}(s)$, The rational Matrix $\hat{\mathbf{Q}}$ of $m \times m$ could be considered as diagonally dominance, if the following are fulfilled (Dutton et al. , 1997);

$$|\hat{q}_{ii}(s)| > r_i \text{ for } 1 \leq i \leq m \text{ for all } \mathbf{s} \text{ values on } D \text{ contour,}$$

$$\text{where } |\hat{q}_{ii}(s)| = \sum_{j=1, j \neq i}^m |q_{ij}(s)| \text{ for row dominance,} \quad (3.49)$$

$$\text{Or } |\hat{q}_{ii}(s)| = \sum_{j=1, j \neq i}^m |q_{ji}(s)| \text{ for all column dominance} \quad (3.50)$$

The circles for on each S on D , has a diagonal element of radius:

$$d_i(s) = \sum_{j=1, j \neq i}^m \hat{q}_{ij}(s) \quad (3.51)$$

With center on a suitable point of $\hat{q}_{ii}(s)$. Figure 3.12 shows Sketch to define the dominance of a rational matrix $\mathbf{Q}(s)$ (Hawkins and McMorran, 1973).

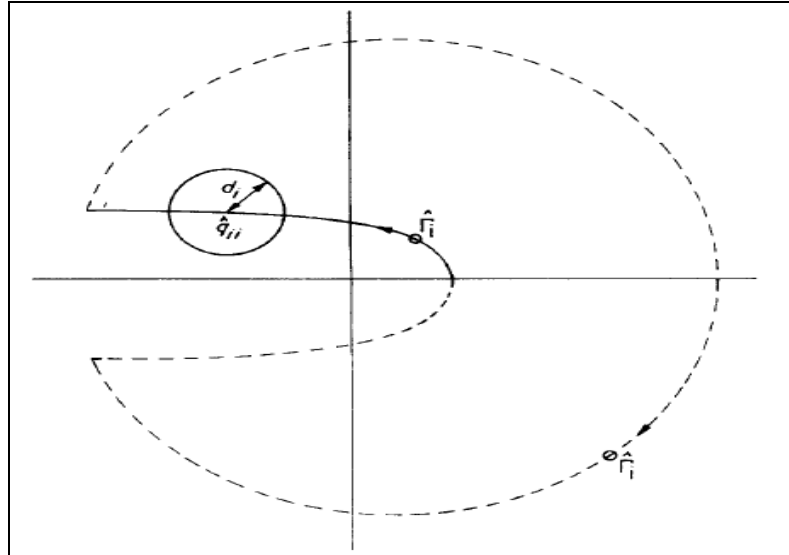


Figure 3.12, Sketch to define the Dominance of a rational matrix $\mathbf{Q}(s)$
(Hawkins and McMorran, 1973)

The diagonal dominance of $\hat{\mathbf{Q}}$ matrix can be examined by plotting Gershgorin circles (1932), on the Nyquist graph, as explained in the Figure 3.13.

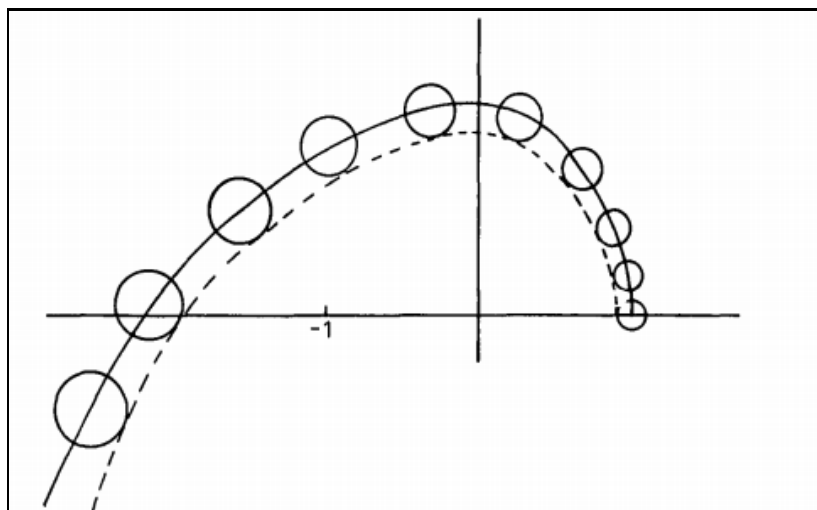


Figure 3.13, Inverse Nyquist Diagram of $\hat{q}_{ii}(s)$
(Hawkins and McMorran, 1973)

if each of circle group (bands) eliminate the origin for $i = 1, \dots, m$, that is means $\hat{Q}(s)$ is row dominant, on D . Similarly, for column dominance would achieved by adopting circles with radius

$$d_i(s) = \sum_{j=1, j \neq i}^m \hat{q}_{ji}(s) \quad (3.52)$$

In general, the matrix \hat{Q} is considered row (or column) dominant, If none of the bands formed by these circles enclosed the origin, at any frequency (Munro, 1972).

3.4.2. System Stability

The stability of the system as stated by Nyquist's principles, is mainly depends on the encirclement of the origin of the system in order to guarantee stability, The general form of Nyquist method which represents stability could be written as:

$$\sum_{i=1}^m \hat{N}_{qi} - \sum_{i=1}^m \hat{N}_{hi} = p_o - p_c \quad (3.53)$$

Where \hat{N}_{qi} and \hat{N}_{hi} are the times of encircle the point origin by mapping the contour D with \hat{q}_{ii} and \hat{h}_{ii} respectively, and p_o and p_c are the zeros in the right-side plan of the open loop and closed loop characteristics polynomial respectively (Munro, 1972).

After achieving diagonally dominant, the system would be considered as two independent single loops, under a dynamic compensator could be designed for each loop in order to improve performance (Dutton, 1997).

The decoupling component $K_d(s)$ of the controller, could be obtained by using traditional methods for controlling the open loop systems, for example PID.

3.4.3. Graphical Criteria for Stability

The general form of stability defined in the equation (3.40) would be satisfied if the band of each diagonal component of $\hat{q}_{ii}(s)$ snapped by the circles leaves the real axis between the origin and $-k_i$. For stability for:

$$h_i^{-1}(s) = h_{ii}^{-1}(s) - f_i \quad (3.54)$$

where $h_i^{-1}(s)$ the inverted transfer function for the i th input the output for all loops closed, while $h_{ii}^{-1}(s)$ is the inverse transfer function for the i th loop when this is open with the others closed. Equation (5.13) is controlled within the bands snapped by the Gershgorin circles, centered on $\hat{q}_{ii}(s)$, and this is applicable for all values of feed-back gain f_i , in each loop between the origin and the k_i loop. Once the closed-loop system gains f_i are selected, stability is achieved, then the measured gain margin for each loop, could be obtained by drawing smaller (Ostrowski) bands using the reduction element $\phi_i(s)$ which is defined in equation (3.55) (Munro, 1972).

The smaller bands could also reduce the region of probability by:

$$\phi_i(s) = \max_{j \neq i} \frac{d_j(s)}{|f_i + q_{jj}(s)|} \quad (3.55)$$

The $h_i^{-1}(s)$ band based on $\hat{q}_{ii}(s)$, which is defined through circle of radius

$$r_i(s) = \phi_i(s)d_j(s) \quad (3.56)$$

where $i = 1, 2, \dots, m$, and $J = 1, 2, \dots, m$, $i \neq j$

3.5. H_∞ - Robust Optimal Control Method

The H-infinity problem was created by Zames in 1960's when discovered the "small gain theorem" (Zames, 1966). It was announced by Zames on 1976 on two occasions. The first was in 1976 at the IEEE CDC, while the second was presented in the "Allerton Conference in 1979". In 1981 the problem was issued officially. Then, in 2006 Apkarian P. and Noll solved the H-infinity problem (Apkarian and Noll, 2006).

3.5.1. H_∞ -Infinity Control

The H_∞ design method addressed the robustness case by deriving a controller which keeps all the signals, responses and errors of the system within the initially defined tolerances and references. Figure 3.14 shows the common multivariable closed loop system with plant $G(s)$, controller $K(s)$, and disturbance d ,

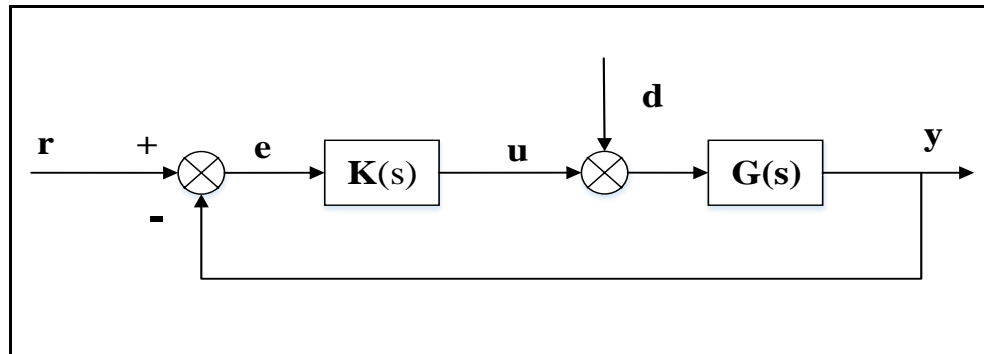


Figure 3.14, General Description of the system

3.5.2. The Over-All Control Problem Formation,

Several methods were implemented to solve the feedback problems which H_∞ optimization created. Practically, it will be more valuable if a standard design procedures was adopted to manipulate specific problems. Figure 3.15 shows the general formulation structure .

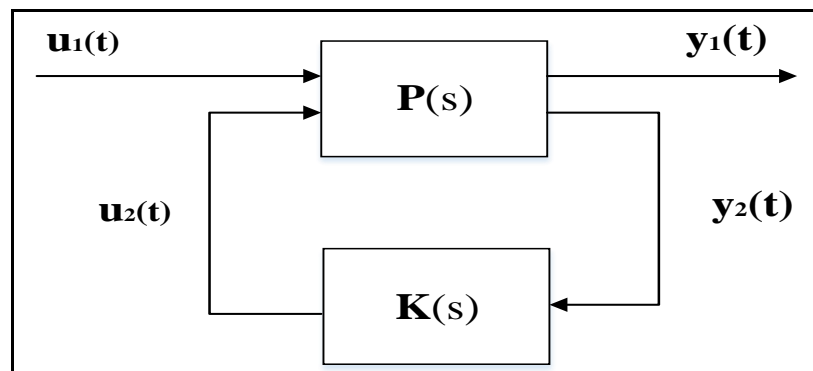


Figure 3.15, Feedback Control Structures

It can be seen from Figure 3.15 that the closed loop system with a feedback control structure, it is made of the augmented plant model $\mathbf{P}(s)$. This plant is proper a model via continuous or discrete-time, linear, time invariant procedure which includes both plant model $\mathbf{G}(s)$ and the disturbances \mathbf{d} , the controller $\mathbf{K}(s)$, external input and output vectors are $\mathbf{u}_1(t)$ and $\mathbf{y}_1(t)$ respectively, and the plant input and output vectors are $\mathbf{u}_2(t)$, and $\mathbf{y}_2(t)$, respectively,

Then

$$\begin{bmatrix} \mathbf{y}_1(t) \\ \mathbf{y}_2(t) \end{bmatrix} = \mathbf{P}(s) \begin{bmatrix} \mathbf{u}_1(t) \\ \mathbf{u}_2(t) \end{bmatrix} \quad (3.57)$$

and by partitioning:

$$\mathbf{P}(s) = \begin{bmatrix} \mathbf{P}_{11}(s) & \mathbf{P}_{12}(s) \\ \mathbf{P}_{21}(s) & \mathbf{P}_{22}(s) \end{bmatrix} \quad (3.58)$$

The control law equation is: $\mathbf{U}(s) = \mathbf{K}(s)\mathbf{Y}(s)$ (3.59)

Substitution equation (3.57) & (3.58), in equation (3.59), enables the relationship between the errors vector $\mathbf{y}_1(\mathbf{s})$ and the external input vector $\mathbf{u}_1(\mathbf{s})$

$$\mathbf{y}_1(\mathbf{s}) = [\mathbf{P}_{11}(\mathbf{s}) + \mathbf{P}_{12}(\mathbf{s})[\mathbf{I} - \mathbf{K}(\mathbf{s})\mathbf{P}_{22}(\mathbf{s})]^{-1}\mathbf{K}(\mathbf{s})\mathbf{P}_{21}(\mathbf{s})]\mathbf{u}_1(\mathbf{s}) \quad (3.60)$$

The general augmented plant model as in the following matrix:

$$\mathbf{P}(s) = \begin{bmatrix} \mathbf{A} & \mathbf{B}_1 & \mathbf{B}_2 \\ \mathbf{C}_1 & \mathbf{D}_{11} & \mathbf{D}_{12} \\ \mathbf{C}_2 & \mathbf{D}_{21} & \mathbf{D}_{22} \end{bmatrix} \quad (3.61)$$

The system \mathbf{P} is partitioned where inputs to \mathbf{B}_1 are the disturbances, and inputs to \mathbf{B}_2 are the control inputs, the outputs of \mathbf{C}_1 are errors to be kept small, and the outputs of \mathbf{C}_2 are the outputs measurements for the controller. Then the state space formula is

$$\dot{\mathbf{x}} = \mathbf{A}\mathbf{x}(s) + [\mathbf{B}_1 \ \mathbf{B}_2] \begin{bmatrix} \mathbf{u}_1(s) \\ \mathbf{u}_2(s) \end{bmatrix}, \begin{bmatrix} \mathbf{y}_1(s) \\ \mathbf{y}_2(s) \end{bmatrix} = \begin{bmatrix} \mathbf{C}_1 \\ \mathbf{C}_2 \end{bmatrix} \mathbf{x} + \begin{bmatrix} \mathbf{D}_{11} & \mathbf{D}_{12} \\ \mathbf{D}_{21} & \mathbf{D}_{22} \end{bmatrix} \begin{bmatrix} \mathbf{u}_1(s) \\ \mathbf{u}_2(s) \end{bmatrix} \quad (3.62)$$

For simplicity the notation, of equation (3.60) can be rephrases as

$$\mathbf{y}_1(s) = \mathbf{T}_{y_1u_1}(s)\mathbf{u}_1(s) \quad (3.63)$$

Then the closed loop transfer function relates the plant outputs and inputs so that

$$\mathbf{T}_{y_1u_1}(s) = \mathbf{P}_{11}(s) + \mathbf{P}_{12}(s)[\mathbf{I} - \mathbf{K}(s)\mathbf{P}_{22}(s)]^{-1}\mathbf{K}(s)\mathbf{P}_{21}(s) \quad (3.64)$$

The \mathbf{H}_∞ optimal control synthesis procedure consist of finding a controller $\mathbf{u}_2(s) = \mathbf{K}(s)\mathbf{y}_2(s)$, so that the \mathbf{H}_∞ norm of closed-loop transfer function $\mathbf{T}(s)$ is minimized, i.e. For \mathbf{H}_∞ Optimal control $\|\mathbf{T}_{y_1u_1}(s)\|_\infty < 1$, and for standard \mathbf{H}_∞ robust control $\min_{\mathbf{K}(s)}\|\mathbf{T}_{y_1u_1}(s)\|_\infty$ should be selected, The output feedback assumptions are:

$$\mathbf{P}(s) = \begin{bmatrix} A & B_1 & B_2 \\ C_1 & 0 & D_{12} \\ C_2 & D_{21} & 0 \end{bmatrix} \quad (3.65)$$

3.5.3. The General Case of Controller Design

As a common case, the concentration will be for a two-port system form for \mathbf{H}_∞ control. As explained in the figure 54, the main goal of this design is to obtain a robust controller $\mathbf{K}(s)$, to ensure the closed loop of the \mathbf{H}_∞ norm is restricted by a positive value of γ . To achieve that, first the internal stability of the system, and second the \mathbf{H}_∞ norm of the transfer function should be smaller than γ , i.e.

$$\|\mathbf{T}_{y_1u_1}(s)\|_\infty < \gamma$$

where γ is selected as the positive and less than 1, therefore the controller matrix can be written as:

$$\mathbf{K}(s) = \left[\begin{array}{c|c} A_f & -ZL \\ \hline - & - \\ F & 0 \end{array} \right] \quad (3.66)$$

where:

$$\begin{aligned} A_f &= A + \gamma^{-2}B_1B_1^T X + B_2F + ZL C_2, \\ F &= -B_2^T X, \quad L = -YC_2, \quad Z = (I - \gamma^{-2}YX)^{-1} \end{aligned} \quad (3.67)$$

X and Y are the solutions including:

$$\begin{aligned} A^T X + XA + X(\gamma^{-2}B_1B_1^T - B_2B_2^T)X + C_1C_1^T &= 0, \\ AY + YA^T + Y(\gamma^{-2}C_1C_1^T - C_2C_2^T)Y + B_1B_1^T &= 0. \end{aligned} \quad (3.68)$$

and the two AREs are the Hamilton matrices:

$$H_\infty = \begin{bmatrix} A & \gamma^{-2}B_1B_1^T - B_2B_2^T \\ -C_1^T C_1 & -A^T \end{bmatrix} \quad (3.69)$$

$$J_\infty = \begin{bmatrix} A^T & \gamma^{-2}C_1C_1^T - C_2C_2^T \\ -B_1^T B_1 & -A \end{bmatrix} \quad (3.70)$$

The conditions for reality of the H_∞ controller are listed in (Tewari, A., 2002). The augmented model with weighting functions is presented in figure 3.16.

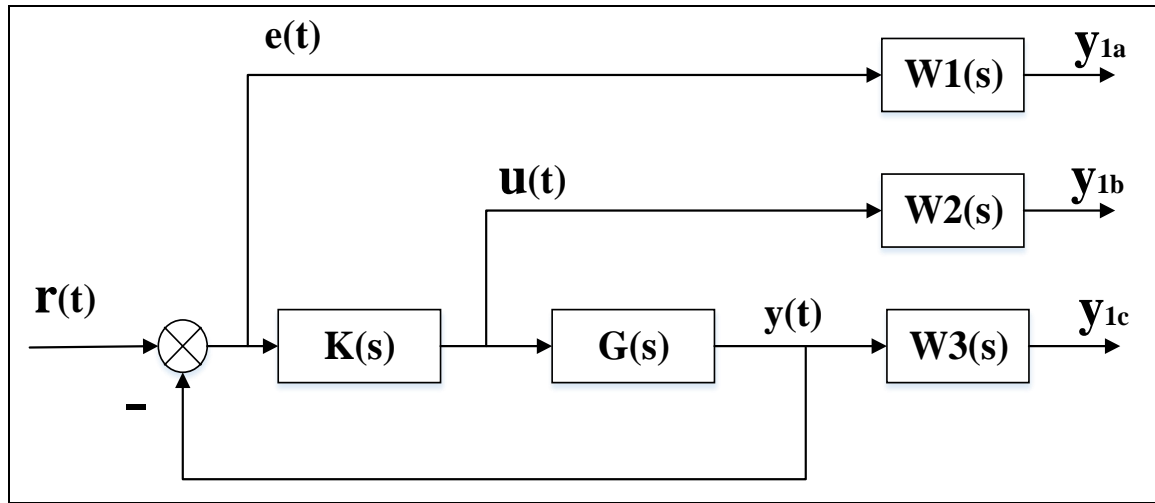


Figure 3.16, Feedback with Weighing Functions

(Doyle et al., 1989).

The $W_1(s)$, $W_2(s)$, and $W_3(s)$, are the weighting filters which can be as two-row matrices. All $G(s)$, $W_1(s)$ and $W_3(s)$ are all proper function. The design of H_∞ controller can be obtained by implementing the concept of the augmented state space model.

Chapter 4

Controller Design and Simulation Results Discussions

4.1. Least Effort Controller

4.1.1. Mathematical -Least Effort Controller Design

The transfer function with the pure integrators results in instability in performance.

Therefore pre- compensator using two filters, the transfer function model for the system becomes:

$$\mathbf{G}(s) = \begin{bmatrix} \frac{68271.3s+2,741,092.695}{s^3+1135s} & \frac{553.29s-1,817,557.65}{s^3+1135s} \\ \frac{553.29s-1,817,557.65}{s^3+1135s} & \frac{68271.3s+2,741,092.695}{s^3+1135s} \end{bmatrix} \begin{bmatrix} \frac{s}{(s+10)} & 0 \\ 0 & \frac{s}{(s+10)} \end{bmatrix} \begin{bmatrix} \frac{s}{(s+100)} & 0 \\ 0 & \frac{s}{(s+100)} \end{bmatrix} \quad (4.1)$$

Figure 4.1 shows the open loop block diagram representation for the transfer function matrix.

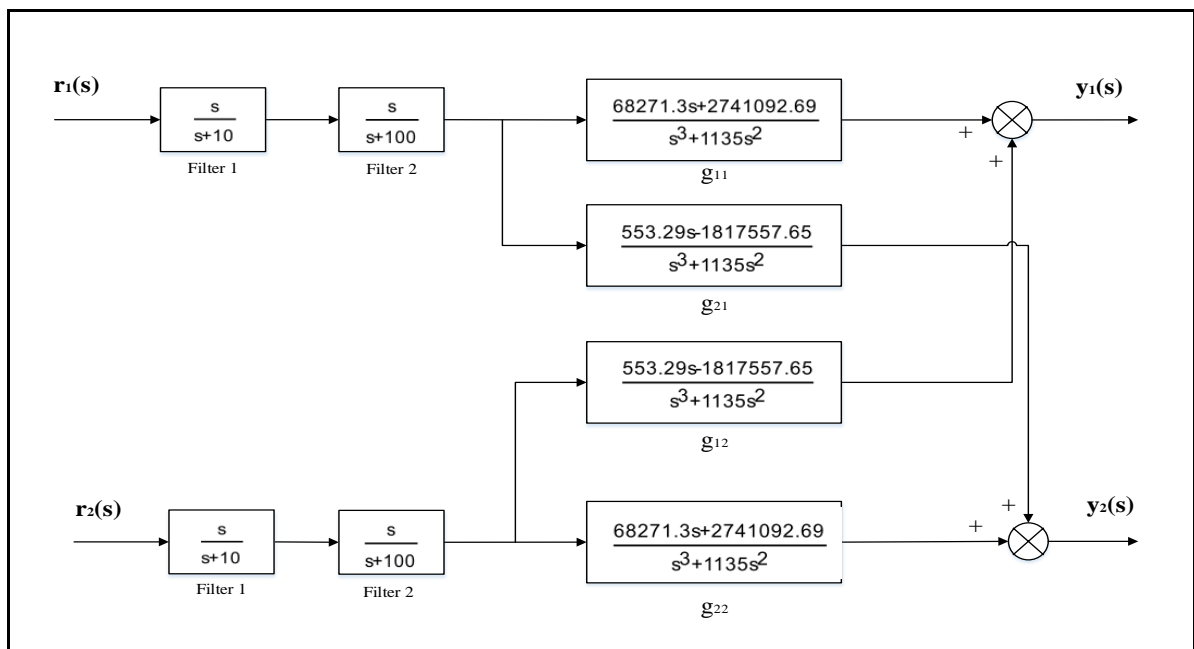


Figure 4.1, Block Diagram Representation For Open Loop System

Multiplying the matrices, the general form of

$$\mathbf{G}(s) = L(s) \frac{A(s)}{d(s)} R(s) \Gamma(s) \quad (4.2)$$

$$\mathbf{G}(s) = \frac{1}{(s+1135)(s+10)(s+100)} \begin{bmatrix} 68271.3s + 2,741,092.695 & 553.29s - 1,817,557.65 \\ 553.29s - 1,817,557.65 & 68271.3s + 2,741,092.695 \end{bmatrix} \quad (4.3)$$

$$\text{where: } \mathbf{L}(s) = \begin{bmatrix} \frac{1}{(s+1135)(s+10)(s+100)} & 0 \\ 0 & \frac{1}{(s+1135)(s+10)(s+100)} \end{bmatrix}, \mathbf{R}(s) = \mathbf{I}, \mathbf{\Gamma}(s) = \mathbf{I},$$

$$\mathbf{A}(s) = \begin{bmatrix} 68271.3s + 2,741,092.695 & 553.29s - 1,817,557.65 \\ 553.29s - 1,817,557.65 & 68271.3s + 2,741,092.695 \end{bmatrix}$$

$$\text{and } d(s) = s^3 + 1245s^2 + 125850s + 1135000$$

$$\text{the rational transfer function is } \mathbf{y}(s) = \mathbf{G}(s)\mathbf{u}(s) \quad (4.4)$$

where:

$$g_{11} = \frac{68271.3s + 2,741,092.695}{s^3 + 1245s^2 + 125850s + 1135000}, \quad g_{12} = \frac{553.29s - 1,817,557.65}{s^3 + 1245s^2 + 125850s + 1135000}$$

$$g_{21} = \frac{553.29s - 1,817,557.65}{s^3 + 1245s^2 + 125850s + 1135000}, \quad g_{22} = \frac{68271.3s + 2,741,092.695}{s^3 + 1245s^2 + 125850s + 1135000}$$

Will be employed.

$$\mathbf{G}(s) = \frac{\mathbf{A}(s)}{d(s)} = \frac{\begin{bmatrix} 68271.3s + 2,741,092.695 & 553.29s - 1,817,557.65 \\ 553.29s - 1,817,557.65 & 68271.3s + 2,741,092.695 \end{bmatrix}}{(s^3 + 1245s^2 + 125850s + 1135000)} \quad (4.5)$$

4.1.2. Inner loop design:

According to equation (4.1)

$$\langle \mathbf{hA}(s)\mathbf{k} \rangle = [\mathbf{h}_1 \ \mathbf{h}_2] \begin{bmatrix} 68271.3s + 2,741,092.695 & 553.29s - 1,817,557.65 \\ 553.29s - 1,817,557.65 & 68271.3s + 2,741,092.695 \end{bmatrix} \begin{bmatrix} \mathbf{k}_1 \\ \mathbf{k}_2 \end{bmatrix}$$

$$\begin{aligned}
&= [(68271.3s + 2,741,092.695)h_1k_1 + (553.29s - 1,817,557.65)h_2k_2 + (553.29s \\
&\quad - 1,817,557.65)h_2k_1 + (68271.3s + 2,741,092.695)h_2k_2] \\
&= [1 \ s] \begin{bmatrix} 2,741,092.695 & -1,817,557.65 & -1,817,557.65 & 2,741,092.695 \\ 68271.3 & 553.29 & 553.29 & 68271.3 \end{bmatrix} \begin{bmatrix} k_1h_1 \\ k_2h_1 \\ k_1h_2 \\ k_2h_2 \end{bmatrix}
\end{aligned}$$

According to $k_2 = nk_1, \dots \dots k_m$ gives

$$\langle h \frac{A(s)}{d(s)} k \rangle =$$

$$k_1 \frac{[1 \ s]}{d(s)} \begin{bmatrix} 2,741,092.695 - 1,817,557.65n & 2,741,092.695n - 1,817,557.65 \\ 68271.3 + 553.29n & 553.29 + 68271.3n \end{bmatrix} \begin{bmatrix} h_1 \\ h_2 \end{bmatrix}$$

To formulated the Q matrix, with $k_1 = 1$ yealding :

$$Q = \begin{bmatrix} 2,741,092.695 - 1,817,557.65n & 2,741,092.695n - 1,817,557.65 \\ 68271.3 + 553.29n & 553.29 + 68271.3n \end{bmatrix} \quad (4.6)$$

$$\text{and } \langle h \frac{A(s)}{d(s)} k \rangle = \frac{b(s)}{d(s)}$$

$$\text{where } d(s) = (s + 1135)(s + 10)(s + 100) = s^3 + 1245s^2 + 125850s + 1135000 \quad (4.7)$$

System poles can be found from equation (3.36). Let $b(s) = s + 10$, so that this stable zero at $s = -10$ will attract the pole at $s = -10$ away from the imaginary axis causing a reduction in settling time. This leads to closed loop stability

$$\langle h \frac{A(s)}{d(s)} k \rangle = \frac{b_0(s + x)}{s^3 + 1245s^2 + 125850s + 1135000}$$

where $b(s) = b_0(s + x)$,

If the values of $x = -10$, and b_0 can be obtained by plotting the root locus diagram for

$\frac{b(s)}{d(s)} = -1$, the root locus plot should be stable for b_0 , from the plot in the Figure 4.2, can

select value of $b_0 = 10000$

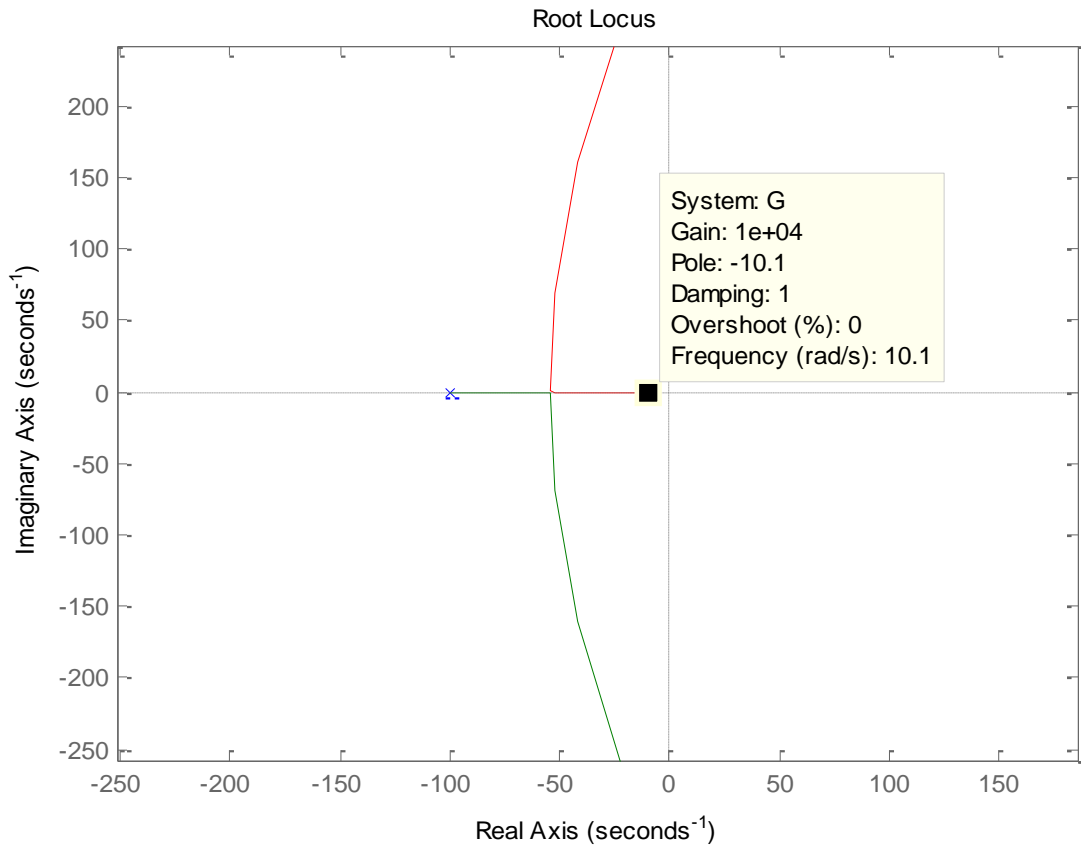


Figure 4.2, Root Locus Diagram

$$\text{Then } \langle h \frac{A(s)}{d(s)} k \rangle b_0(s + 10) = b_0[1 \text{ s}] \begin{bmatrix} 10 \\ 1 \end{bmatrix},$$

$$\text{According to the equation } \mathbf{k}_1[\mathbf{Q}][\mathbf{h}] = \mathbf{b}$$

Then:

$$k_1[1 \text{ s}] \begin{bmatrix} 2,741,092.695 - 1,817,557.65n & 2,741,092.695n - 1,817,557.65 \\ 68271.3 + 553.29n & 553.29 + 68271.3n \end{bmatrix} \begin{bmatrix} h_1 \\ h_2 \end{bmatrix} = b_0[1 \text{ s}] \begin{bmatrix} 10 \\ 1 \end{bmatrix}$$

$$\text{Where } \mathbf{Q} = \begin{bmatrix} 2,741,092.695 - 1,817,557.65n & 2,741,092.695n - 1,817,557.65 \\ 68271.3 + 553.29n & 553.29 + 68271.3n \end{bmatrix}, \quad [\mathbf{h}] = \begin{bmatrix} h_1 \\ h_2 \end{bmatrix},$$

And $\mathbf{b} = b_0[1 \text{ s}] \begin{bmatrix} 10 \\ 1 \end{bmatrix}$ are the coefficients of numerator of $b(s)$, $k_1 = 1$

$$\text{Then } \mathbf{Qh} = b_0[1 \text{ s}] \begin{bmatrix} 10 \\ 1 \end{bmatrix}, \quad \text{and} \quad \mathbf{h} = \mathbf{Q}^{-1} \begin{bmatrix} 10 \\ 1 \end{bmatrix} b_0 \quad (4.8)$$

The value of n required to minimize the control energy,

$$(|k_1 \quad h_1| + |k_2 \quad h_1|)y_1(t) + (k_1h_2 + k_2h_1)y_2(t) = E(t)$$

$$E(t) = \int_0^{t=T} (\sum_{j=1}^n k_j^2 \sum_k^n h_k^2) y_k^2 d(t) \quad (4.9)$$

For arbitrary change in outputs $y_2(t)$ following arbitrary disturbance minimizing performance index J

$$J = \sum_{j=1}^n k_j^2 \sum_k^n h_k^2 \quad \text{would minimize J} \quad (4.10)$$

Here $J(n) = (k_1^2)[1 + n^2][h_1^2 + h_2^2] = (k_1^2)[1 + n^2][h_1 \quad h_2] \begin{bmatrix} h_1 \\ h_2 \end{bmatrix}$, and $\mathbf{h} = \mathbf{Q}^{-1} \begin{bmatrix} x \\ 1 \end{bmatrix} \mathbf{b}_0$

$$\text{Then } J(n) = (k^2)[1 + n^2] \mathbf{b}_0 [x \quad 1] (\mathbf{Q}^{-1})^T \mathbf{Q}^{-1} \begin{bmatrix} x \\ 1 \end{bmatrix} \mathbf{b}_0 \quad (4.11)$$

$$\text{By selecting } k_1 = 1, \mathbf{b}_0 = 10000, \text{ then } \mathbf{b} = \begin{bmatrix} 10 \\ 1 \end{bmatrix}$$

Substituting for $k_1, \mathbf{Q}, \mathbf{b}, \mathbf{b}_0, x$ in (3.39) yields the performance index:

$$J(n) = 1(1 + n^2) \mathbf{1} \mathbf{b}^T (\mathbf{Q}^{-1})^T \mathbf{Q}^{-1} \begin{bmatrix} 10 \\ 1 \end{bmatrix} 10^4$$

$$J = \frac{4.6117 \times 10^{20} (n^2 + 1) (2.2316 \times 10^{35} \times n^2 - 4.4244 \times 10^{35} n + 2.22613 \times 10^{35})}{(-4.63396 \times 10^{32} n^2 + 3.35282 \times 10^{30} n + 4.583393 \times 10^{32})^2}$$

It can be seen from the Figure 4.3, the relation of the performance index J against to gain ratio n, to find the absolute minimum value of performance index, differentiating J with respect to gain ratio and equating to zero so that:

$$\frac{\partial J}{\partial n} = 0$$

Reveal that there four supremum values for J, where J_{\min} arises when : $n = 1.6559$

where $J = 2.7015 \times 10^{-10}$ (minimum).

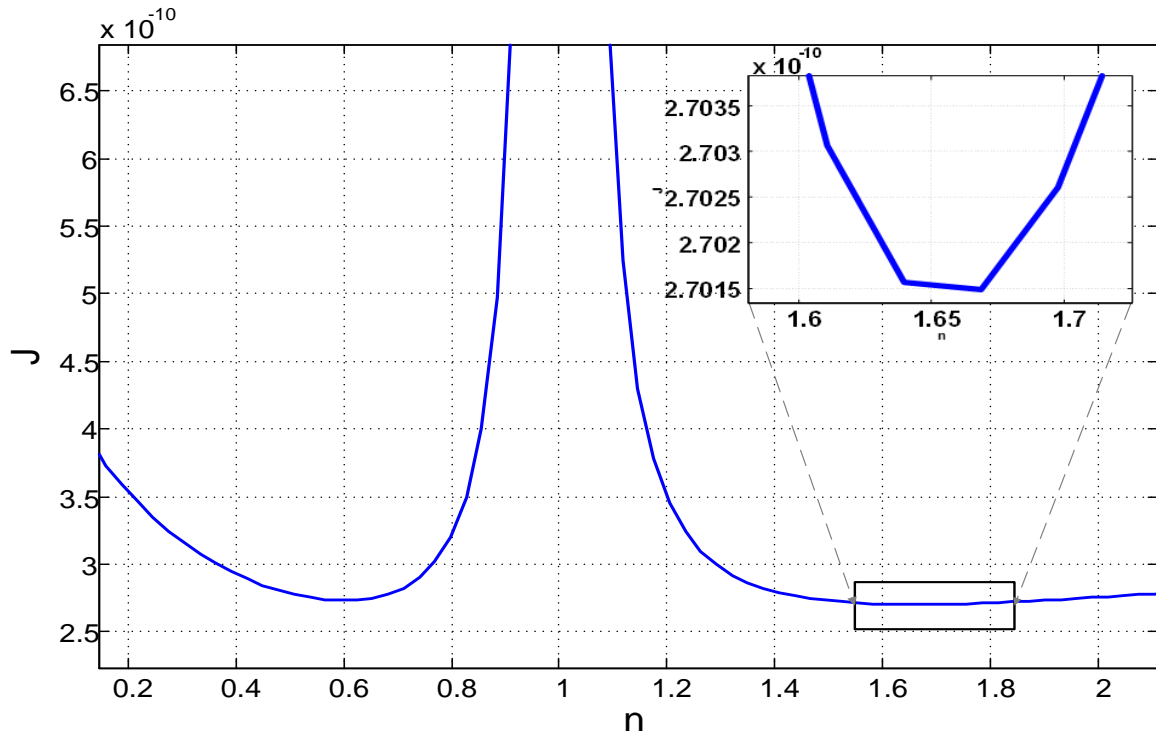


Figure 4.3, The performance Index J against Gain ratio n

Hence the inner loop forward gain values becomes:

$$k_1 = 1, k_2 = 1.6559, \text{ then } \mathbf{k}(0) = \begin{bmatrix} 1 \\ 1.6559 \end{bmatrix}$$

Then \mathbf{Q} can be found by substituting value of n in (4.6)

$$\mathbf{Q} = \begin{bmatrix} -0.2685e6 & 2.7213e6 \\ 0.0692e6 & 0.1131e6 \end{bmatrix} \quad (4.12)$$

\mathbf{h}_0 then can be found by substituting values of \mathbf{Q} , $\mathbf{b} = \begin{bmatrix} 10 \\ 1 \end{bmatrix}$ in to the equation (4.8), then

the inner loop feedback gain values can be found from

$$\mathbf{h}(0) = \frac{\mathbf{Q}^{-1}\mathbf{b}}{k_1} = [0.0727 \quad 0.0439] \quad (4.13)$$

4.1.3. Outer Loop Design

In order to design the outer loop, required to obtain feed forward and feedback gain

matrices $\mathbf{k}(0)$, $\mathbf{h}(0)$, s_s , $\mathbf{G}(0)$ and \mathbf{F} ,

Transfer function matrix for the steady state open loop given by $\mathbf{G}(0)$, and the steady state interaction due to coupling in the outputs will be restricted in the close loop 10%:

$$\text{Then } \mathbf{s}_s = \begin{bmatrix} 1 & 0.1 \\ 0.1 & 1 \end{bmatrix}$$

$$\mathbf{P} \text{ will be calculated by equation } \mathbf{P} = \{\mathbf{G}^{-1}(\mathbf{0}) + \mathbf{k}(\mathbf{0}) \succ \mathbf{h}(\mathbf{0})\} \mathbf{S}_s (\mathbf{I}_2 - \mathbf{F} \mathbf{S}_s)^{-1}$$

$$\mathbf{H} \text{ will be calculated by the equation } \mathbf{H} = \mathbf{P}^{-1} \mathbf{k} \succ \mathbf{h} + \mathbf{F}$$

The effect of increasing feedback gain from 0.1 to 0.8 was investigated. The outer loop design for different outer loop feedback gain values, selected for $0 < f < 1$, $f_1 = f_2 = 0.1, 0.3, 0.5$ and 0.8 . In order to complete the control system strategy the disturbance rejection will also be investigated .

$$\text{For the first outer loop feedback gain value } f = 0.1, \text{ then } \mathbf{F} = \begin{bmatrix} 0.1 & 0 \\ 0 & 0.1 \end{bmatrix}$$

$$\mathbf{P} = \begin{bmatrix} 0.9691 & 0.6946 \\ 0.7793 & 0.9787 \end{bmatrix}, \text{ and } \mathbf{H} = \begin{bmatrix} 0.0695 & -0.0185 \\ 0.1470 & 0.1890 \end{bmatrix}$$

$$\text{For the second outer loop feedback gain value } f = 0.3, \text{ then } \mathbf{F} = \begin{bmatrix} 0.3 & 0 \\ 0 & 0.3 \end{bmatrix}$$

$$\mathbf{P} = \begin{bmatrix} 1.2761 & 0.9339 \\ 1.0434 & 1.2919 \end{bmatrix}, \text{ and } \mathbf{H} = \begin{bmatrix} 0.2726 & -0.0166 \\ 0.115 & 0.3697 \end{bmatrix}$$

$$\text{For the third outer loop feedback gain value } f = 0.5, \text{ then } \mathbf{F} = \begin{bmatrix} 0.5 & 0 \\ 0 & 0.5 \end{bmatrix}$$

$$\mathbf{P} = \begin{bmatrix} 1.8723 & 1.4181 \\ 1.5735 & 1.9035 \end{bmatrix}, \text{ and } \mathbf{H} = \begin{bmatrix} 0.4758 & -0.0147 \\ 0.0831 & 0.5503 \end{bmatrix}$$

$$\text{For the fourth outer loop feedback gain value } f = 0.8, \text{ then } \mathbf{F} = \begin{bmatrix} 0.8 & 0 \\ 0 & 0.8 \end{bmatrix}$$

$$\mathbf{P} = \begin{bmatrix} 6.6156 & 5.7235 \\ 6.1955 & 6.8435 \end{bmatrix}, \text{ and } \mathbf{H} = \begin{bmatrix} 0.8821 & -0.0108 \\ 0.0192 & 0.9116 \end{bmatrix}$$

4.1.4. Simulation Results

For values of feedback $f < 0.8$ the compensators \mathbf{P} and \mathbf{H} have element of smaller moduli, the closed loop response was simulated using Matlab-Simulink with various values of outer loop feedback gain, in the range of $0.1 \leq f \leq 0.8$, By rotating unit step change inputs on both references for the magnetically levitation system model, considering $\mathbf{r}_1(s)$ as the first input reference for the air gap1, while $\mathbf{r}_2(s)$ the second input reference for the air gap 2, the response results shown in the figures 4.4, to figure 11.

These traces describe acceptable response variation with steady state interaction limited to 10 percent, as selected.

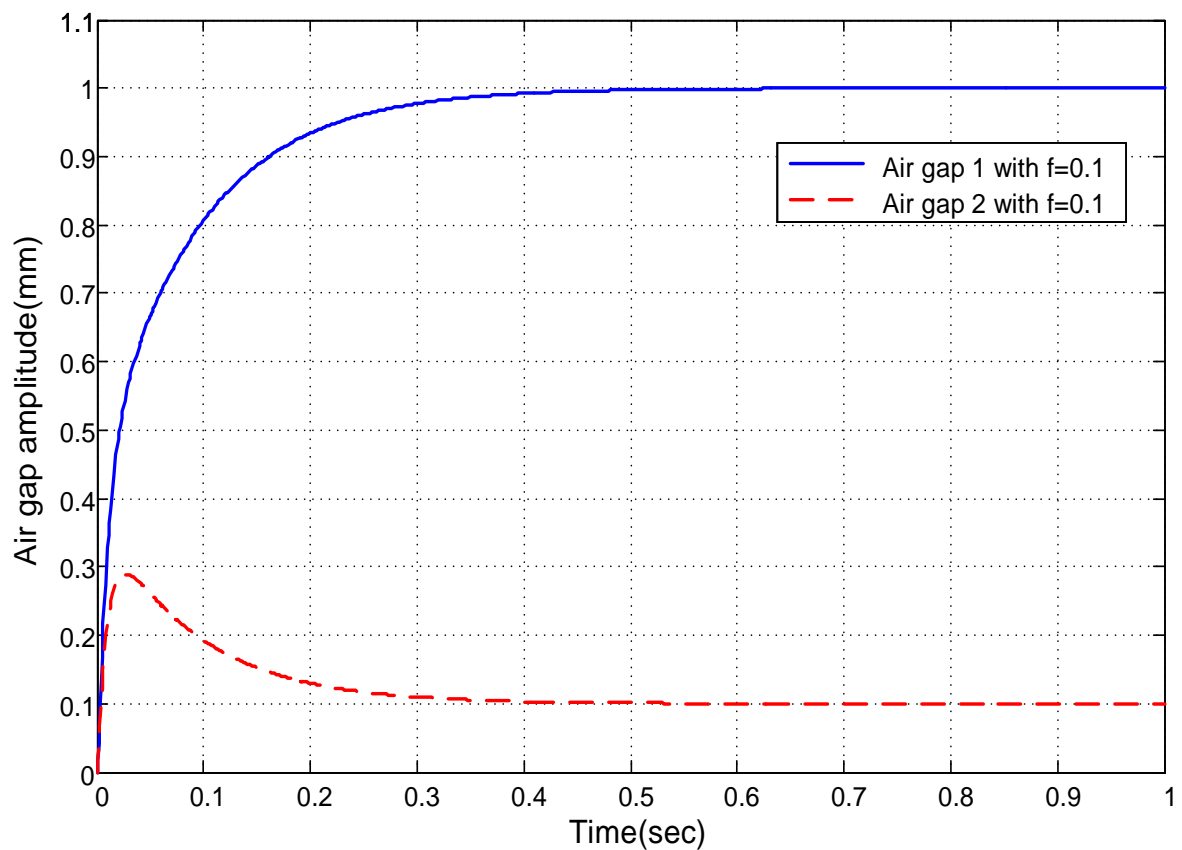


Figure 4.4, Closed loop response with $f=0.1$, following unit step input at $\mathbf{r}_1(s)$

The first value of outer loop feedback gain $f = 0.1$, for the simulation for the closed loop system model, with a unit step applied on $\mathbf{r}_1(\mathbf{s})$, with $\mathbf{r}_2(\mathbf{s}) = \mathbf{0}$, gives the output responses shown in the Figure 4.4. The first output (air gap 1) transient is overdamped with a settling time of approx. 0.7 sec. to reach its steady state value, the second output response (air gap 2) shows small overshoot which is recovered within 0.6 seconds to steady state conditions. The interaction between the outputs was maintained at 10 percent as determined by the steady state matrix S_s .

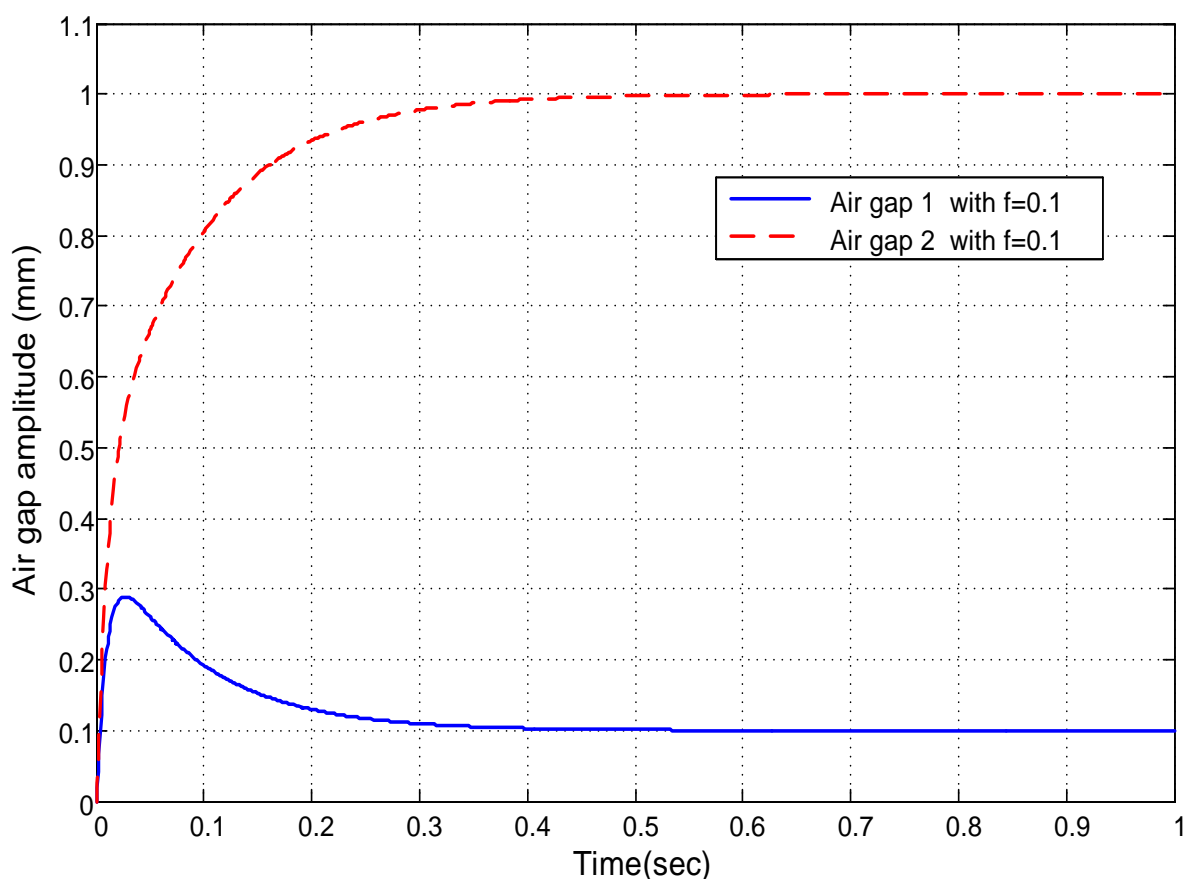


Figure 4.5, Closed Loop Response with $f=0.1$,
Following Unit Step Input at $\mathbf{r}_2(\mathbf{s})$

Then, with changing the input reference to on the second reference $\mathbf{r}_2(\mathbf{s})$, the output results presented in the Figure 4.5, the responses shows the similar behavior as in the first input

on $r_1(s)$, the first output recovers rapidly to steady state within 4.7 seconds, while the second output (air gap 2), is overdamped, and taken 0.56 seconds to reach steady state conditions. With the second value of $f = 0.3$, the same procedure was used to investigate the closed loop system responses to a unit step input applied on second input reference $r_1(s)$. The output results can be seen in the Figure 4.6, the first output (air gap 1) is overdamped, with small improvement in the time required to steady state. The response time was reduced from 0.7 sec. when $f = 0.1$ to 0.47sec. when $f = 0.3$

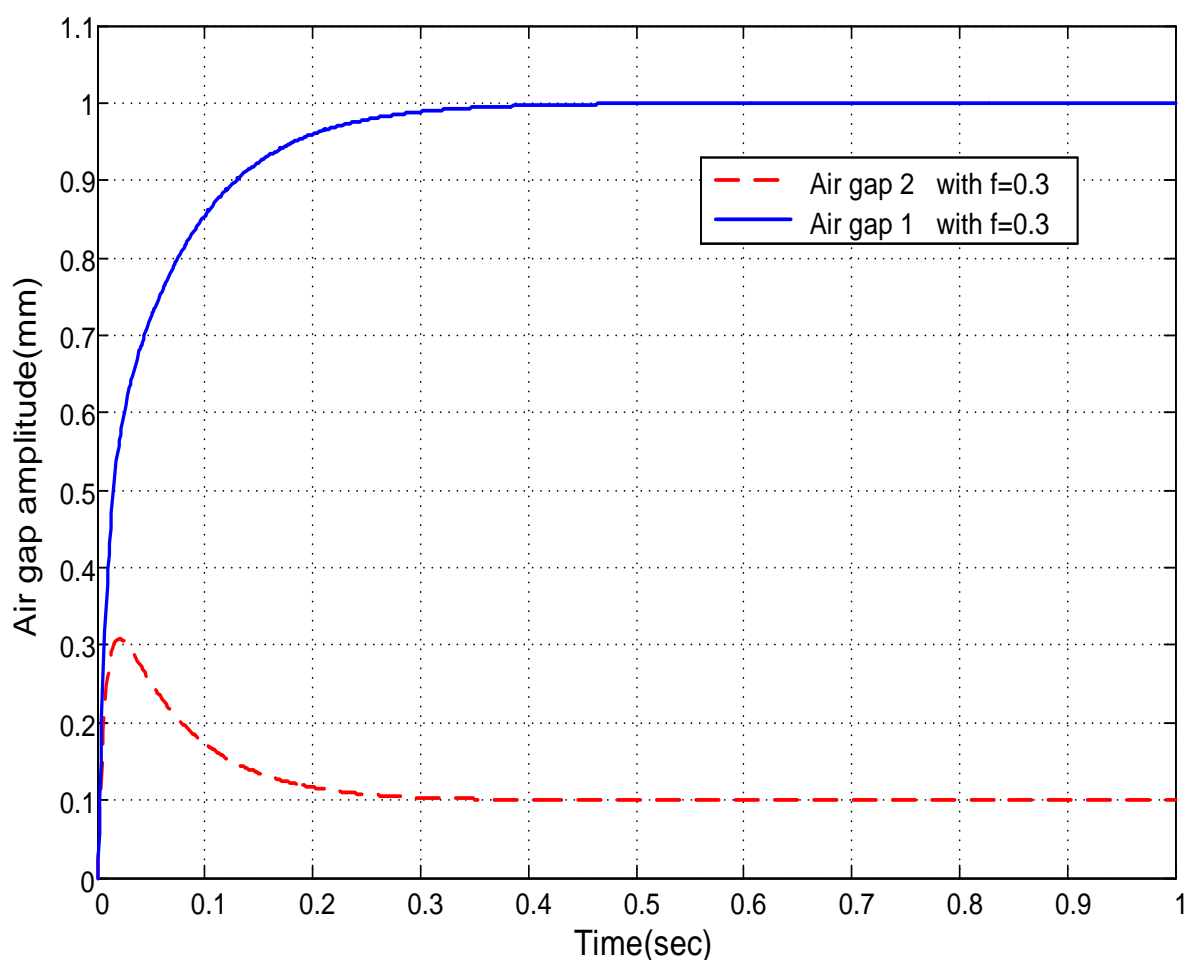


Figure 4.6, Closed Loop Response With $f=0.3$,
Following Unit Step Input at $r_1(s)$

on the other hand, as illustrated in the Figure 4.7, the second output also shows an improvement

has a similar overshoot as in first output, but with rise and settling time of about 0.36 sec. which is less than the previous trial with $f = 0.1$

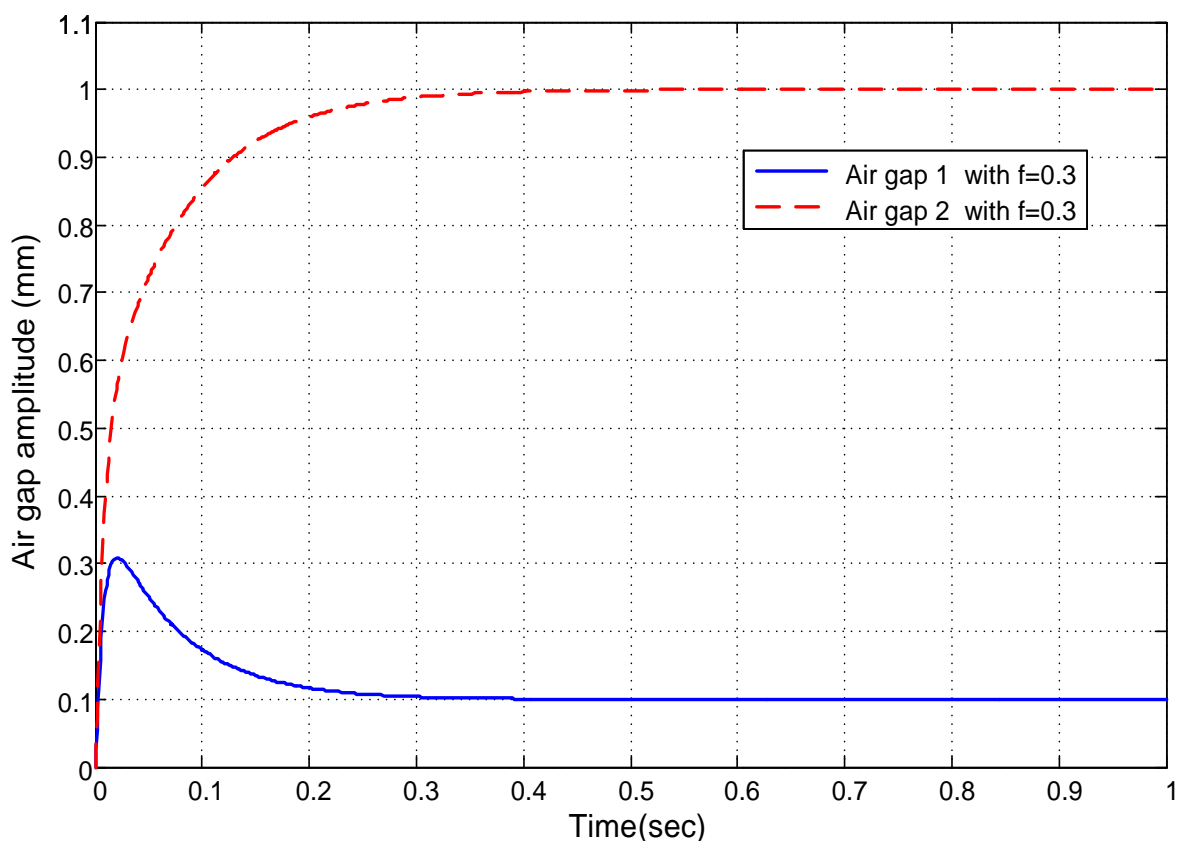


Figure 4.7, Closed Loop Response With $f=0.3$,
Following Unit Step Input at $r_2(s)$

For the same outer loop feedback gain $f = 0.3$, but the unit step input on the $r_2(s)$, the simulation results are as shown in the figure 32. The output of air gap 1, has similar pattern of the second output (air gap 2) when input at $r_1(s)$. However, now it is faster, showing an acceptable overshoot, of only 0.44 sec to reach the designed steady state value of 0.1, as limited by the Ss matrix.

The next trial, for the system response with external loop feedback gain higher of, $f = 0.5$, with unit step input on the $r_1(s)$, the out puts responses were as in the Figure 4.8. Is expected, the results has similar pattern of the previous cases, with an improvement in the rising and de

settling time, with the first output is over damped, maintaining the steady state value, as in the

designed level, the recorded transient time (rise and settling time) of about 0.38 sec. which is less than the previous trail, while the second output only 0.25 seconds are requires to reach the recommended steady state. This is also less than the previous case.

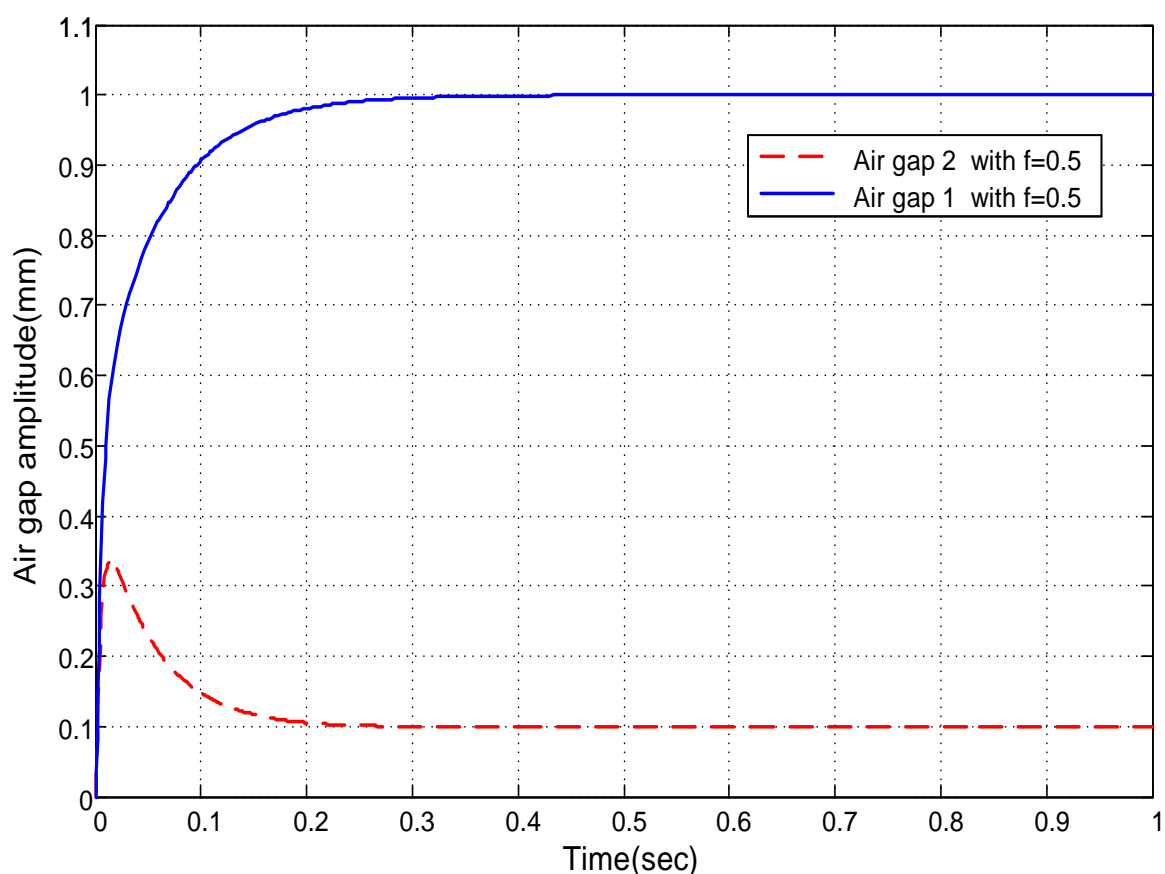


Figure 4.8, Closed Loop Response With $f=0.5$,
Following Unit Step Input at $r_1(s)$

Now, with the input on the second reference $r_2(s)$, the outputs almost inverted from the previous case, as shown in the Figure 4.9, the first output requires only 0.28 seconds to go to the lowest value of the Ss matrix which is 0.1, while the second output is raised to the highest value of the Ss matrix, within 0.5 second.

The system responses when outer loop feedback $f=0.5$ for both references showing improvement in output results better than the previous trial when $f=0.3$,

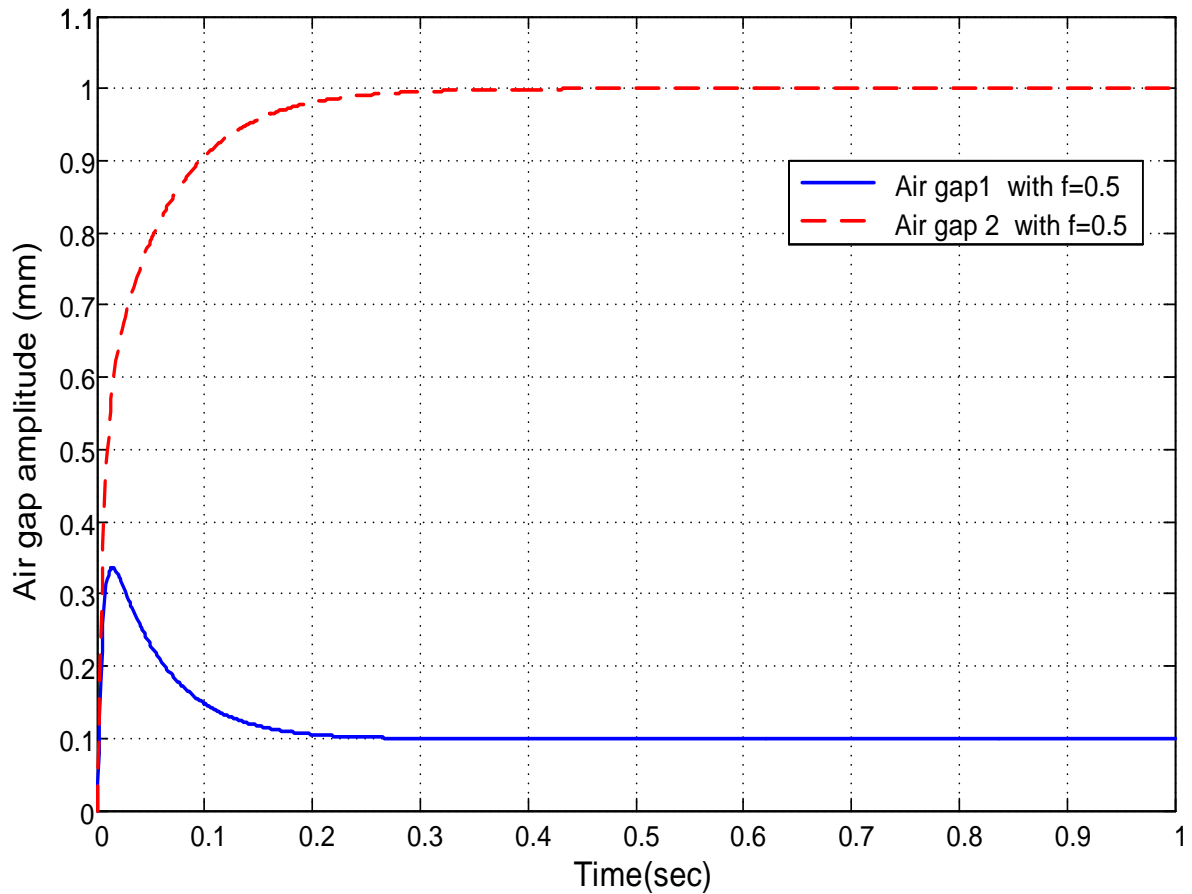


Figure 4.9, Closed Loop Response With $f=0.5$,
Following Unit Step Input at $r_2(s)$

For the last investigation with the outer loop feedback gain of $f = 0.8$, the simulation results in the responses shown in Figure 4.10. This is a good improvement in system responses, following the unit step input on the first reference $r_1(s)$.

The first output (air gap 1) was critically damped, and reached the designed steady state in 0.2 seconds , with very small steady state errors, which would not affecting the system performance.

The second output requires only 0.15 second to reach to the designed steady state, with an accepted overshoot, Then, the unit step to the second reference $r_2(s)$, as in the Figure 4.11.

The simulation results show good improvements in the system outputs to meet the targeted values very quickly, since the first output time is only 0.15 second, to reach the desired value, while the second output reached steady state in 0.33 seconds, which is less than the previous time for $f = 0.5$,

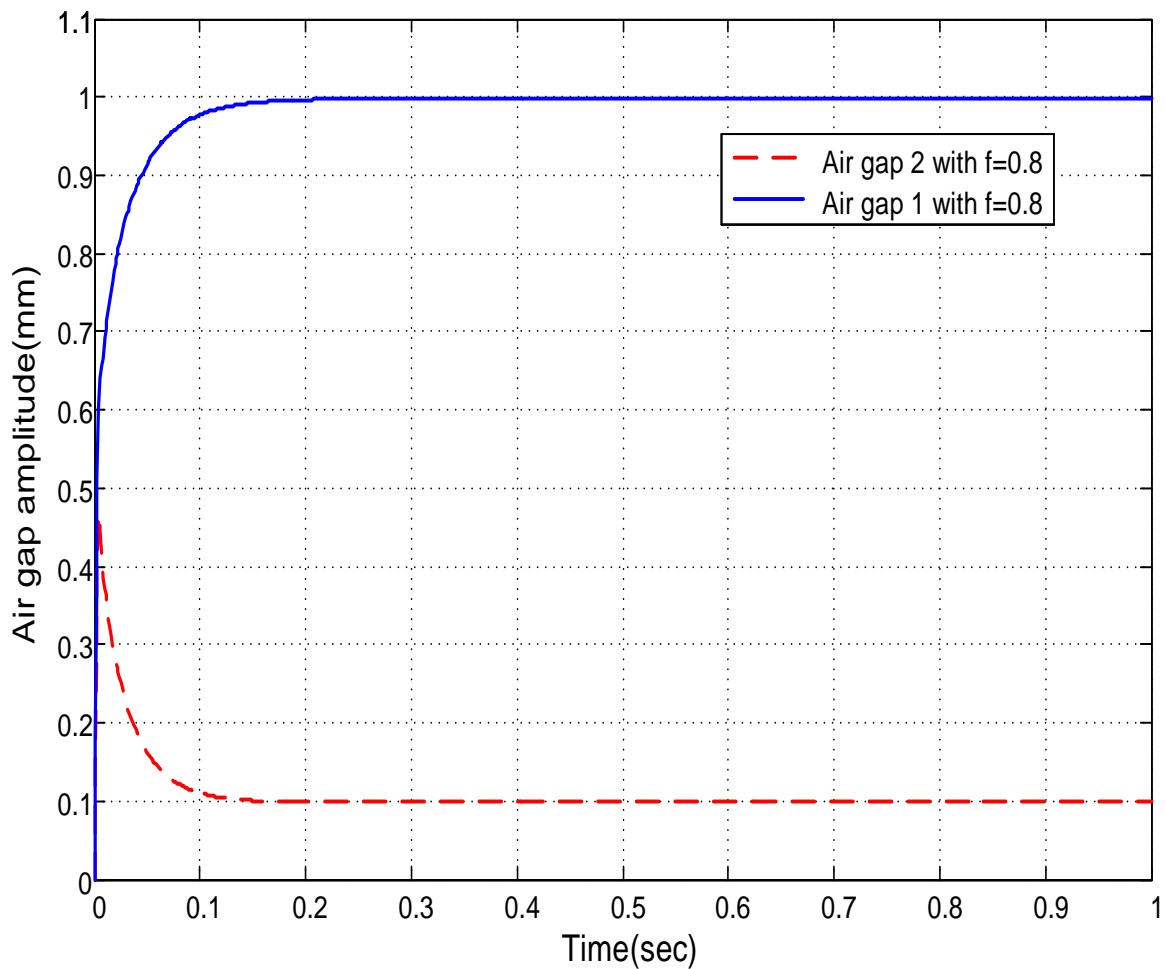


Figure 4.10, Closed Loop Response With $f=0.8$,

Following Unit Step Input at $r_1(s)$

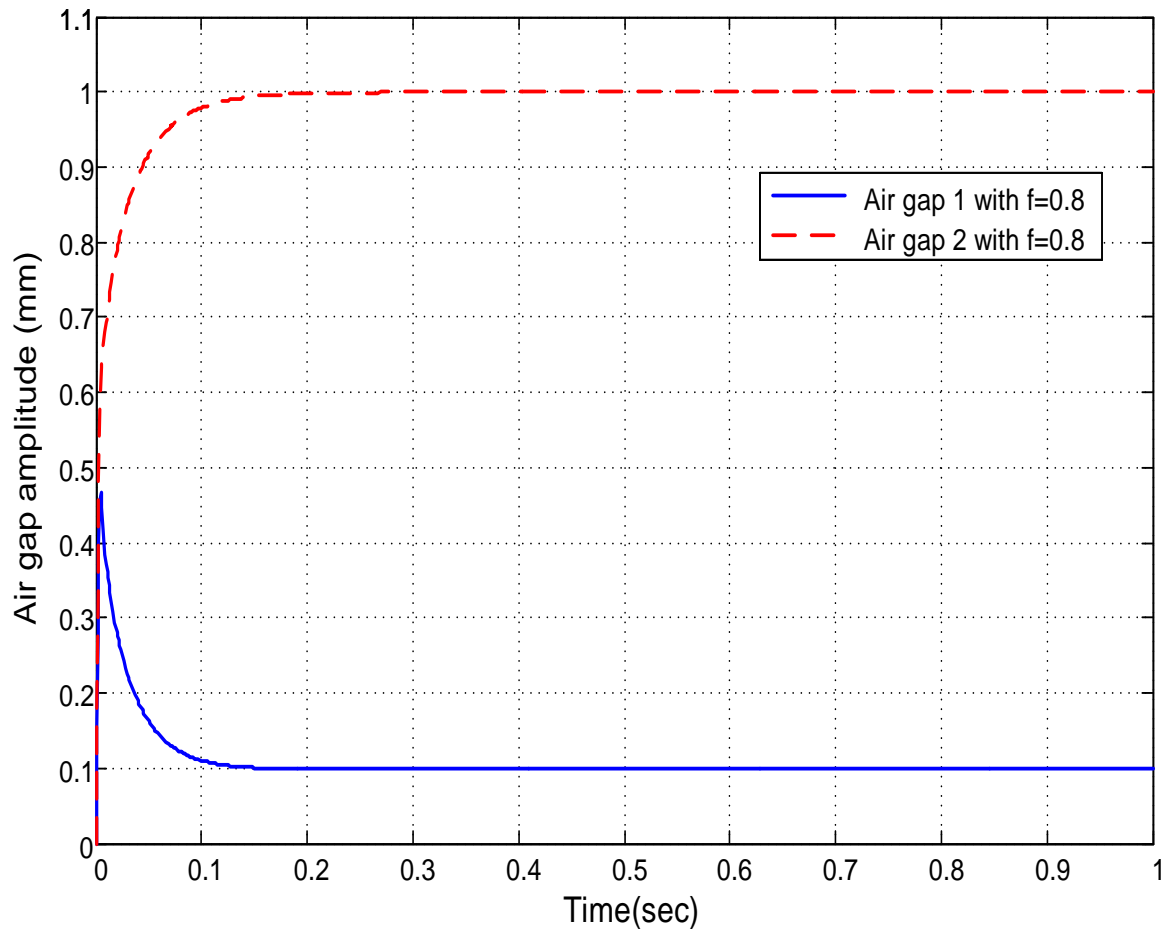


Figure 4.11, Closed Loop Response With $f=0.8$,
Following Unit Step Input at $r_2(s)$

From the previous analysis, it could be concluded that the closed loop system responses show significant improvements with increasing outer-loop feedback gain from $f = 0.1$ to $f = 0.8$. The best responses obtained with feedback $f = 0.8$, give acceptable overshoot and steady state errors. Also the response for all f values show similar interaction between the outputs which is limited to 10%.

From Figure 4.12, and Figure 4.13, to understand the overall system responses with all values of outer loop feedback gain, for unit step inputs on each input reference respectively.

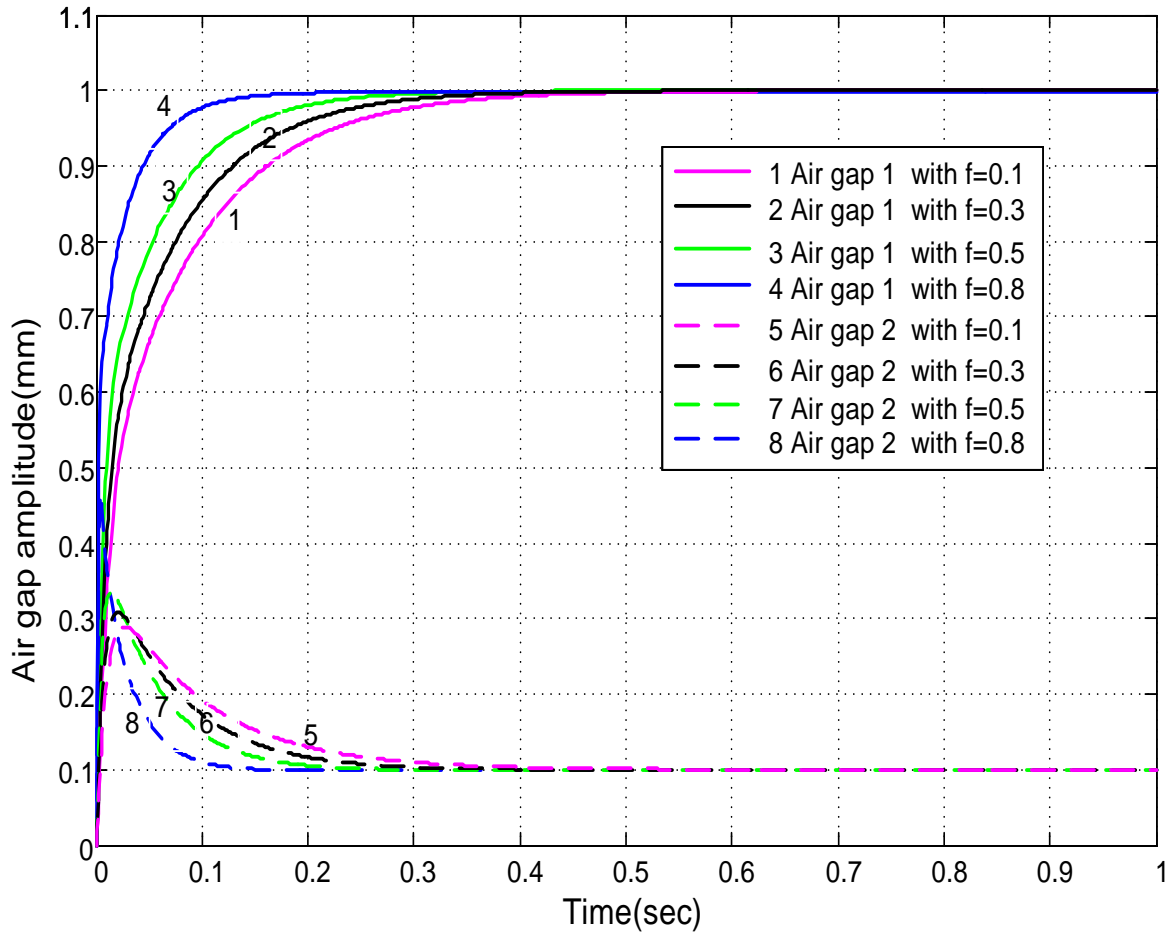


Figure 4.12, Closed Loop Response Following

Unit step input at $\mathbf{r}_1(s)$, $\mathbf{r}_2(s) = 0$

The disadvantages in this procedure, take place when increasing the outer loop feedback gain value up to 0.9 or 1, the simulation with $f = 0.9$, and $f = 1$ shows unacceptable dynamics for the closed loop system. The output responses attract large oscillations showing the best selection of \mathbf{f} for this system was in the range $0.5 \leq f \leq 0.8$,

Notice that other least effort designs could be delivered, according to the selection of steady state matrix \mathbf{S}_s , and value of (b_0) .

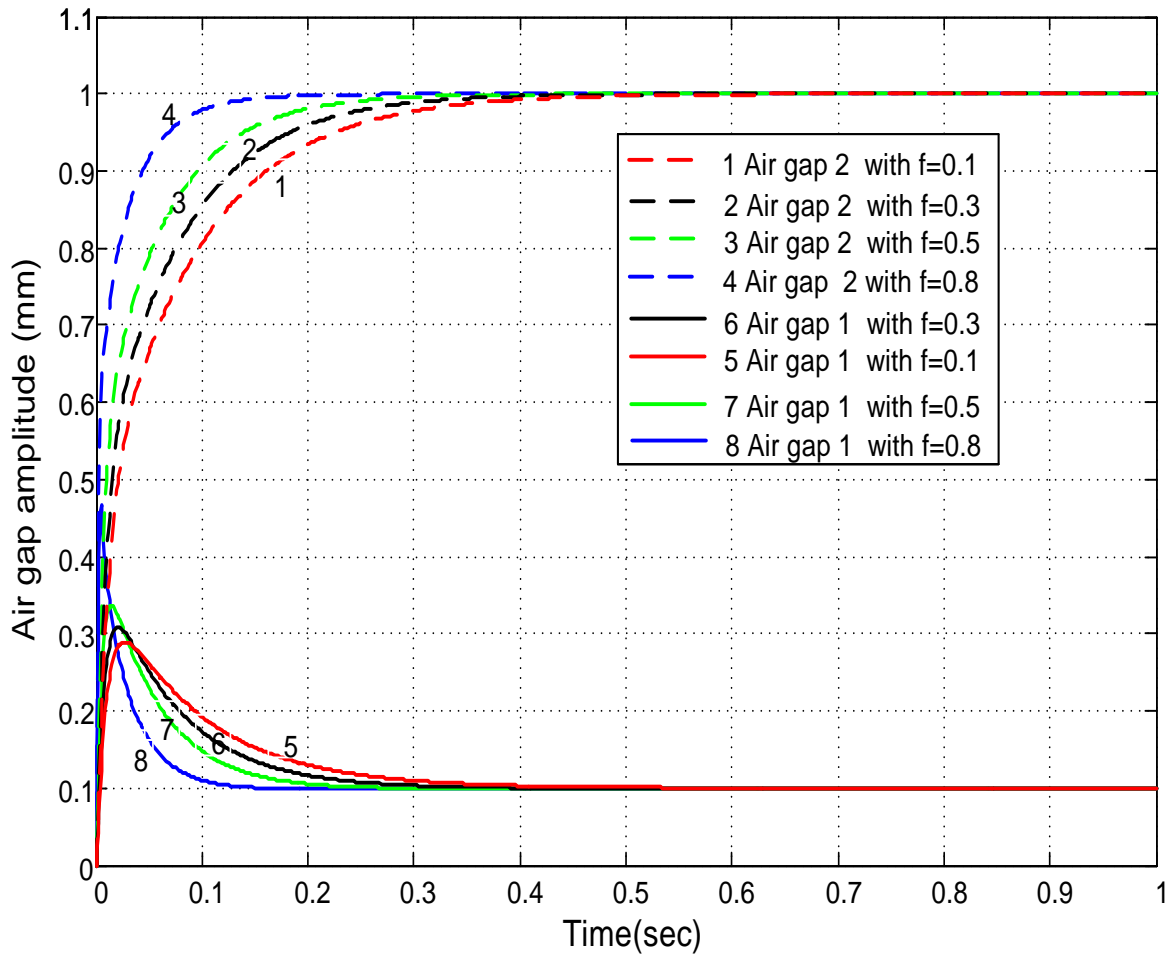


Figure 4.13, Closed Loop Response Following

Unit step input at $r_1(s)$, $r_2(s) = 0$

4.1.5. Disturbance Rejection:

The system performance has also investigated for disturbance rejection, in order to ensure the capability to recover when subjected to external load disturbances. This system was investigated by apply unit step loads on the first output (air gap 1), and increasing the external loop feedback gain f in the range $0.1 < f < 0.8$, where $f_1 = 0.1$, $f_2 = 0.3$, $f_3 = 0.5$, $f_4 = 0.8$, The output results for each value of f will be investigated.

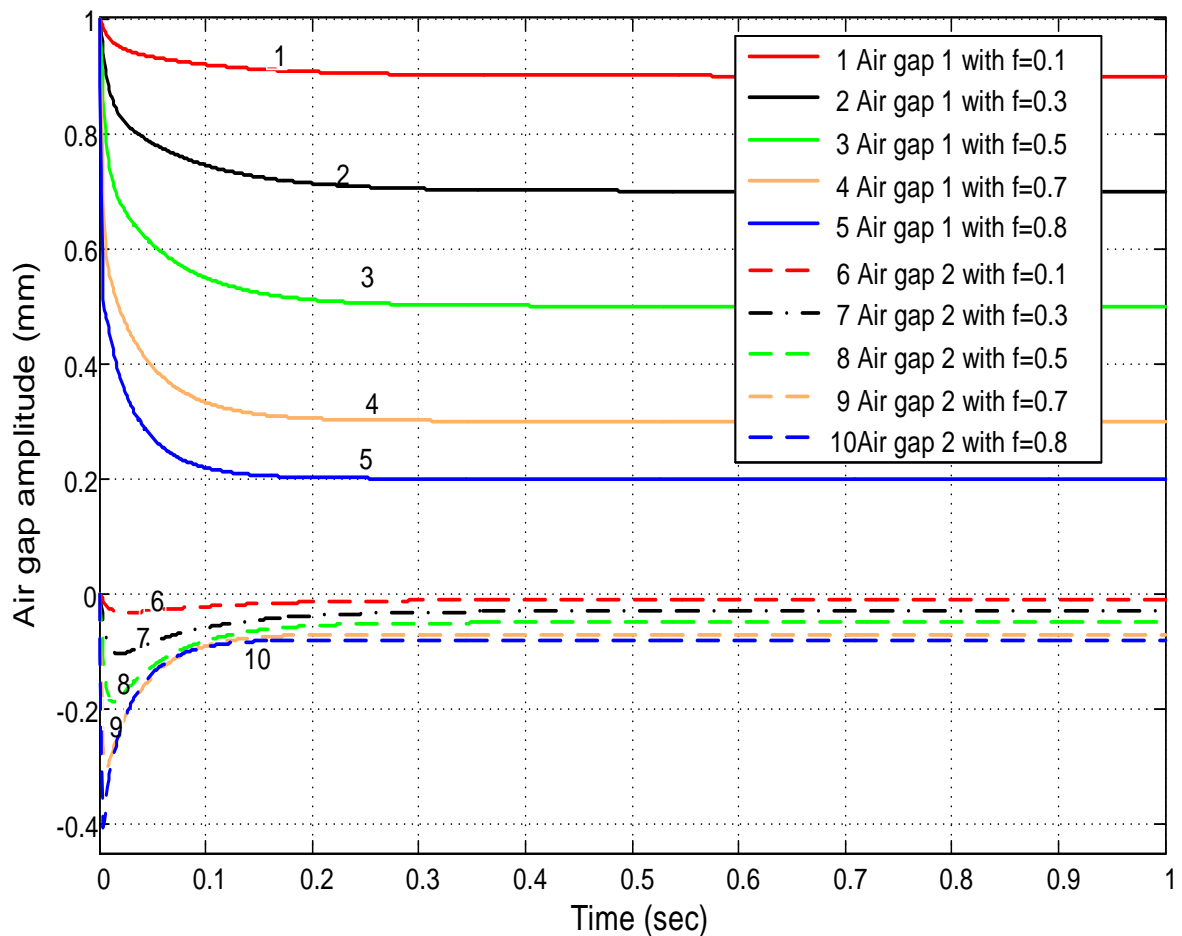


Figure 4.14, Disturbance Rejection With Input at

$$\mathbf{d}_1, \text{ and } \mathbf{r}_1(s) = \mathbf{r}_2(s) = \mathbf{d}_2 = \mathbf{0}$$

The simulation employed on the system model is as shown in the appendix. The output responses can be seen in the Figure 4.14. It is clear from this figure, that the system shows improvements in the disturbance recovery, with $f = 0.1$ where weak disturbance recovery, of about 10 % takes place of up to 30% for $f = 0.3$, with settling time about 0.5 second, with increases up to 50% with $f = 0.5$ for 0.3 sec. The best recovery of 80 % obtained with $f = 0.8$, in a time of 0.38 sec.

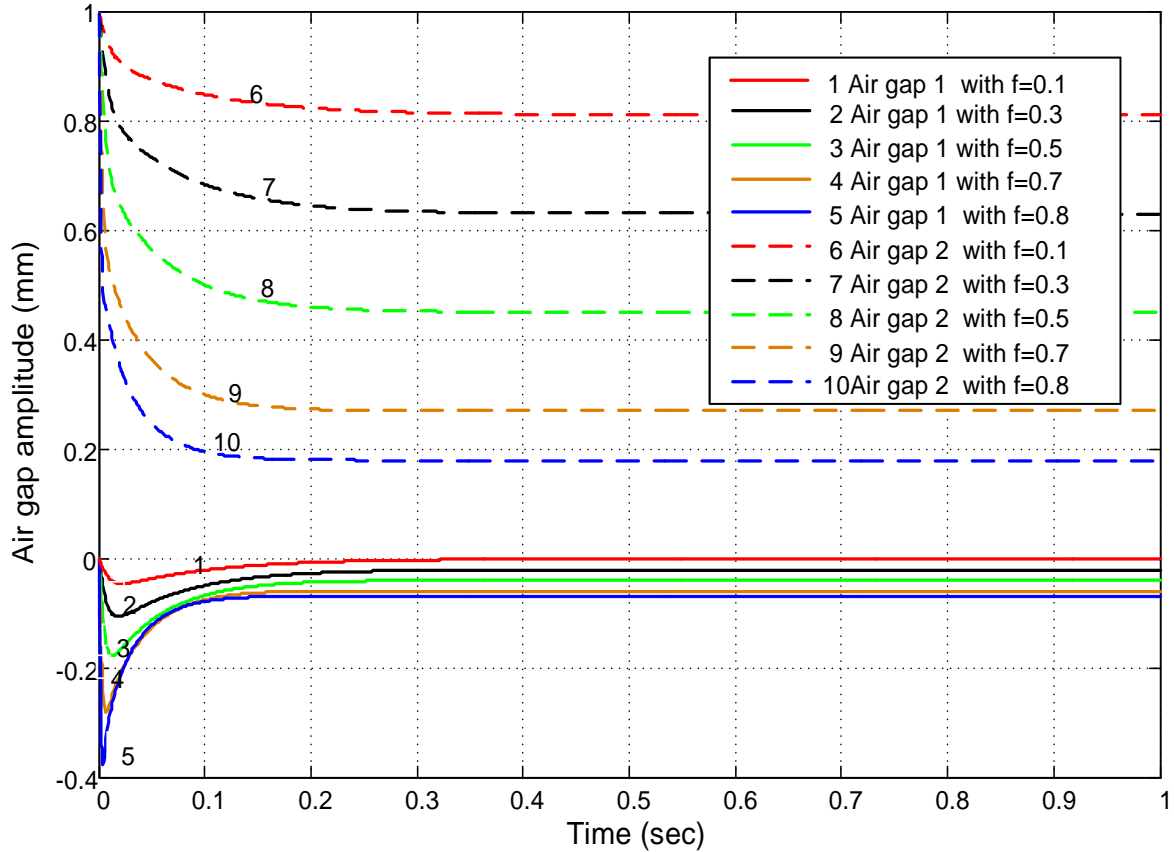


Figure 4.15, Disturbance rejection with unit step input at \mathbf{d}_2 , and $\mathbf{r}_1(s) = \mathbf{r}_2(s) = \mathbf{d}_1 = \mathbf{0}$

In the second investigation, with a unit step disturbance applied on the second output (air gap 2), the system shows similar improvement, as in the first trial. The rate of disturbance recovery increased rapidly in this case following the increasing external loop feedback value. The best results followed $f = 0.8$, with time about 0.2 sec. From the responses it can be seen that the best performance for closed loop system was achieved with external feedback gain of $0.5 \leq f \leq 0.8$, as shown in the Figure 4.15. and demonstrated by minimum rise and settling times, Figure 4.14 & Figure 4.15 shows the response following unit step disturbances on $\mathbf{d}_1(t)$ and then on $\mathbf{d}_2(t)$. These curves illustrate that increasing steady state disturbance suppression has been achieved for $f_1, f_2 > 0.1$ with no ‘cross-talk’ between the outputs.

4.1.6. Control Energy Dissipation

In many cases the required filter has to be realized digitally, attracting thereby implementation costs (Whalley and Ebrahimi, 2006).

As shown in the Figure 4.16, the energy consumed by each of the three controllers can be computed during suppressing random disturbance corresponding to

$$E(t) = \int_0^{t=T} \left(\sum_{j=1}^n k_{y_j}^2 \sum_k^n h_k^2 \right) y_k^2 d(t)$$

With $r_1(t) = r_2(t) = 0$, as illustration in fig (energy fig), the outer- loop gain has been set to $f_1 = f_2 = 0.3$ for purpose of explanation for the minimum effort regulator.

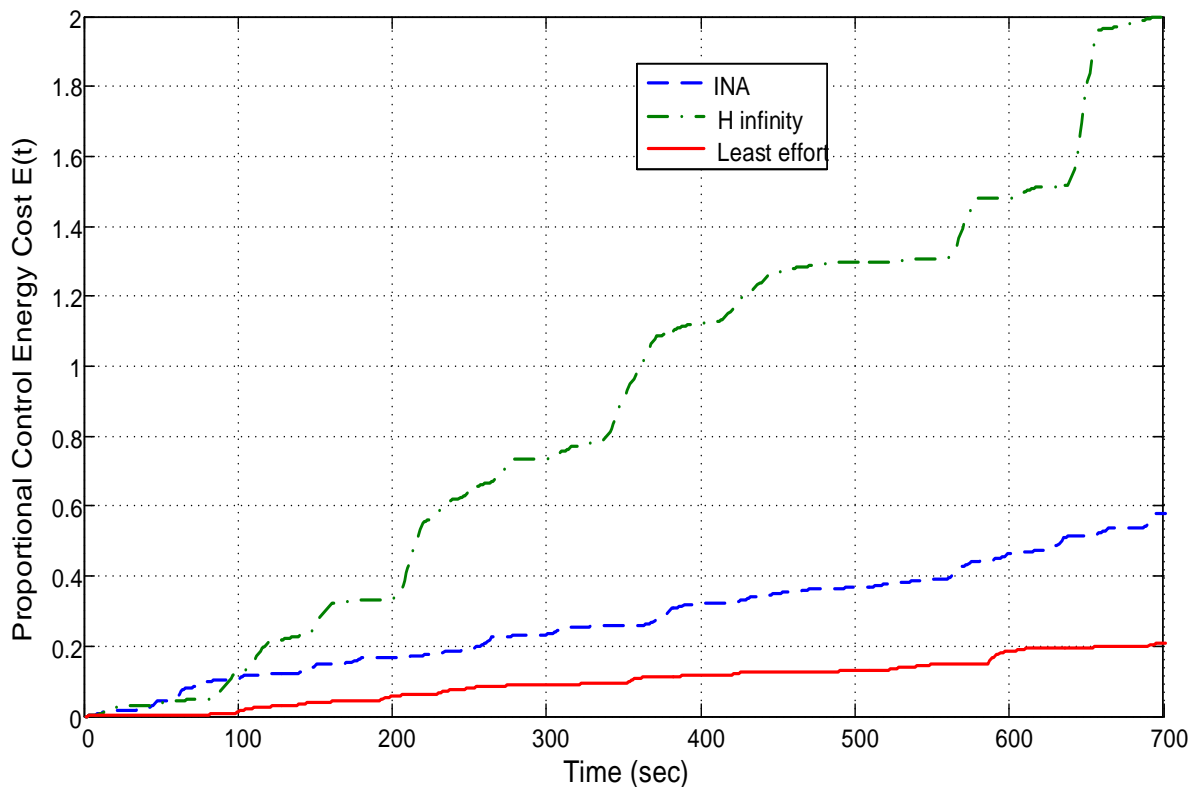


Figure 4.16, Energy Consumed Compared Between Least Effort, INA and H-infinity

It can be seen from the graph that the energy consumed by INA, H infinity controller increases in comparison to that consumed when operating under optimum least effort conditions. This diverging energy difference would manifest itself in terms of increasing control system actuator activity and component wear, generating heat, aging, and noise attracting thereby additional maintenance, wear and power cost.

From the results it can be concluded that the system responses obtained from the new technique (least effort) seems to be more suitable and well behaved. This guarantees the flexibility of the design strategy. The transient response improved by designing the inner loop, while the interaction in the outputs has been reduced by designing the outer loop, by improved disturbance recovery.

4.2. Inverse Nyquist Array Controller Design

The system model transfer function given by equation (4.14) is:

$$G(s) = \frac{1}{(s+1135)(s+10)(s+100)} \begin{bmatrix} 68271.3s + 2,741,092.695 & 553.29s - 1,817,557.65 \\ 553.29s - 1,817,557.65 & 68271.3s + 2,741,092.695 \end{bmatrix} \quad (4.14)$$

$G(s)$ can be inverted, to $\hat{G} =$

$$\begin{bmatrix} \frac{1.465 \times 10^{-5} s^4 + 0.01883 s^3 + 2.576 s^2 + 90.64 s + 667.5}{s^2 + 80.74 s + 903.3} & \frac{-1.187 \times 10^{-7} s^4 + 0.2422 \times 10^{-3} s^3 + 0.4706 s^2 + 48.94 s + 442.6}{s^2 + 80.74 s + 903.3} \\ \frac{-1.187 \times 10^{-7} s^4 + 0.2422 \times 10^{-3} s^3 + 0.4706 s^2 + 48.94 s + 442.6}{s^2 + 80.74 s + 903.3} & \frac{1.465 \times 10^{-5} s^4 + 0.01883 s^3 + 2.576 s^2 + 90.64 s + 667.5}{s^2 + 80.74 s + 903.3} \end{bmatrix} \quad (4.15)$$

The diagonally dominant of \hat{G} can be investigated by plotting Nyquist diagrams with Gershgorin circles using m-file cod (Appendix B) for the inverted transfer function matrix \hat{G} , Figure 4.17, and figure 4.18 showing Nyquist plot with Gershgorin bands for \hat{g}_{11} , \hat{g}_{22} respectively. It can be seen from the graph that the system is column dominant since the Nyquist diagram for each \hat{g}_{11} , \hat{g}_{22} shows that none of the Gershgorin circles are enclose the origin.

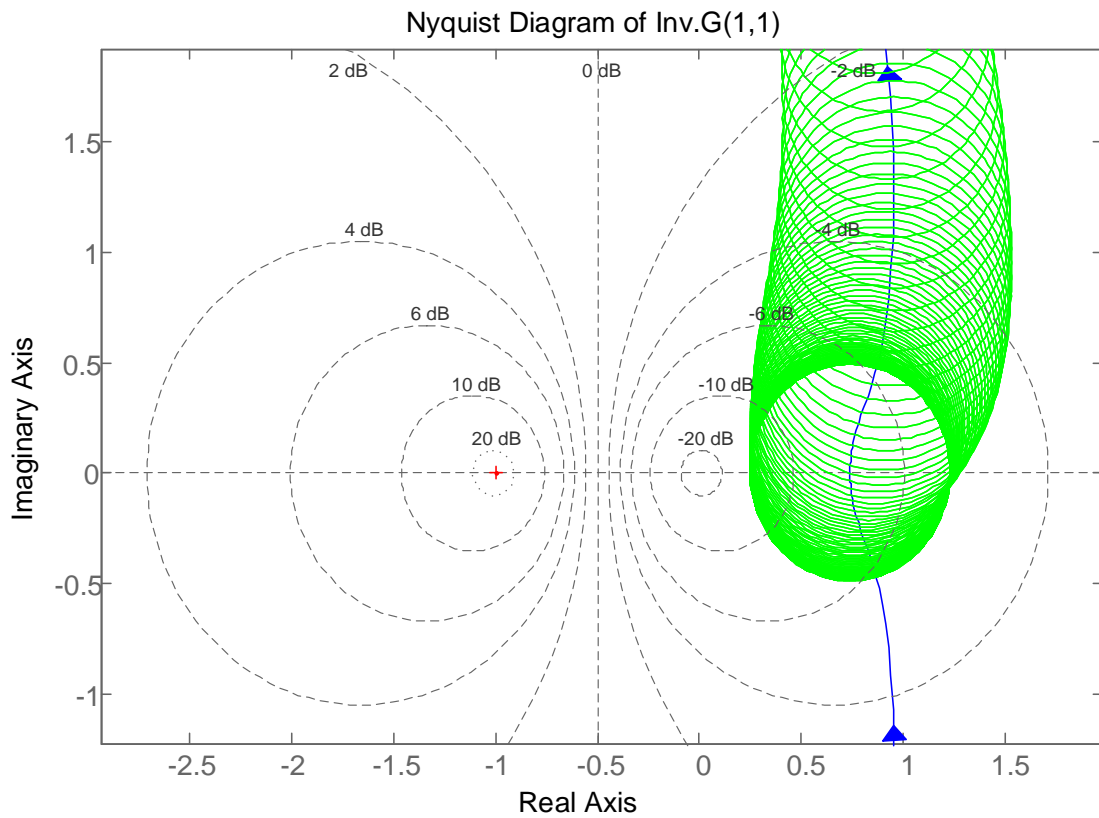


Figure 4.17, Nyquist diagram of \hat{g}_{11} with Gershgorin bands

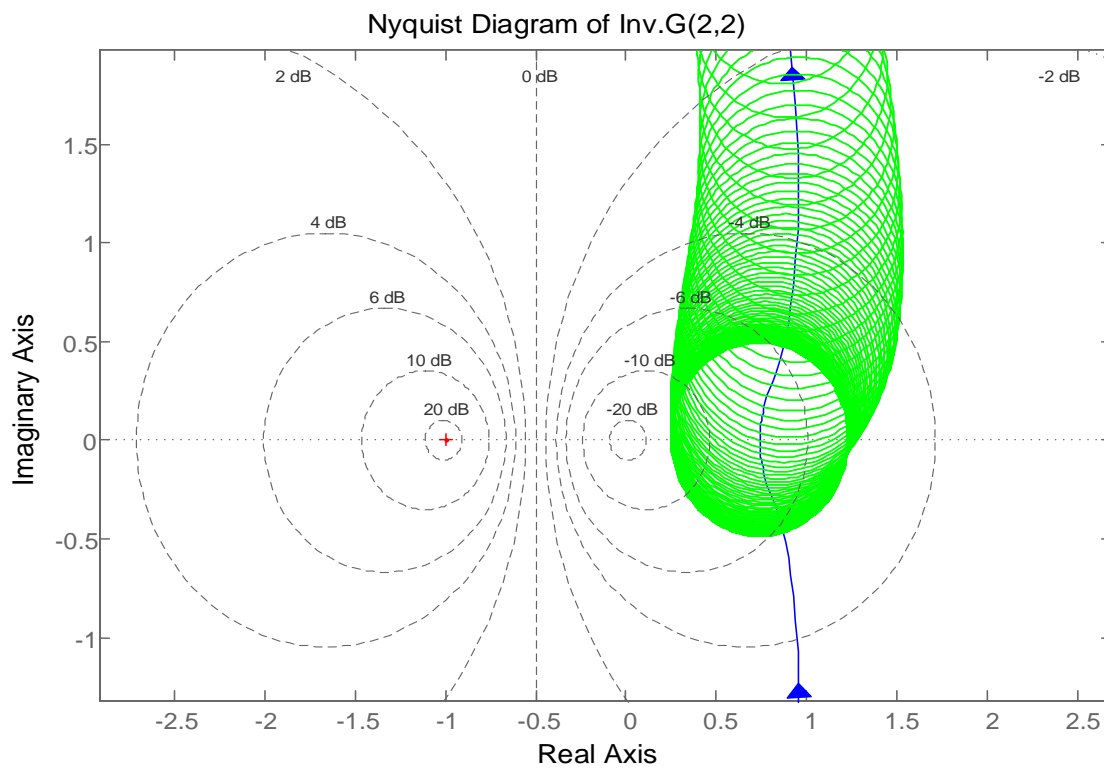


Figure 4.18, Nyquist diagram of \hat{g}_{22} with Gershgorin bands

By using elementary matrix operation, for row (or column) elements of \hat{G} the dominance condition can be changed. According to the equation (3.41), the next step is to select a pre compensator $\hat{k}(s)$ in order to achieve the diagonally dominant of invers matrix $\hat{Q}(s)$ let set $\hat{k}(s) = \hat{k}_1(s)\hat{k}_2(s)$, Then the equation (3.41) become

$$\hat{Q}(s) = \hat{k}_1(s)\hat{k}_2(s)\hat{G}(s) \quad (4.16)$$

$$\text{Let } \hat{k}_1(s) = \begin{bmatrix} 1 & -0.03 \\ -0.03 & 1 \end{bmatrix}, \quad \text{and} \quad \hat{k}_2(s) = \begin{bmatrix} 2 & 0 \\ 0 & 2 \end{bmatrix}$$

$$\text{Hence } \hat{Q}(s) = \begin{bmatrix} 1 & -0.03 \\ -0.03 & 1 \end{bmatrix} \begin{bmatrix} 2 & 0 \\ 0 & 2 \end{bmatrix}$$

$$\begin{bmatrix} \frac{1.465 \times 10^{-5} s^4 + 0.01883 s^3 + 2.576 s^2 + 90.64 s + 667.5}{s^2 + 80.74 s + 903.3} & \frac{-1.187 \times 10^{-7} s^4 + 0.2422 \times 10^{-3} s^3 + 0.4706 s^2 + 48.94 s + 442.6}{s^2 + 80.74 s + 903.3} \\ \frac{-1.187 \times 10^{-7} s^4 + 0.2422 \times 10^{-3} s^3 + 0.4706 s^2 + 48.94 s + 442.6}{s^2 + 80.74 s + 903.3} & \frac{1.465 \times 10^{-5} s^4 + 0.01883 s^3 + 2.576 s^2 + 90.64 s + 667.5}{s^2 + 80.74 s + 903.3} \end{bmatrix} \quad (4.17)$$

In similar procedure, by plotting Nyquist diagram for equation (4.17), the general view of the Nyquist diagram for \hat{q}_{11} with Gershgorin bands shown in Figure 4.19.

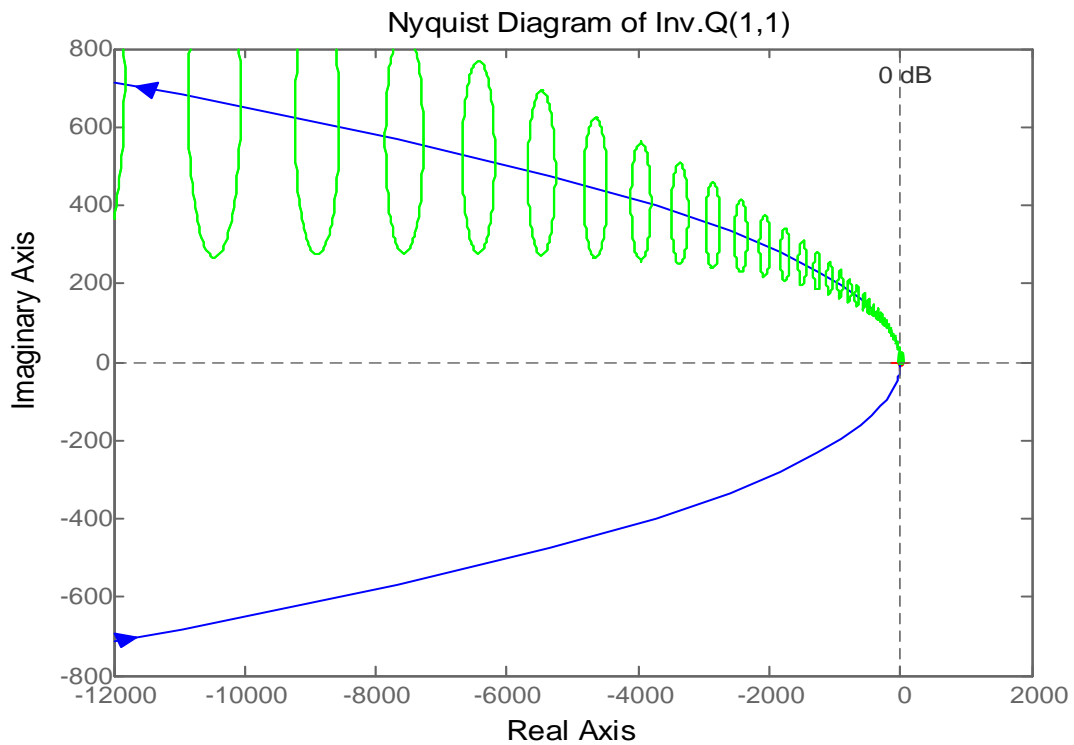


Figure 4.19, Overview Of Nyquist Plot With Gershgorin Circles For Element \hat{q}_{11}

It is clear from figure 4.19, there is no intersection with the negative real axis. For the enlarged Nyquist plot with Gershgorin circles for \hat{q}_{11} and \hat{q}_{22} , shown in Figure 4.20 and Figure 4.21 respectively.

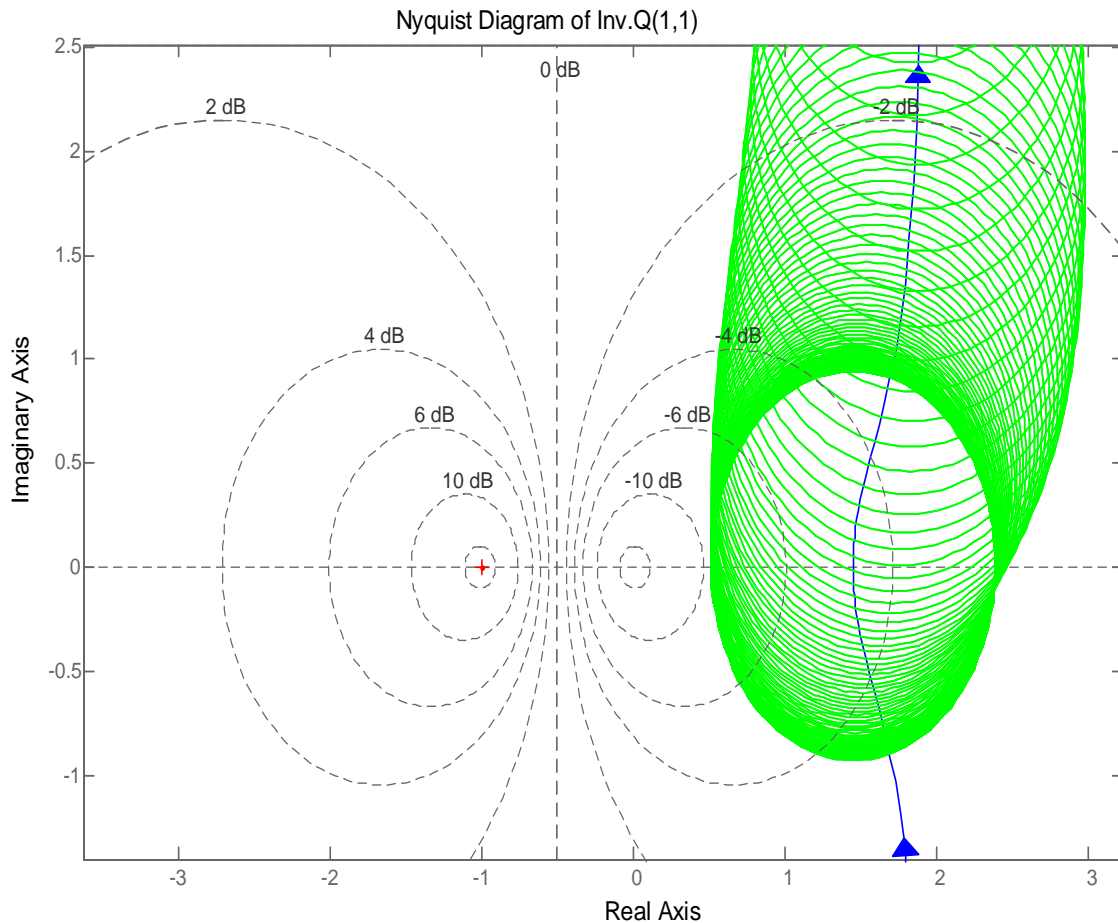


Figure 4.20, Nyquist diagram of \hat{q}_{11} with Gershgorin circles

The Nyquist plot of the first column element \hat{q}_{11} shows that none of the circles enclose the origin, so the system is column diagonally dominant, and the Nyquist plot for the second column element \hat{q}_{22} , again shows none of Gershgorin circles encircle the origin, so that the system is second column diagonally dominant.

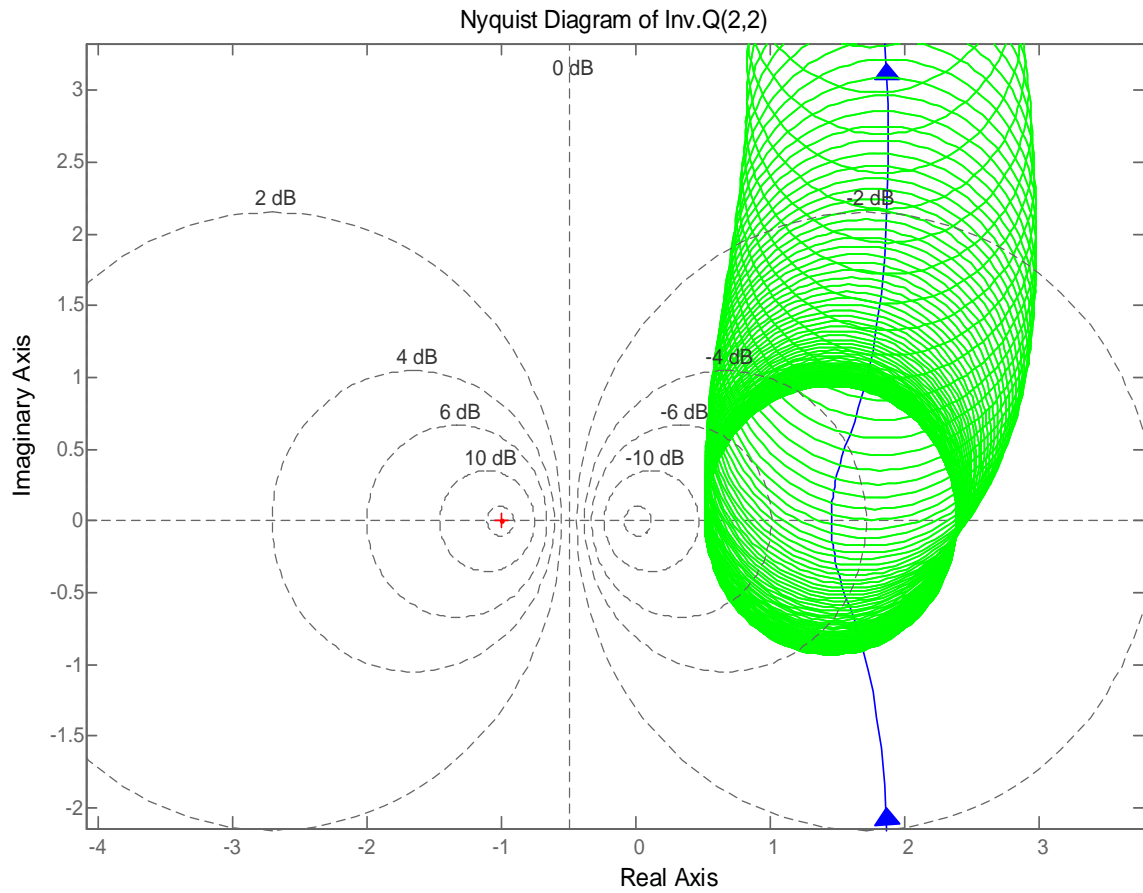


Figure 4.21, Nyquist Diagram of \hat{q}_{22} with Gershgorin Circles

4.2.1. Dynamic Controller

Since the diagonally dominance is achieved, in the next step a dynamic controller for each loop designed. Initially, default to a unity P+I compensator and having transfer function matrix of:

$$K_3(s) = \begin{bmatrix} \frac{s+50}{s} & 0 \\ 0 & \frac{s+50}{s} \end{bmatrix} \quad (4.18)$$

Then the overall controller would be

$$k(s) = [\hat{k}_2 \hat{k}_1]^{-1} K_3(s) = \left\{ \begin{bmatrix} 2 & 0 \\ 0 & 2 \end{bmatrix} \begin{bmatrix} 1 & -0.03 \\ -0.03 & 1 \end{bmatrix} \right\}^{-1} \begin{bmatrix} \frac{s+50}{s} & 0 \\ 0 & \frac{s+50}{s} \end{bmatrix}$$

$$\text{Then } k(s) = \frac{1}{s} \begin{bmatrix} 0.5005s + 25.02 & 0.0150s + 0.7507 \\ 0.0150s + 0.7507 & 0.5005s + 25.02 \end{bmatrix} \quad (4.19)$$

The final simulation model is given in Appendix 2, the closed loop feedback gain f would be unity for each loop. Figure 22 and figure 23, shows the simulation results for the closed loop response following unit step change on $\mathbf{r}_1(s)$ and then on $\mathbf{r}_2(s)$, respectively.

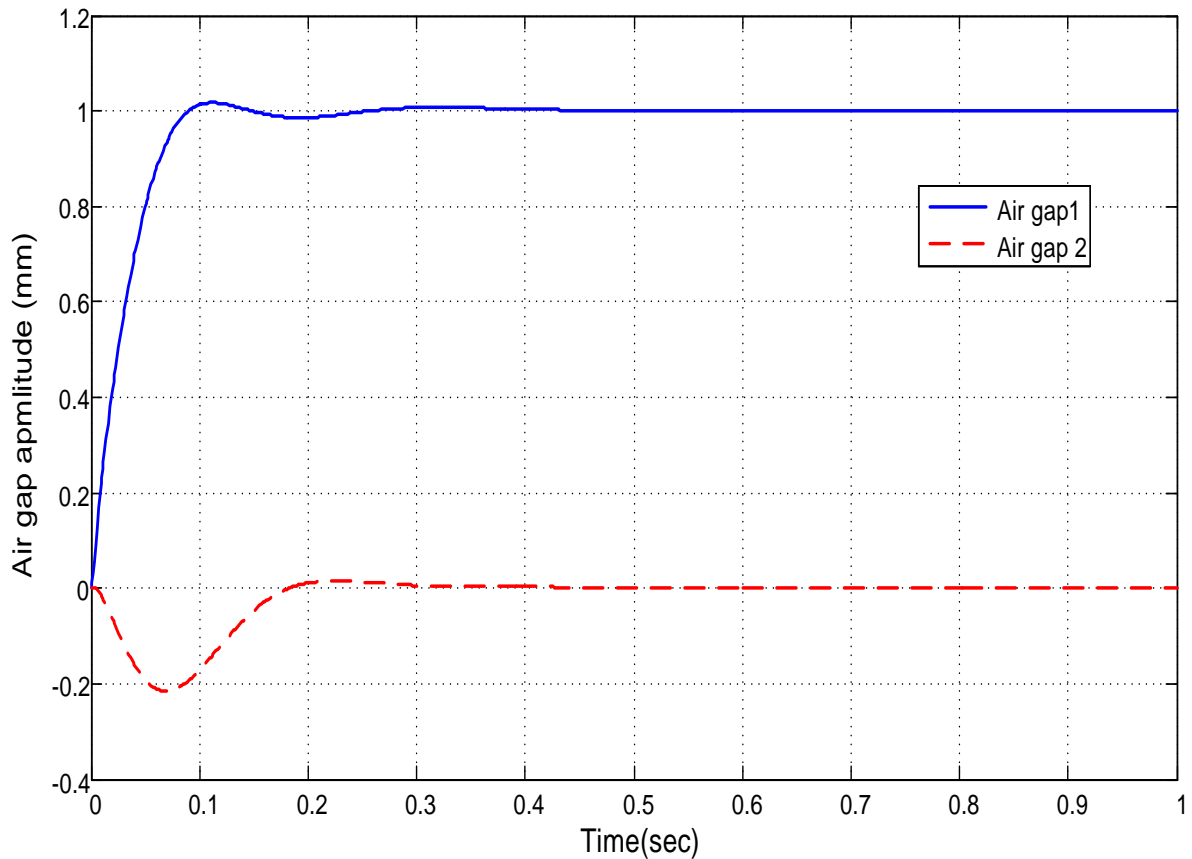


Figure 4.22, INA -Closed Loop Response Following Unit Step Input at $\mathbf{r}_1(s)$

The first output following a unit step change on the first input $\mathbf{r}_1(s)$, can be seen from Figure 4.22 giving the system response for air gap 1. With a settling time about 0.45sec. There is a steady state error introduced in the first output response, while the output response for air gap 2, for the same input, has acceptable dynamics with a higher steady state error and settling time of about 0.75 sec. with the system completely decoupled.

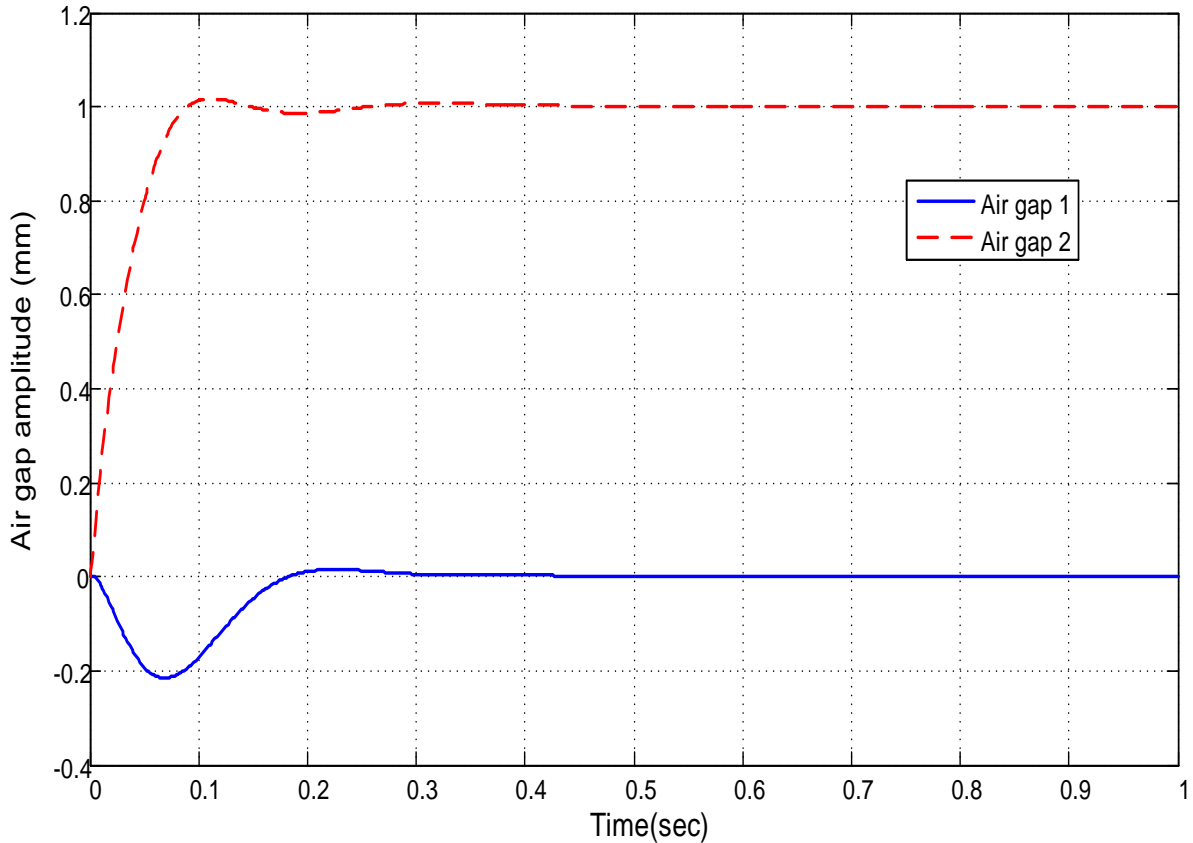


Figure 4.23, INA -Closed Loop Response Following Unit Step Input at $r_2(s)$

For the system responses following unit step change in $r_2(s)$, shown in Figure 4.23, it can be seen that the outputs responses for both air gap 1 and air gap 2 acceptable and the output response for air gap 1 shows good dynamics with a small steady state error and settling time about 0.75 sec, with a very small overshoot. The output of air gap 2 response is also very good with a minor overshoot, and small settling time of about 0.45sec. The system is completely decoupled with little output cross talk.

4.3. H_∞ -Controller Design

The controller design procedure explained in chapter 3, by selecting frequency weighing matrix $\mathbf{W}(i\omega)$, considering that the largest singular value of $\mathbf{W}(i\omega)$ is closed to unity, in a

specific frequency range $0 \leq \omega \leq \omega_0$, with roped decay to zero for higher frequency in $\omega > \omega_0$, so that we could select weight's functions as

$$\mathbf{W}_1 = \begin{bmatrix} \frac{100}{s+0.5} & 0 \\ 0 & \frac{100}{s+1} \end{bmatrix}, \quad \mathbf{W}_2 = \mathbf{I}, \text{ to avoid the singularity issues, and } \mathbf{W}_3 = \begin{bmatrix} \frac{s}{1000} & 0 \\ 0 & \frac{s}{200} \end{bmatrix}$$

By using MATLAB command code 'augf' as in the attached appendix, the variable Gamma (γ) of the system transfer function can be obtained, by using the command "hinftot". In MATLAB we can obtain \mathcal{H}_∞ optimal which following the interaction used to obtain minimum Gamma (γ_{\min})

```

<< H-Infinity Optimal Control Synthesis >>
No      Gamma    D11<=1  P-Exist  P>=0    S-Exist  S>=0    lam(PS)<1  C.L.
-----
1  1.0000e+00  OK      FAIL     FAIL     OK       OK       OK          UNST
2  5.0000e-01  OK      OK       OK       OK       OK       OK          STAB
3  7.5000e-01  OK      FAIL     FAIL     OK       OK       OK          UNST
4  6.2500e-01  OK      OK       FAIL     OK       OK       OK          UNST
5  5.6250e-01  OK      OK       FAIL     OK       OK       OK          UNST
6  5.3125e-01  OK      OK       OK       OK       OK       OK          STAB
7  5.4688e-01  OK      OK       OK       OK       OK       OK          STAB
8  5.5469e-01  OK      OK       FAIL     OK       OK       OK          UNST
9  5.5078e-01  OK      OK       FAIL     OK       OK       OK          UNST

Iteration no. 7 is your best answer under the tolerance: 0.0100.

```

Table 1, Results Obtained from MATLAB for \mathcal{H}_∞ Optimal Control Synthesis

As it clear from the table 1, the interaction number 7 is the best answer, with

$\gamma_{\min} = 5.4688e - 01$, therefore the controller equation

$$\mathbf{K}(s) = \begin{bmatrix} K_{11}(s) & K_{12}(s) \\ K_{21}(s) & K_{22}(s) \end{bmatrix} \quad (4.20)$$

where:

$$K_{11}(s) = \frac{4695.2 (s + 1135) (s + 1144) (s + 449.4) (s + 100) (s + 47.63) (s + 10) (s + 1)}{(s + 5088) (s + 1307) (s + 1139) (s + 258.5) (s + 71.07) (s + 17.99) (s + 1) (s + 0.5)}$$

$$K_{12}(s) = \frac{4553.1 (s + 1187) (s + 1135) (s + 100) (s + 10) (s + 0.5) (s^2 + 162.7s + 1.516e04)}{(s + 5088) (s + 1307) (s + 1139) (s + 258.5) (s + 71.07) (s + 17.99) (s + 1) (s + 0.5)}$$

$$K_{21}(s) = \frac{4538.7 (s + 1135) (s + 1137) (s + 100) (s + 10) (s + 1) (s^2 + 166.4s + 1.6e04)}{(s + 5088) (s + 1307) (s + 1139) (s + 258.5) (s + 71.07) (s + 17.99) (s + 1) (s + 0.5)}$$

$$K_{22}(s) = \frac{4939.2 (s + 1135) (s + 1090) (s + 443.2) (s + 100) (s + 47.68) (s + 10) (s + 0.5)}{(s + 5088) (s + 1307) (s + 1139) (s + 258.5) (s + 71.07) (s + 17.99) (s + 1) (s + 0.5)}$$

Then the controller $K(s)$, could be written in the final form:

$$K(s) = \left[\begin{array}{c} \frac{4695.2 (s+1135) (s+1144) (s+449.4) (s+100) (s+47.63) (s+10) (s+1)}{(s+5088) (s+1307) (s+1139) (s+258.5) (s+71.07) (s+17.99) (s+1) (s+0.5)} \\ \frac{4538.7 (s+1135) (s+1137) (s+100) (s+10) (s+1) (s^2 + 166.4s + 1.6e04)}{(s+5088) (s+1307) (s+1139) (s+258.5) (s+71.07) (s+17.99) (s+1) (s+0.5)} \\ \frac{4553.1 (s+1187) (s+1135) (s+100) (s+10) (s+0.5) (s^2 + 162.7s + 1.516e04)}{(s+5088) (s+1307) (s+1139) (s+258.5) (s+71.07) (s+17.99) (s+1) (s+0.5)} \\ \frac{4939.2 (s+1135) (s+1090) (s+443.2) (s+100) (s+47.68) (s+10) (s+0.5)}{(s+5088) (s+1307) (s+1139) (s+258.5) (s+71.07) (s+17.99) (s+1) (s+0.5)} \end{array} \right] \quad (4.21)$$

It is clear from the equation (4.21), that the compensator functions are very complex sub-systems, non-minimum phase, with high order, since the numerator order is 7, while for the denominator it is of order 8. The system will be investigated with the designed controller by using the simulated model in Matlab. H-infinity system block diagram and simulation model can be seen in the appendix (A).

Unit step changes applied on the first input $r_1(s)$, and then on the second input $r_2(s)$, will be applied. The responses of the closed-loop system following a unit step change as in the Figure 4.24, on the first input set point $r_1(s)$,

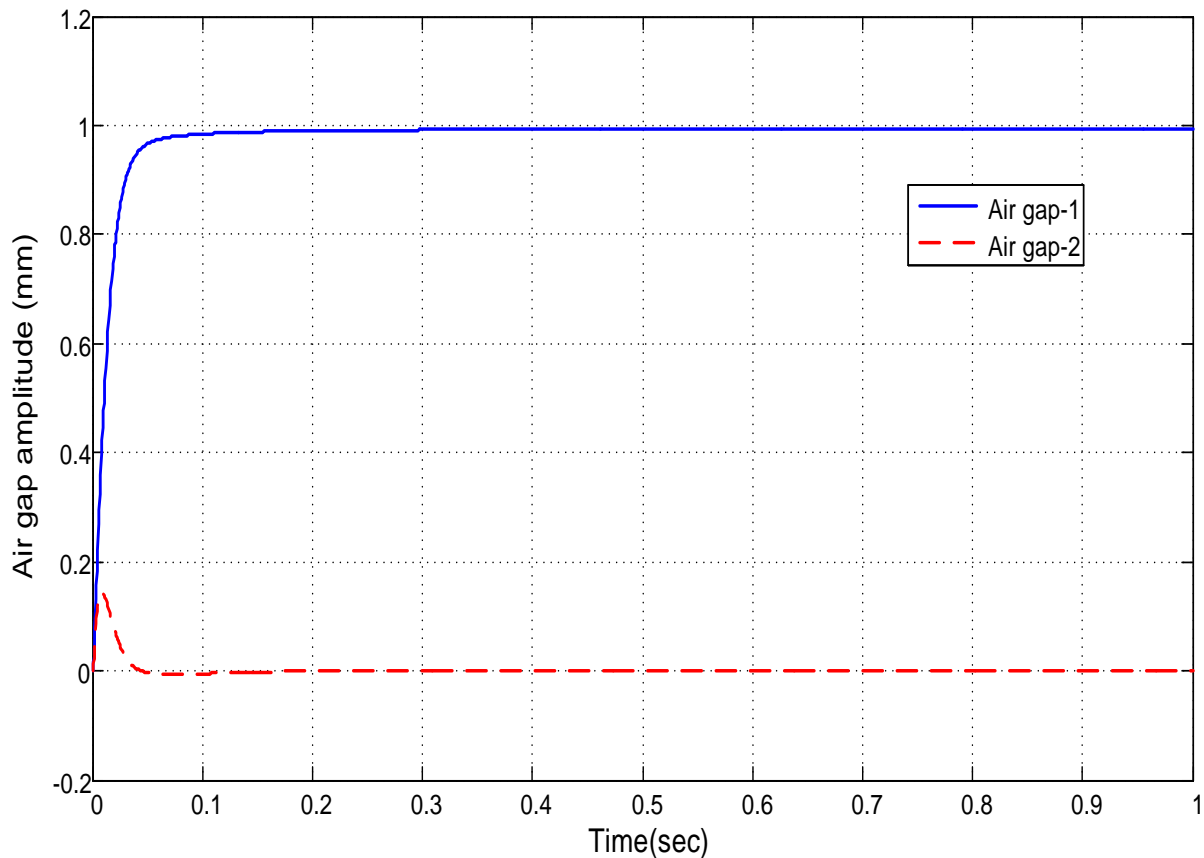


Figure 4.24, System Response Following
Unit Step Change On $r_1(s)$

The first output, air gap 1 displays critically damped transients with rapid response with a small steady state error with the required time (both rising and settling time) of about 0.2 second. The second output (air gap 2) also has the similar behavior, results rapid, stable responses in time about 0.1 sec to reach the steady state, It is clear from the graph that there are zero interaction between outputs and no cross talk.

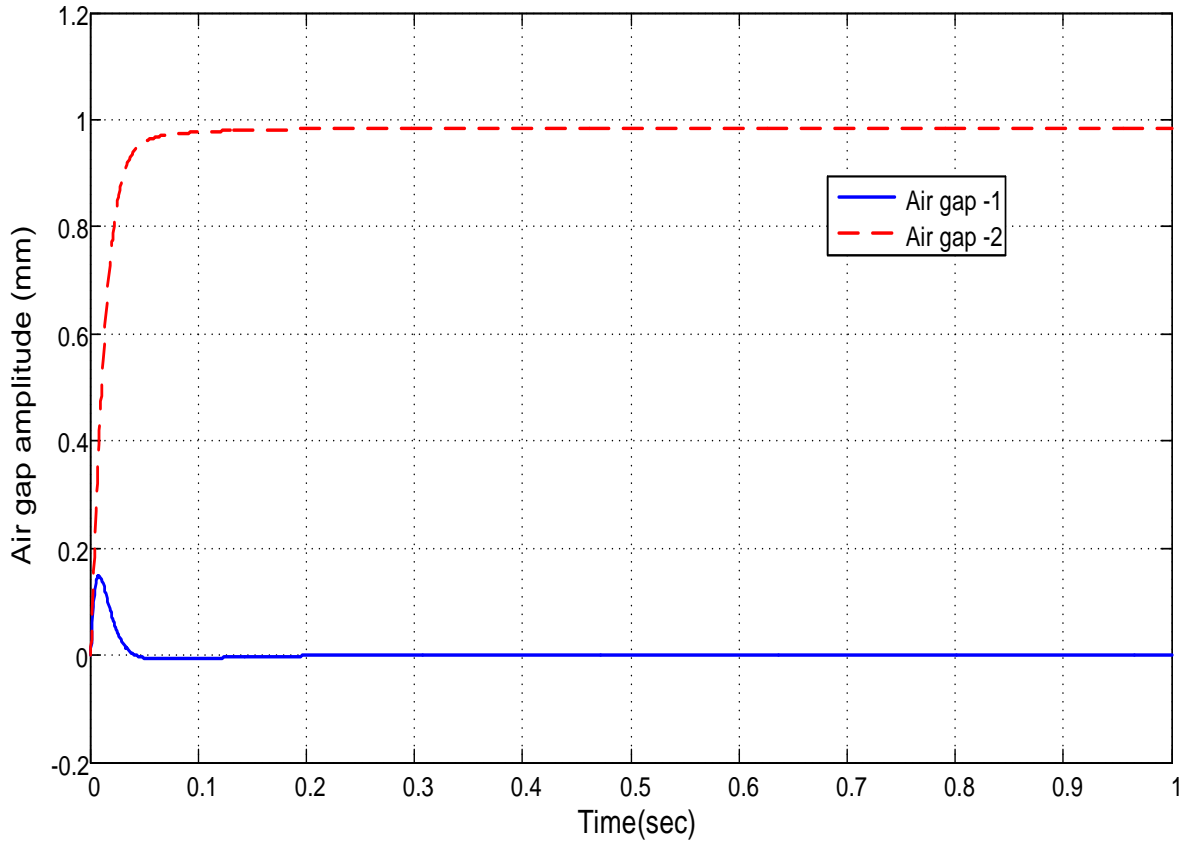


Figure 4.25, System Response Following
Unit Step Change On $r_2(s)$

In the second case, a unit step input is applied on the second reference $r_2(s)$, The output response is shown t in the figure 4.25, Both responses for air gap 1 and air gap 2 are fast and stable. The first response is critically damped, showing no steady state error and the second response (air gap 2) is fast and stable with no interaction. Generally, the responses in both cases are similar. This similarity is due to similarity in the system transfer function matrix.

4.4.Comparison study

Three significant system control techniques were studied in this research, Least effort technique, Inverse Nyquist Array (INA), and H-infinity methodology. The areas of comparison were, the restrictions and difficulties of practical application, outputs responses for the closed-loop system following unit step changes separately on each of system inputs,

the rejection of external disturbance, and stability of each system for each control technique by applying step change separately on each output of the closed loop system, the investigated methods (technique) allow multivariable systems to be expanded from a frequency domain rather than the state-space standpoint.

The main investigated technique was the Least effort approach with attempt to analyse the system inner and outer loop, system optimization in order to minimize the performance index, disturbance rejection and stability. The inner loop design gives an effective method for improving the transient response, while the outer loop design is constructed to achieve robustness by reducing output interaction to enhance the disturbance rejection performance. The main purpose of this technique is to minimize the control effort required.

The Inverse Nyquist Array (INA) method has also been studied, which aims to approximate diagonalization, by achieving transfer function diagonal dominance, in order to remove the interaction between the system outputs. Then an independent compensator could be designed by using normal SISO methods. In addition, the H-Infinity approach was considered which directly addresses the problem of robustness by deriving a controller which maintains system response and errors within allowable tolerances, reducing noise in the system. The main step to achieve that by partitioning the system, the controller generated H-Infinity technique is of higher order and more complicated than the controller created by the other methods.

4.4.1. Closed Loop Responses Comparisons

The Closed-loop response following the application of these controllers was similar with each almost identical. All of them show performance and good responses to the inputs, and disturbance recovery. However, each of these methods has different features depending on the complexity of system transfer equation.

The least effort controller response are robust, rapid and well performed, it is succeeded to minimize the interaction in system outputs which were maintained at the designed value which is 10%. In comparison, the least effort controller is simpler and require less control effort than the INA and H-infinity, which employ perfect integrators and relatively high gain. In comparison on system response following step change at r_1 for all three methods shown in Figure 4.26.

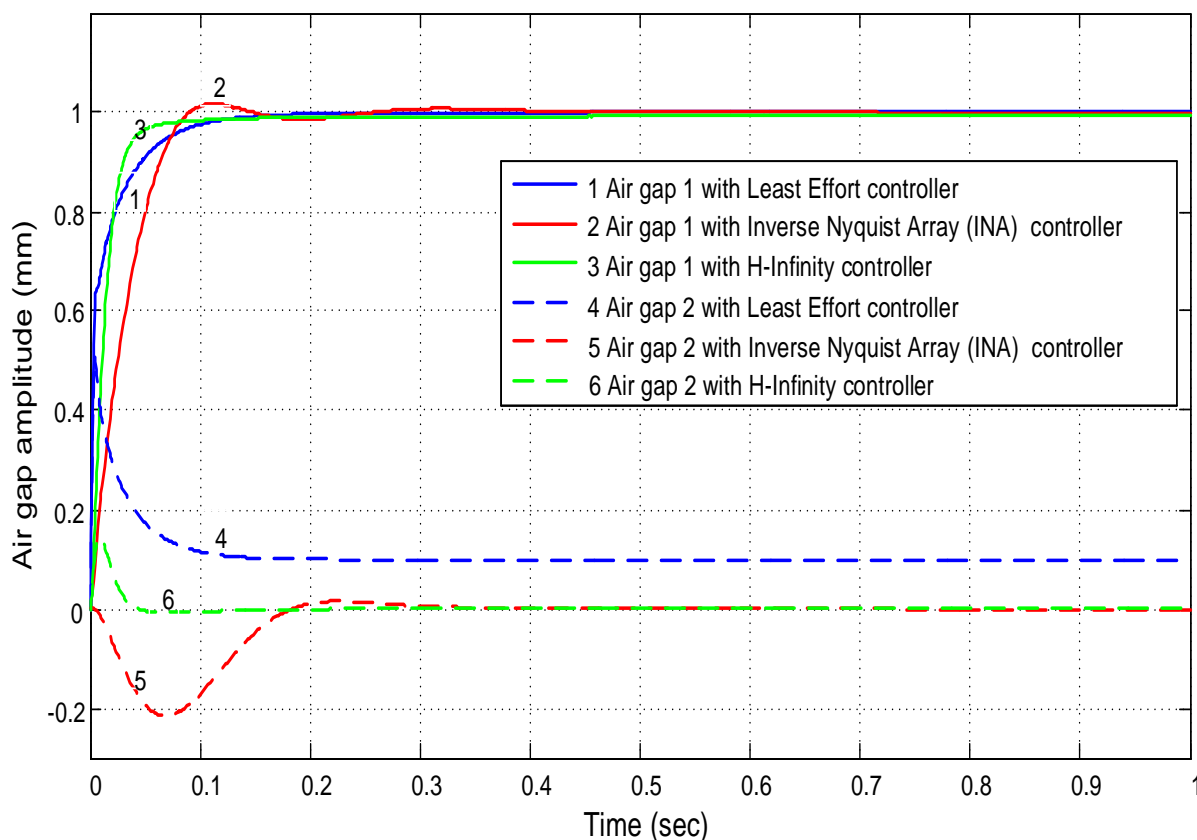


Figure 4.26, System response following step change at $r_1(s)$ for all three controllers

It can be seen that the response of Least effort controller reaches to steady state for the first output air gap with critical damping, very fast to reach the designed steady state with about 0.2 second , with very small steady state errors, which do not affecting the system performance, The second output took only 0.15 second to reach the designed steady state, with a small, accepted overshoot.

For the INA the system response for air gap 1, is very rapid and stable required 0.45 sec in the response for INA controller with slight over shoot. There is a steady state error introduced in the first output response, while the output response for air gap 2 for the same input, has acceptable dynamics with higher steady state error and a settling time about 0.75 sec. The system is completely decoupled. while for H-infinity controller responses following unit step change on the first input set point $r_1(s)$, the first output (air gap 1) display critically damped system with rapid response with steady state error, the required time (both rising and settling time) was about 0.2 second. The second output (air gap 2) also have the similar behavior were quick and stable with responses time of about 0.1 sec to reach the steady state. It is clear from the graph that zero interactions between the outputs and no cross talk was achieved.

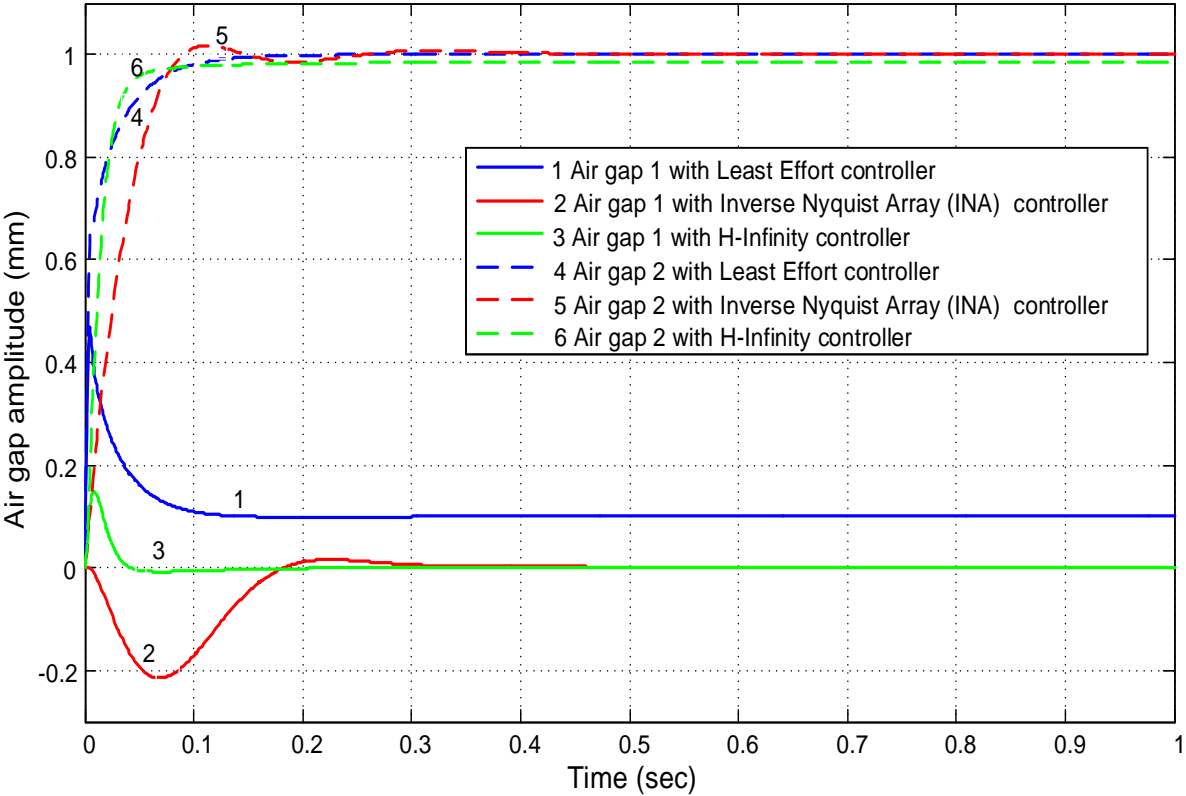


Figure 4.27, Comparison responses following step change

at $r_2(s)$ for all three methods

Rotating the input to the reference $\mathbf{r}_2(s)$, the output responses for three of technique shown in the Figure 4.27, it can be seen that the results are similar to these obtained in the first input, the simulation results with Least effort controller showing good improvements in the system outputs to meet the targeted values very quickly, since the first output registered time of only 0.15 second, to reach the desired value, while the second output achieved the suggested steady state within 0.33 seconds.

The steady state errors has been minimized with INA controller by using PI, it can be seen from Figure 4.27 the outputs response for both air gap 1 and air gap 2 are well performed. The output response for air gap 1 has acceptable dynamics with a small steady state error and settling time about 0.75 sec, and very small overshoot, while the output of air gap 2 transient response is very good with a minor overshoot, small settling time about 0.45sec. The system is completely decoupled with no output cross talk.

The Inverse Nyquist array methodology is not easy to apply for many applications, because it depends on the identification of a pre compensator in order to achieve diagonally dominance, for the inverted open loop system transfer function. Since there is no regular or typical procedure for this, each system model has to be investigated. The system model studied in this research with the consideration of the suggested filters, is almost diagonally dominant, for small values of the pre compensator matrices.

The controller designed by H-infinity approach shows good response with small steady state errors about 0.04% less than the reference set point of air gap, indicating decidability of the controller to reach the designed set point. Attention is immediately draw to the very complexity of controller functions generated by H-infinity technique. Devotees of this choice of regulation may suggest that the reduction methods could be engaged to provide lower order controller functions. However, stability couldn't be guaranteed by this approach let alone optimality.

It was clearly noticed from the response following the controller for the INA and H infinity, that the second output of air gap was 0 mm, which means the possibility of physical contact between the car body and the train guideway, would take place, while the least effort controller showing very good results, the response of air gap reach to the value exactly same as reference set point with no steady state errors. The second response of air gap value of 0.1 mm, which is exactly same as the designed value of (Ss) matrix.

4.4.2. Disturbance Rejection Results

The other significant area of comparison between these three control design techniques, is the capability of the control system to recover from external disturbances, in the similar manner, the closed loop system simulated with the application of unit step disturbances on each output, in turn. First applying disturbance d_1 on the first output, , the responses shown in Figure 4.28.

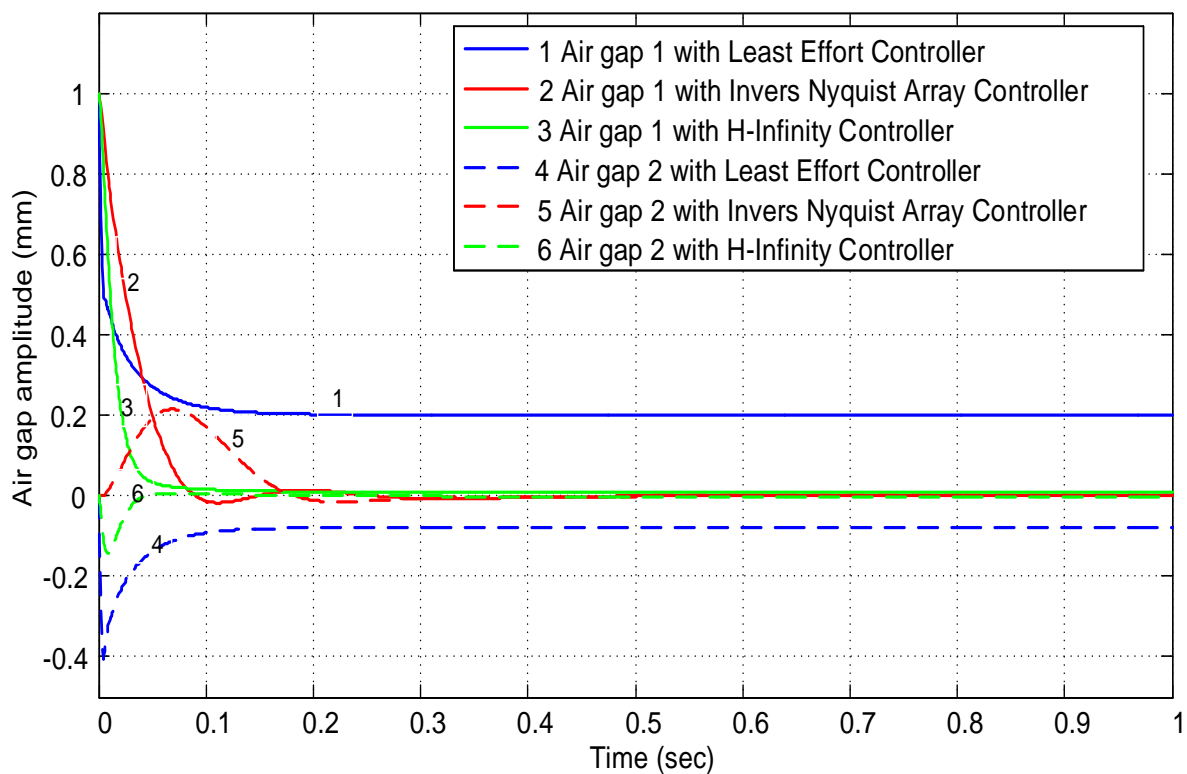


Figure 4.28, Closed-loop Responses following unit step disturbance on d_1 comparing between Least Effort, Invers Nyquist Array and H-Infinity

the H-infinity controller shows a good recovery of the disturbances for both outputs, which is registered less than second to suppress the disturbance for both air gaps, while the Least effort controller recover 80 percent of disturbance with 0.15 second, and the Inverse Nyquist array controller shows more time than the other controllers to recover 95 percent of the disturbance by about 0.38 seconds for both outputs.

For the second simulation round with rotation the disturbance d_2 to the second output of the system for each of three controllers, as shown in the figure 4.29, the output results also shows that the H-Infinity controller results best disturbance recovery for both outputs (air gaps), the registered time was less than 0.1 second to recover 95 percent of disturbance for both air gaps, Similarly the INA shows good disturbances recovery for the second air gap with less 0.1 second, while the results on first air gap shows about 0.4 second for disturbance recovery,

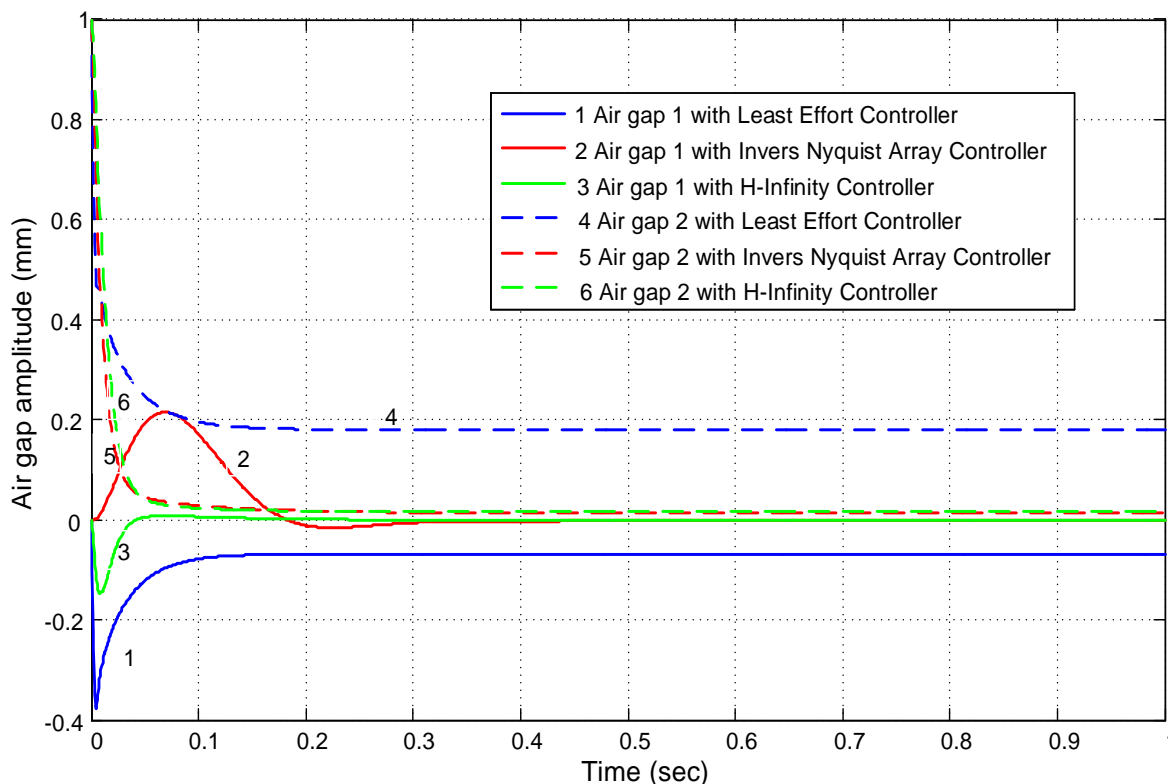


Figure 4.29, Closed-loop responses following unit step disturbance on d_2 comparing between Least Effort, Invers Nyquist Array and H-Infinity

The Least effort controller shows almost similar disturbance recovery for both outputs as in the first input reference, this indicates that the least effort controller is more stable for both input references, and it recommended for implements purposes for multivariable control system applications.

4.4.3. Energy Consumption

The energy consumptions comparison for each controller has also been investigated in figure 4.30, it can be seen from the graph that the energy consumed by INA and H infinity controller sensationally increasing in comparison to that consumed when operation under optimum least effort conditions.

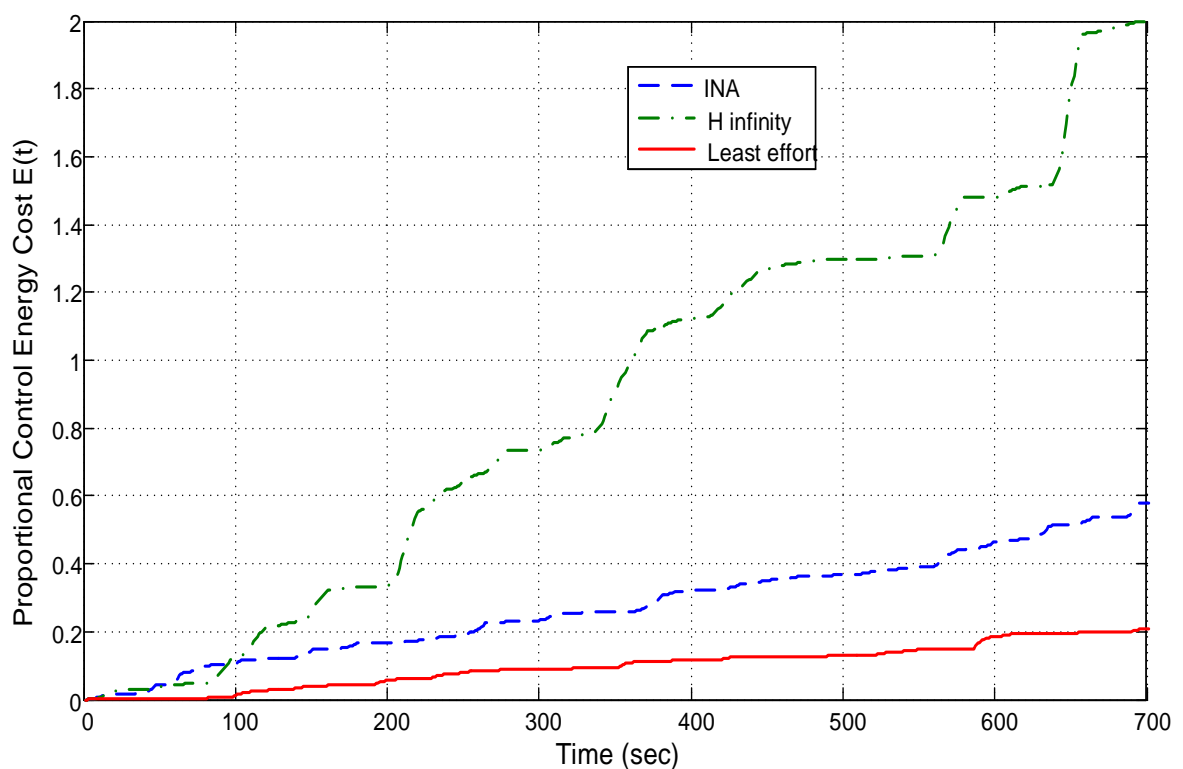


Figure 4.30, Energy Consumed Compared between, least effort, INA and H-infinity

This diverting energy difference would manifest itself in term of control system actuator and component wear, generating heat, aging, and noise attracting thereby additional maintenance, capital and power cost.

The investigation show that the energy consumption for each one of the three controllers, in figure 4.30 that the least effort controller dissipates less energy than the other controllers to recover the system under random disturbance, and the highest value of energy consumed is with the H-infinity controller.

Chapter 5

Conclusions and Recommendations

5.1. Conclusions

In this investigation three automatic control strategies were examined. These were the least effort approach, H-infinity and Inverse Nyquist Array (INA), to controller design, for the electromagnetic levitation system for the Maglev train. The closed loop performance, following the application of these regulators was similar for each producing almost identical, over damped transients and substantial disturbance suppression characteristics.

The question remaining relates to the energy dissipation difference, between these three, distinctly different, feedback control strategies.

Clearly, this energy consumption difference does not manifest itself in improving the dynamic or steady state, system response condition since the three methods provide almost equivalent, closed loop performance.

In view of this comparison, the logical conclusion to be drawn is that since the regulation energy difference between the three methods, does not improve performance it is devoted to promoting increased actuator activity and the generation of heat, wear and noise. In effect, this additional inefficient energy consumption is instrumental in reducing the working life of the system whilst attracting higher maintenance and capital replacement costs with diminishing system reliability. This is the penalty, for poor design selection and the reduction of the long term, life cycle duration of the system.

Firstly, compensation was allowed for the open loop transfer function, in order to avoid the effect of the double integrator appearing in the system models characteristic equation. This compensation will increase the performance the controller of maglev train levitation system, by adding two first order filter on each system input.

As per the requirements of least effort method, internal and external loops were engaged. In the controller design procedure for least effort technique, the outer loop was designed to regulate the steady state of system output with the required steady state disturbance offset conditions by adjusting the external loop gain (f) value which is recommended to be in the range of $0 < f < 1$ (Whalley, R. and Ebrahimi, M. 2006).

While the internal loop design permits to good transient system response, and system stability, this can be achieved by selecting the best value of b_0 and the steady state matrix S_s . The performance index (J) value was defined and investigated to be minimized. The minimum value was achieved through minimizing the sum of the squared elements, and then a suitable value of ratio (n) could be calculated. This value ensures minimal energy to recover the performance of the system under arbitrary disturbance conditions.

The controller generated / created with least effort technique is a more reliable and efficient controller. It shows good behavior to meet the design requirements and control objectives of electromagnetic levitation system (Maglev train), keeping the air gap value within the desired level, this is evident from the system responses.

In this research, the Inverse Nyquist and H-infinity controller were also investigated and selected as second and third choice respectively. A pre compensator was designed implant the diagonally dominance procedure. A small gain matrix was their able to enhance the diagonally dominance conditions of system transfer function model. For the controller designed by H-infinity technique, the weighting matrices were selected on an arbitrary basis, The main restrictions applying to the H-infinity methodology is the complexity of the system characteristics equation i.e. High order systems, and the systems with more than two inputs- two outputs, approximations would be required in order to minimize the transfer function order and eliminate the multiple integrators required. However these restrictions can easily be

overcome with the application of Least Effort control, in comparison with the difficulties of achieving diagonally dominance as in Inverse Nyquist Array (INA), and selecting of weighting matrix for the H- Infinity control technique.

5.2.Recommendations

Based on the results obtained previously, the Least Effort Technique (controller) was simpler in design and application, and the research objectives are clearly fulfilled by implementing it, in comparison with the alternative control methods,

I recommended that the Least Effort control technique is employed for implementation in the due to the best system performance and low cost of application, and improvement in the maglev train suspension system efficiency. Controlling the air gap with less energy consumption and the reduction in the maintenance costs is a highly desirable objective.

Chapter 6

References and Appendix

6.1. References

- Allwright, J. (1970). Commutative controllers. *Electronics Letters*, 6(9), p.276.
- Al-Saadi z. (2014). *A Design Study for a Multivariable Feedback Controller for Aircraft Carrier Landing*. MSc Systems Engineering-Faculty of Engineering. BUiD.
- Alshehhi K. (2014). *Combined Armature And Field Voltage Control Of DC Motor*. MSc Systems Engineering-Faculty of Engineering. BUiD.
- Anderson, B. and Luenberger, D. (1967). Design of multivariable feedback systems. *Proceedings of the Institution of Electrical Engineers*, 114(3), p.395.
- Apkarian, P. and Noll, D. (2006). Non smooth H_{∞} synthesis. *IEEE Transactions on Automatic Control*, 51(1), pp.229-244.
- Apkarian, P. and Noll, D. (2006). The H_{∞} Control Problem is Solved. *ONERA Control System Department*.
- Aslan, Y., Beauvois, D. and Rossiter, J. (1993). Eigen-structure approximations and their use for a commutative controller strategy: Application to a helicopter. *Control Engineering Practice*, Vol.1, No.(2), pp.357-363.
- Belletrutti, J. and MacFarlane, A. (1971). Characteristic loci techniques in multivariable-control-system design. *Proceedings of the Institution of Electrical Engineers*, 118(9), pp. 1291-1297.
- Bennett, S. (1996). A brief history of automatic control. *IEEE Control Systems Magazine*, 16(3), pp.17-25.
- Bissell, C. (1989). Stodola, Hurwitz and the genesis of the stability criterion. *International Journal of Control*, 50(6), pp.2313-2332.
- Bissell, C. (2009). History of Automatic control. In: *Springer Handbook of Automation*, 1st ed. Springer-Verlag Berlin Heidelberg, pp.53-69.
- De-Sheng, L., Jie, L. and Kun, Z. (2006). Design of Nonlinear Decoupling Controller for Double-electromagnet Suspension System. *ACTA Automatica SINICA*, 32(3), pp.322-328.

- Dorf, R. and Bishop, R. (2008). *Modern control systems*. 12th ed. Pearson Education, Inc.
- Doyle, J., Glover, K., Khargonekar, P. and Francis, B. (1989). State-space solutions to standards H₂ and H_∞ control problems. *IEEE Transactions on Automatic Control*, 34(8), pp.831-847.
- Dutton, K., Thompson, S. and Barraclough, B. (1997). *The art of control engineering*. 1st ed. Harlow: Addison Wesley.
- El Hassan, T. (2012). *A Design Study for Multivariable Feedback Control System Regulation for Aircraft Turbo-Jet Engines*. MSc Systems Engineering-Faculty of Engineering. BUiD.
- Evans, W. (1950). Control system synthesis by Root Locus method. *Electrical Engineering*, 69(5), pp.405-405.
- Gahinet, P. and Apkarian, P. (1994). A linear matrix inequality approach to H_∞ control. *International Journal of Robust and Nonlinear Control*, 4(4), pp.421-448.
- Gary G. Leininger (1979). Diagonal dominance for multivariable Nyquist Array Methods using function minimization, *IFAC*. 15, pp.339-345.
- General Atomics, (2002). *Low Speed Maglev Technology Development Program*. U.S. Department of Transportation.
- Gottzein, E. and Lange, B. (1975). Magnetic suspension control systems for the MBB high speed train. *Automatica*, 11(3), pp.271-284.
- Gu, G. (2009). Linear Feedback Control - Analysis and Design with MATLAB (by Dingyu Xue et al; 2007) [Bookshelf]. *IEEE Control Systems Magazine*, 29(1), pp.128-129.
- H. (1967). Reduction of system matrixes. *Electronics Letters*, 3(8), p.368.
- Hawkins, D. and McMorran, P. (1973). Determination of stability regions with the inverse Nyquist array. *Proceedings of the Institution of Electrical Engineers*, 120(11), p.1445.
- Hazen, H. (1934). Theory of servo-mechanisms. *Journal of the Franklin Institute*, 218(3), pp.279-331.
- He, G., Li, J. and Cui, P. (2015). Decoupling Control Design for the Module Suspension Control System in Maglev Train. *Mathematical Problems in Engineering*, 2015, pp.1-13.

- Howell, J. (1986). Aerodynamic response of maglev train models to a crosswind gust. *Journal of Wind Engineering and Industrial Aerodynamics*, 22(2-3), pp.205-213.
- Hyung-Woo Lee, Ki-Chan Kim, and Ju Lee, (2006). Review of maglev train technologies. *IEEE Transactions on Magnetics*, 42(7), pp.1917-1925. (Hyung-Woo Lee et al., 2006).
- Kalman R. and Bucy R. (1961). New Results in Linear Filtering and Prediction Theory. *Journal of Basic Engineering, Transactions of the ASME*, pp.95-108.
- Kalman, R. (1959). On the general theory of control systems. *IRE Transactions on Automatic Control*, 4(3), pp.110-110.
- Kimura, H. (1996). *Chain-scattering approach to H-infinity control*. 1st ed. Boston, Mass.: Birkhäuser Boston.
- Lewis F. (1992). *Applied optimal control & estimation*. New Jersey: Prentice-Hall. Inc.
- Li, Y., He, G. and Li, J. (2013). Nonlinear Robust Observer-Based Fault Detection for Networked Suspension Control System of Maglev Train. *Mathematical Problems in Engineering*, 2013, pp.1-7.
- M., P. and Wiener, N. (1950). The Extrapolation, Interpolation and Smoothing of Stationary Time Series, with Engineering Applications. *Journal of the Royal Statistical Society. Series A (General)*, 113(3), p.413.
- Macfarlane, A. (1970). Two necessary conditions in the frequency domain for the optimality of a multiple-input linear control system. *Proceedings of the Institution of Electrical Engineers*, 117(2), p.464.
- Macfarlane, A. and Belletrutti, J. (1973). The characteristic locus design method. *Automatica*, 9(5), pp.575-588.
- Macfarlane, A. and Postlethwaite, I. (1977). The generalized Nyquist stability criterion and multivariable root loci. *International Journal of Control*, 25(1), pp.81-127. (Macfarlane and Postlethwaite, 1977).
- Maxwell, J. (1868). On Governors. *Proceedings of the Royal Society*, pp. 270-283.
- Mayr, O. (1970). The Origins of Feedback Control. *Scientific American*, 223(4), pp.110-118.
- McMorran, P. (1970). Design of gas-turbine controller using inverse Nyquist method. *Proceedings of the Institution of Electrical Engineers*, 117(10), p.2050.

- Mindell, D. (1995). Engineers, psychologists, and administrators: control systems research in wartime, 1940-45. *IEEE Control Systems*, 15(4), pp.91-99.
- Munro, N. (1972). Design of controllers for open-loop unstable multivariable system using inverse Nyquist array. *Proceedings of the Institution of Electrical Engineers*, 119(9), p.1377.
- Munro, N. (1972). Multivariable systems design using the inverse Nyquist array. *Computer-Aided Design*, 4(5), pp.222-227.
- Munro, N. (1985). Recent Extensions to the Inverse Nyquist Array Design Method. *Proc. 24th IEEE Conference on Decision & Control*, 24, pp.1852-1857.
- Nyquist, H. (1932). Regeneration Theory. *Bell System Technical Journal*, 11(1), pp.126-147.
- Owens, D. and Chotai, A. (1986). Approximate models in multivariable process control. An inverse Nyquist array and robust tuning regulator interpretation. *IEE Proceedings D Control Theory and Applications*, 133(1), p.1.
- Rogg, D. (1984). General survey of the possible applications and development tendencies of magnetic levitation technology. *IEEE Transactions on Magnetics*, 20(5), pp.1696-1701.
- Rosenbrock, H. (1958). Approximate relations between transient and frequency response. *Journal of the British Institution of Radio Engineers*, 18(1), pp.57-68.
- Rosenbrock, H. (1969). Design of multivariable control systems using the inverse Nyquist array. *Proceedings of the Institution of Electrical Engineers*, 116(11), p.1929.
- Rosenbrock, H. (1969). Design of multivariable control systems using the inverse Nyquist array. *Proceedings of the Institution of Electrical Engineers*, 116(11), p.1929.
- Rote, and Coffey, April 1994.
- Shu G., Reinhold I., Shen G. (2007). Modeling and Simulation of Shanghai MAGLEV Train Transrapid with Random Track Irregularities. *Schriftenreihe Georg-Simon-Ohm-Fachhochschule Nürnberg.*, pp.1-12.
- Shu G., Reinhold I., Shen G. (2008). Simulation of a MAGLEV Train with Periodic Guideway Deflections. *IEEE, Asia Simulation Conference — 7th Intl. Conf. on Sys. Simulation and Scientific Computing*, pp.421-425.
- Skogestad, S. and Postlethwaite, I. (2001). *MULTIVARIABLE FEEDBACK CONTROL Analysis and design*. 2nd ed. Chichester: Wiley.

- Song X., Zhiqiang L., Guang H., Ning H., (2012). Sensor Fault Diagnosis of Maglev Train Based on Kalman Filter Group. *IEEE Computer Society, Fifth International Conference on Intelligent Computation Technology and Automation*. pp.312-316.
- Tewari, A. (2002). *Modern Control Design with MATLAB and SIMULINK*. 1st ed. Chichester: John Wiley.
- Wang, T. and Yeou-Kuang Tzeng, (1994). A new electromagnetic levitation system for rapid transit and high speed transportation. *IEEE Transactions on Magnetics*, 30(6), pp.4734-4736.
- Warwick, K. (1996). *An Introduction to Control Systems* 2nd ed. UK: World Scientific Publishing Co. Pte. Ltd.
- Whalley, R. (1988). The application of multivariable system techniques. *Transactions of the Institute of Measurement and Control*, 10(1), pp.2-3. (Whalley, 1988).
- Whalley, R. and Ebrahimi, M. (1999). Multivariable system regulation with minimum control effort. *Proceedings of the Institution of Mechanical Engineers, Part I: Journal of Systems and Control Engineering*, 213(6), pp.505-514.
- Whalley, R. and Ebrahimi, M. (2006). Multivariable System Regulation, *Proc. IMechE, Part C, Journal of Mechanical Engineering Science*, 220(5), pp. 653-667
- Xue, S., Long, Z., He, N. and Chang, W. (2012). A High Precision Position Sensor Design and Its Signal Processing Algorithm for a Maglev Train. *Sensors*, 12(12), pp.5225-5245.
- Yamamura, S. (1976). Magnetic levitation technology of tracked vehicles present status and prospects. *IEEE Transactions on Magnetics*, 12(6), pp.874-878.
- Yongzhi J. Xiao J. (2011). Modeling of gap sensor for High-speed maglev train based on RBF network. *Proceedings of the 2011 IEEE International Conference on Cyber Technology in Automation, Control, and Intelligent Systems*, pp. 279-282
- Yongzhi, J., Zhang, K. and Xiao, J. (2011). Modeling of Gap Sensor for High-speed Maglev Train Based on Fuzzy Neural Network. *IEEE, Eighth International Conference on Fuzzy Systems and Knowledge Discovery*, pp.650-654.
- Zames, G. (1966). On the input-output stability of time-varying nonlinear feedback systems Part one: Conditions derived using concepts of loop gain, conicity, and positivity. *IEEE Transactions on Automatic Control*, 11(2), pp.228-238.

- Zames, G. (1966). On the input-output stability of time-varying nonlinear feedback systems--Part II: Conditions involving circles in the frequency plane and sector nonlinearities. *IEEE Transactions on Automatic Control*, 11(3), pp.465-476.
- Zames, G. (1981). Feedback and optimal sensitivity: Model reference transformations, multiplicative seminorms, and approximate inverses. *IEEE Transactions on Automatic Control*, 26(2), pp.301-320.
- Zhang, W., Li, J., Zhang, K. and Cui, P. (2013). Decoupling Suspension Controller Based on Magnetic Flux Feedback. *Advanced Materials Research*, 709, pp.462-469.
- Zhao, C., She, L., Chang, W. (2009). Design and Implement of Multifunctional Monitoring System for the Suspension and Guidance System of Maglev Train. *IEEE, computer society, 2009 International Conference on Measuring Technology and Mechatronics Automation*, pp. 202-205.
- ZhaoHong D. (2012). Optimal Control Design for Maglev Train Suspension System. *International Conference on Automatic Control and Artificial Intelligence ACAI*, pp.1481-1483.
- Zhigang, L., Zhigang, I. and Xiaolong, L. (2015). *Maglev Trains Key Underling Technology*. 1st ed. Springer-Verlag Berlin Heidelberg: Springer Tracts in Mechanical Engineering.
- Zhiqiang, L., Song, X., Zhizhou, Z. and Yunde, X. (2007). A New Strategy of Active Fault-tolerant Control for Suspension System of Maglev Train. *Proceedings of the IEEE*, pp.88-94.

Appendix-A

Block Diagrams and Simulation Models:

Open loop system

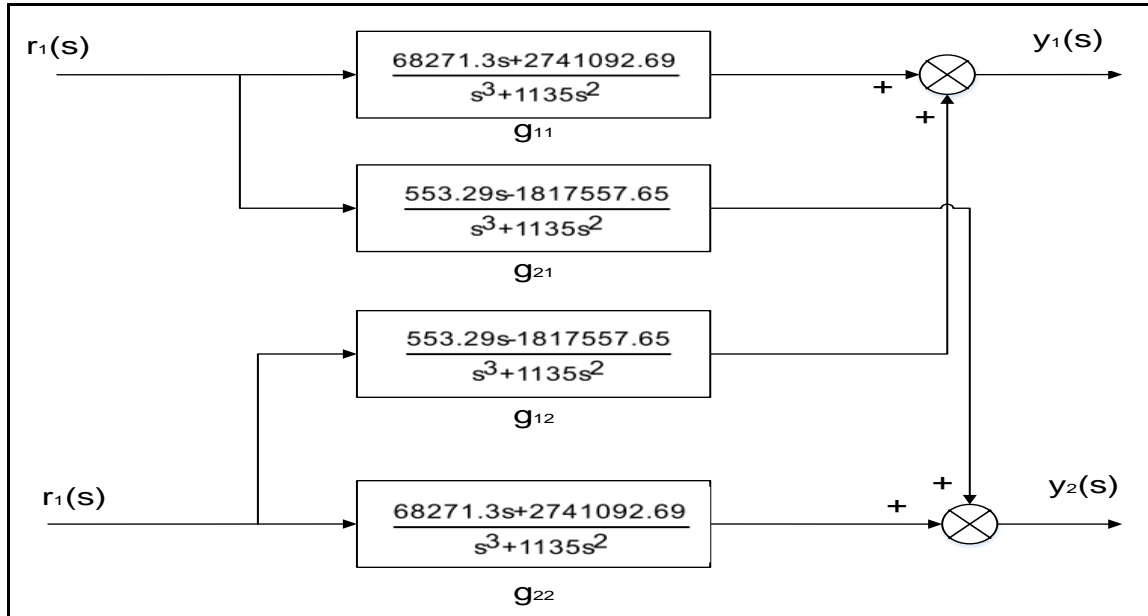


Figure 6.1, Open Loop Simulation Model Prior Including The Filters

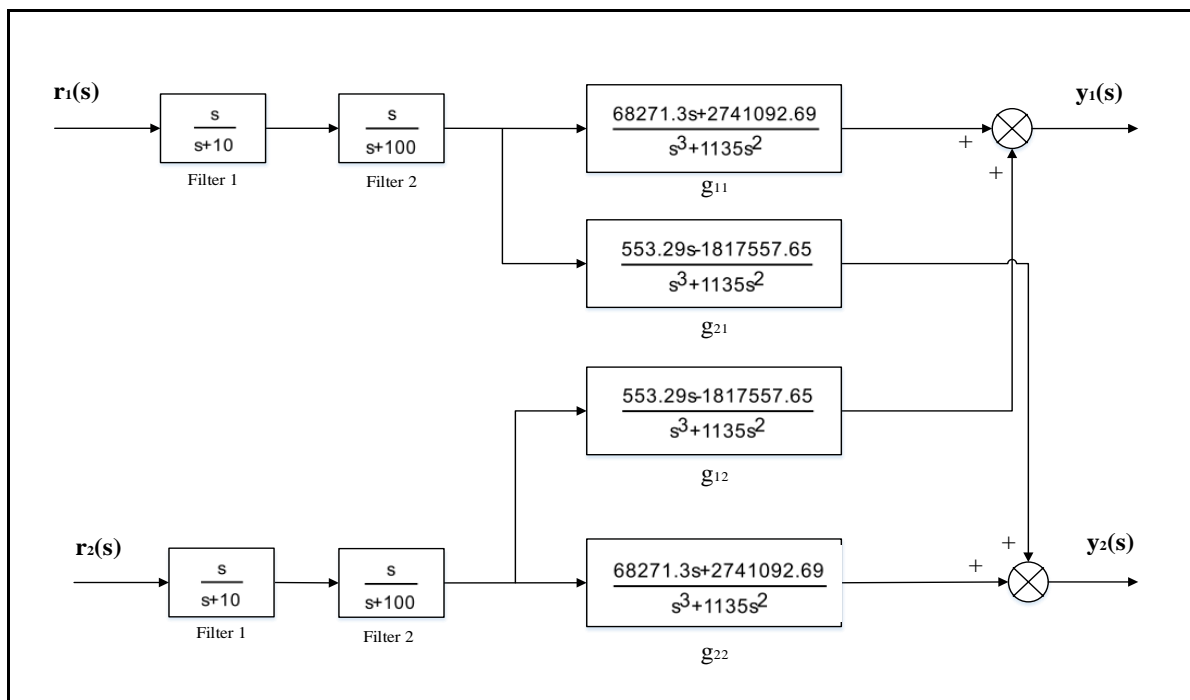


Figure 6.2, Block diagram representation for open loop system with filters

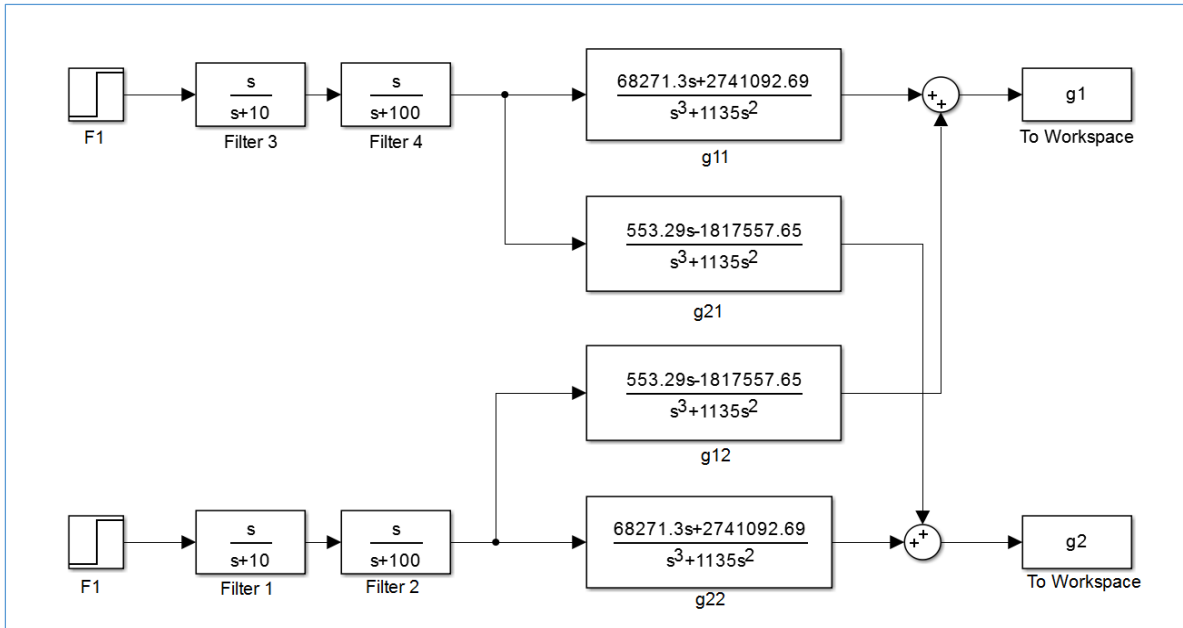


Figure 6.3, Open loop simulation model

Least Effort system model:

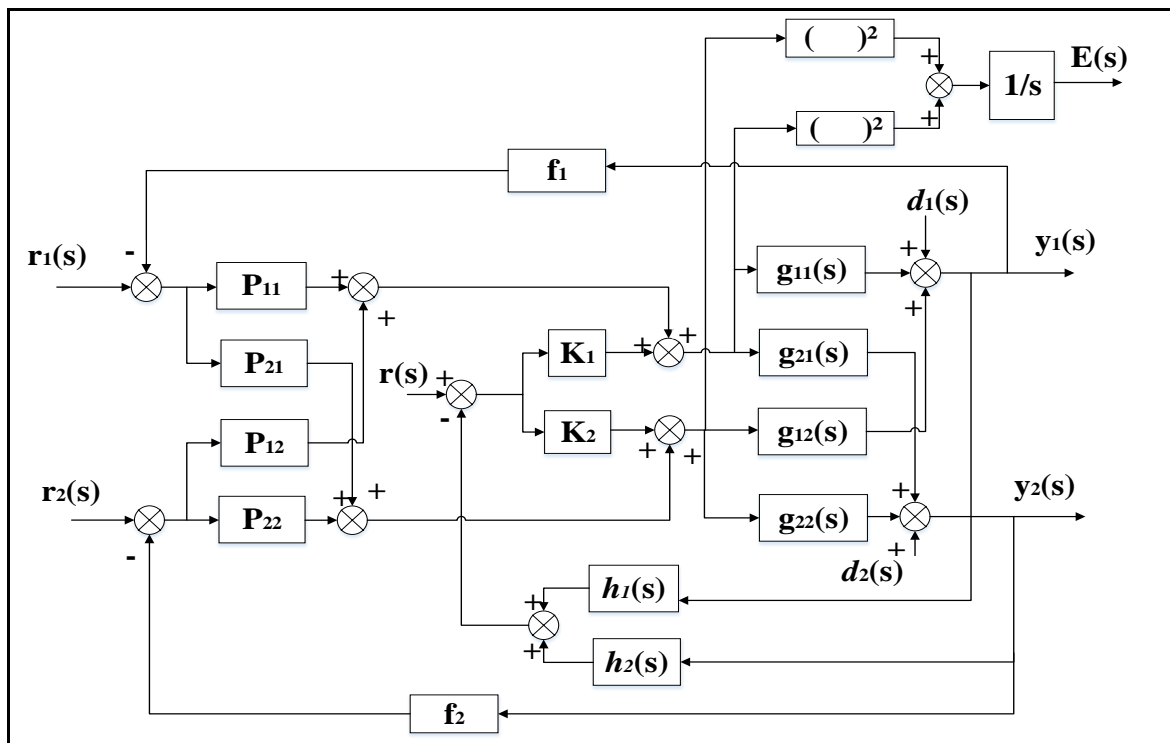


Figure 6.4, Block Diagram Representation For General Closed Loop System For Least Effort Methodology

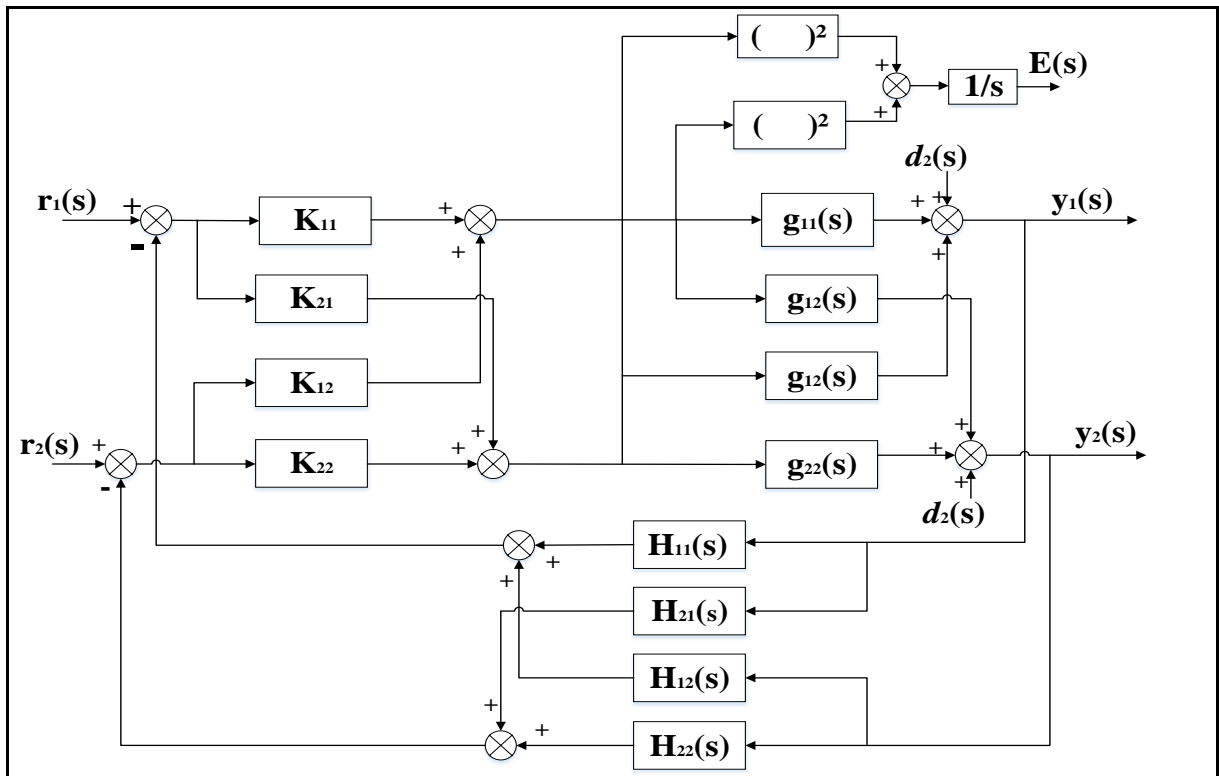


Figure 6.5, Least Effort-Block Diagram representation the conventional of $K(s)$ - $H(s)$

Inverse Nyquist Array (INA) Model:

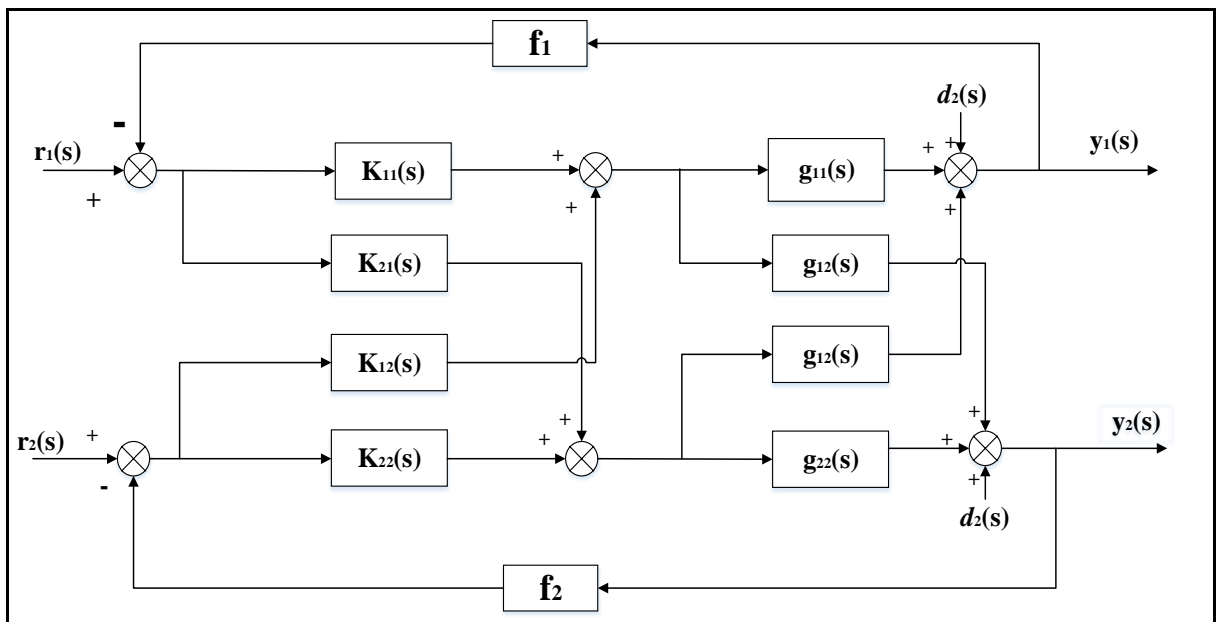


Figure 6.6, General Closed Loop System Block Diagram Representation for INA

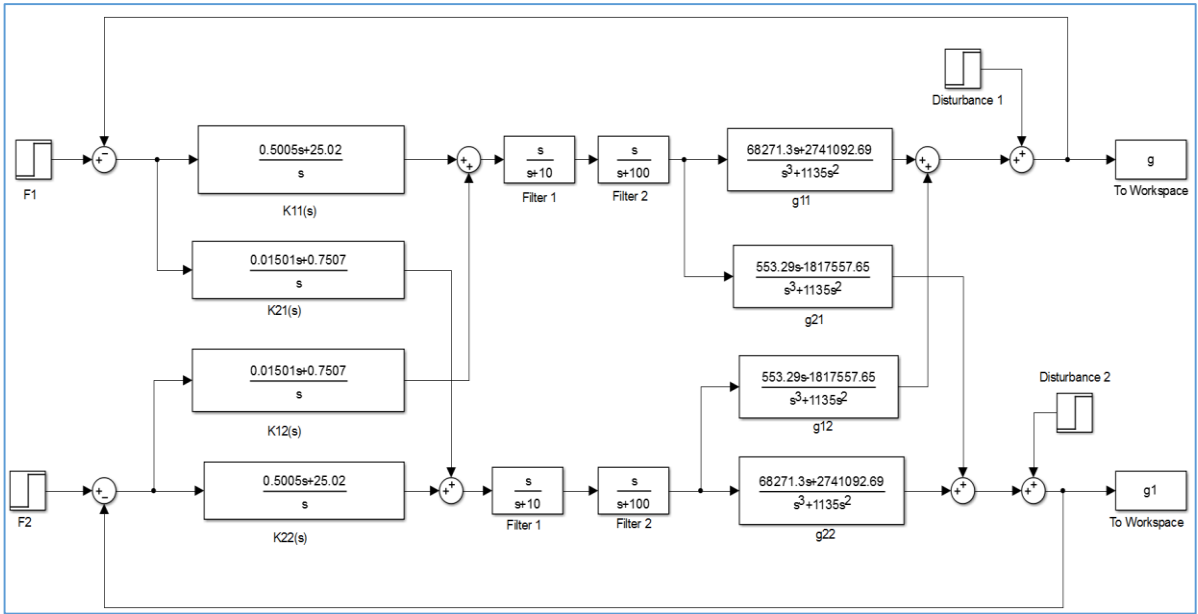


Figure 6.7, Closed loop Simulation model for INA

H-Infinity:

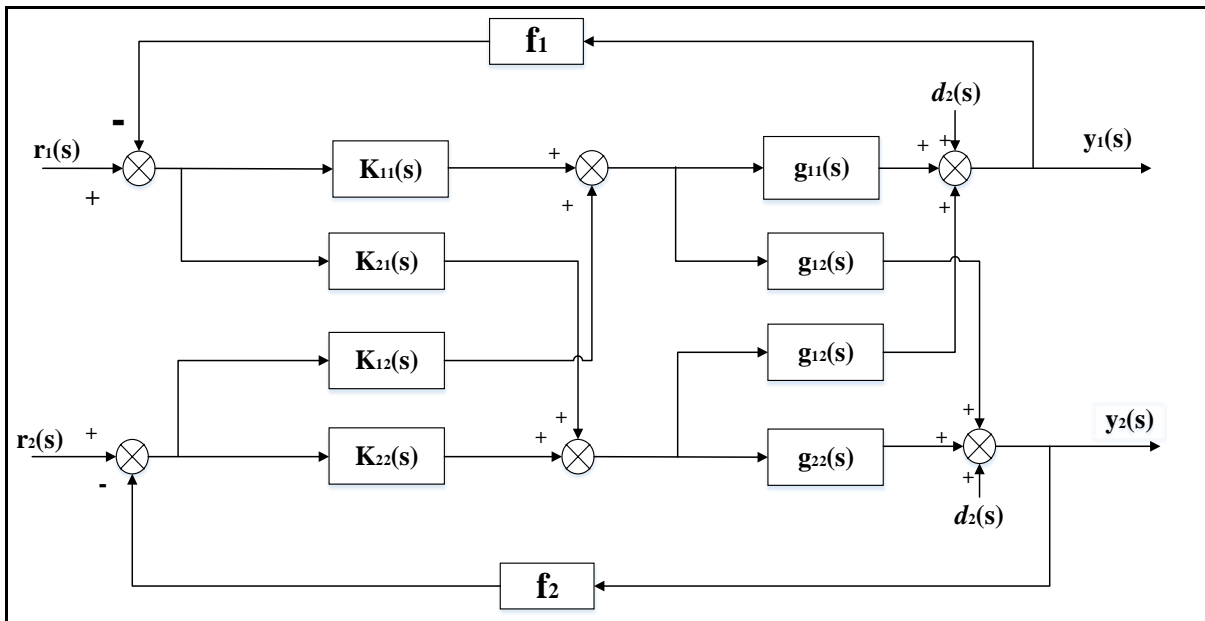


Figure 6.8, General Closed Loop System Block Diagram Representation For H-Infinity

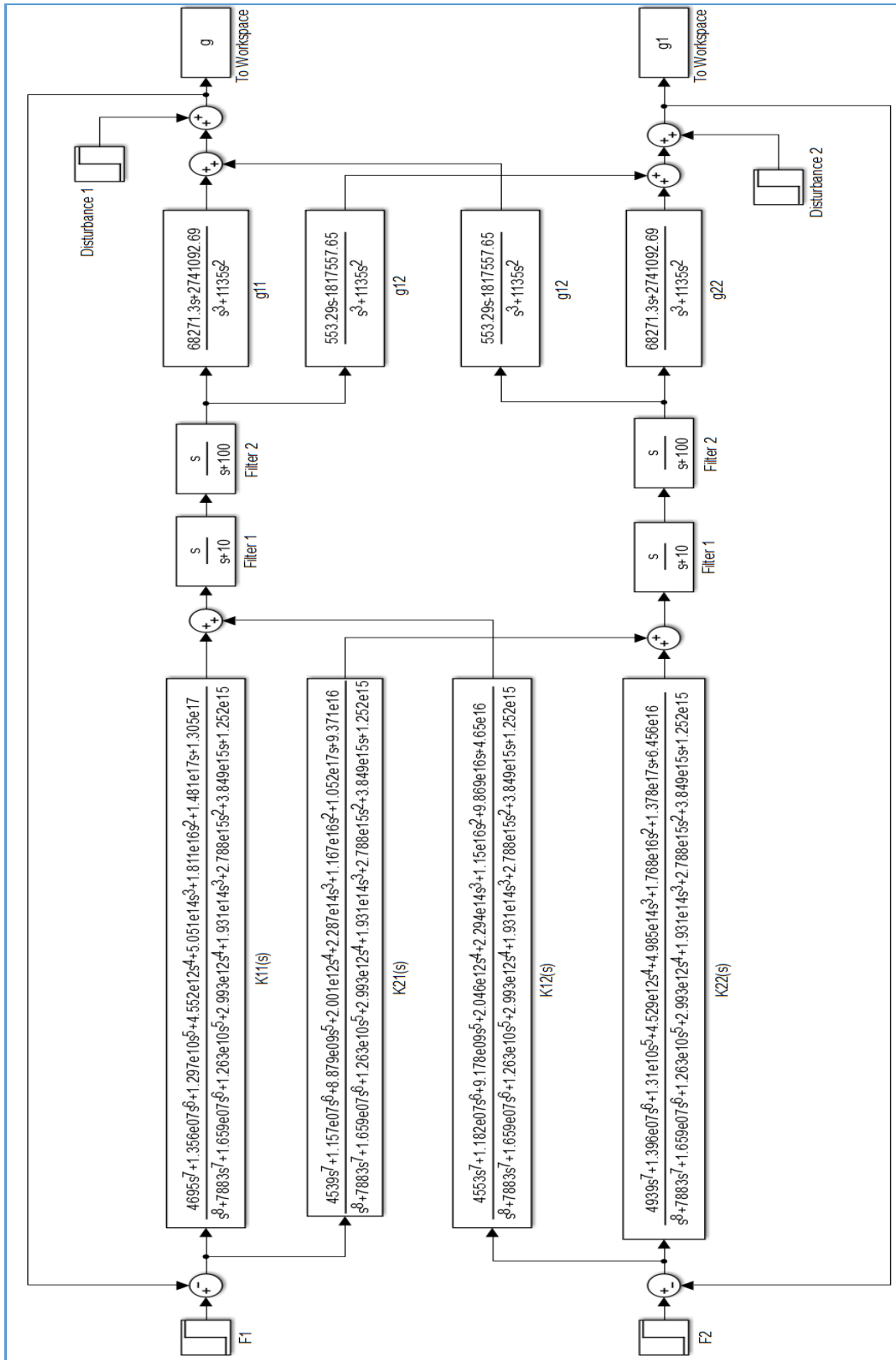


Figure 6.9, Closed loop Simulation model for H-Infinity

Appendix-B

M-files Commands

Least Effort Methodology m-file

```
% A Program For Designing A Least Effort Controller For a
% Maglev train suspension system .
disp(' Least Effort Contrller For Maglev train suspension system System')
disp('*****')
format compact
%% The Open-Loop Transfer Function
syms s
G=1/(s^3+1245*s^2+125850*s+1135000)*[6.8271e+04*s+2.7411e+06 553.2900*s-
1.8176e+06;553.2900*s-1.8176e+06 6.8271e+04*s+2.7411e+06];

disp('The open-loop transfer function of the system, G(s), is')
pretty(G)
disp('-----')
%% Expressing G(S) as G(S)=L(s).A(s)/d(s).R(s).Gamma(s)
[A,D]=numden(G);
d=D(1,1)/2000;
A=d*G;
L=eye(2);
R=eye(2);
Gamma=eye(2);
% Displaying A(S),d(s),L(s) and R(s)
disp('Press Enter to display A(s),d(s),L(s),R(s) and Gamma(s)')
disp('-----')
pause
disp('A(s) is')
pretty(A)
disp('d(s) is')
pretty(d)
disp('L(s) is')
L
disp('R(s) is')
R
disp('Gamma(s) is')
Gamma
%% Forming the inner product <h.A(s).k>
syms h1 h2 k1 k2 n real
hak=[h1 h2]*A*[k1 k2]';
hak=subs(hak,k2,n*k1);
hak=subs(hak,k1,1);
[hak,how]=simple(hak);
disp('=====')
disp('Press Enter to display the inner product<h.A(s).k>')
pause
disp('The inner product is')
pretty(hak)
%% Forming the matix Q
% forming the first colum of Q
hak1=subs(hak,h2,0);
Q(1,1)=simple((subs(hak1,s,0)/h1));
Q(2,1)=simple((hak1-Q(1,1)*h1)/(s*h1));
% forming the second colum of Q
hak1=subs(hak,h1,0);
Q(1,2)=simple((subs(hak1,s,0)/h2));
Q(2,2)=simple((hak1-Q(1,2)*h2)/(s*h2));
```

```

disp('=====')
disp('Press Enter to display the matrix Q')
pause
disp('The Q matrix is')
Q
%% Designing the inner loop
sys=tf(1,sym2poly(d));
% Building the root locus
disp('Press Enter to display the root locus of b(s)/d(s)=-1, with unity
unmerator')
pause
figure(2)
rlocus(sys)
disp('-----')
display('The poles are:')
p=pole(sys)
b=[10;1];
b0=10000
b1=[10;1]*b0;
% Finding the performance index, J
J=(1+n^2)*b1'*inv(Q)'*inv(Q)*b1;
J=simple(J);
disp('-----')
display('Press Enter to display the performance index,J')
pause
pretty(J)
disp('Press Enter to display the graph of J as a function of n')
pause
figure(3)
ezplot(J)
xlabel('n')
ylabel('J')
grid on
% Finding the minimum of J
% Finding the derivative of J
J1=diff(J);
[num,den]=numden(J1);
J1=num/den;
disp('=====')
display('Press Enter to display the derivative of the performance index,J')
pause
pretty(J1)
% Finding the values of 'n' for which J is minimum
syms x
J1=subs(J1,n,x);
n=solve(J1);
n=double(n);
disp('=====')
display('Press Enter to display the the values of n for which J has an
extremum')
pause
n=sort(n)
% Findind the corresponding values of J
J1=subs(J,n)
% Finding the value of n at which J is the minimum
disp('-----')
disp('Press Enter to display the value of n at which J is minimum')
for nn=1:length(n)
if isreal(n(nn))==0
n(nn)=inf;
end

```

```

end
n=n(isfinite(n));
J=subs(J,n);
pause
n=n(find(J==min(J)))
disp('-----')
disp('Press Enter to display the corresponding value of matrix Q')
pause
Q
% Finding the value of h(s)
disp('-----')
disp('Press Enter to display the value of h(s)')
pause
k1=1;
hs=(inv(Q)*b1)
% Finding the value of k
disp('-----')
disp('Press Enter to display the value of vector k')
pause
k2=n*k1;
k=[k1 k2]
% Finding the steady-state value of the transfer function
disp('-----')
disp('Press Enter to display the steady-state value of the transfer
function')
pause
G0=limit(G,s,0)
% Entering Ss
disp('-----')
disp('Press Enter to display the value of Ss')
pause
Ss=[1 0.1;0.1 1]
I=[1 0;0 1]
% Entering the value of f and determining the matrix F
disp('=====')
beep
disp('Entering the value of f')
disp('=====')
f=input('Enter the value of f ')
pause
F=[f 0;0 f]
% Calculating the feed-forward gain of the outer loop
disp('-----')
disp('Press Enter to display the feed-forward gain matrix of the outer
loop,p')
pause
P=(inv(G0)+k*(hs))*Ss*inv(I-F*Ss);
P=double(P)
% Calculating the feed-forward gain of the outer loop
disp('-----')
disp('Press Enter to display the feed-back gain matrix of the outer
loop,H')
pause
H=(inv(P)*k*(hs))+F;
H=double(H)
%%%(Alshehhi K., 2014).%%

```

Inverse Nyquist Array m-file

```
%%%%INVERSE NYQUIST ARRAY mFile%%%%%

% finding the final transfer function G of the system after adding the
% filters%%%%%
a=68271.3;
b=a*40.15;
c=553.29;
d=c*3285;
den=[1 1245 125850 1135000];
g11=[a b];
g12=[c -d];
g21=[c -d];
g22=[a b];
sys11=tf(g11,den);
sys12=tf(g12,den);
sys21=tf(g21,den);
sys22=tf(g22,den);
G=[sys11 sys12;sys21 sys22];
G
%%%Invistigation of diagonally domenance of the TF
gershband(G, 'V')
%%%%%%%%%%%%%%%%%%%%%%%%%%%%%%%%%%%%%%%%%%%%%%%%%%%%%%%%%%%%%%%%%%%%%%%%
%%% Find inversion of the TF%%%%%%%%5%%%%%%%%
H=inv(G);
H
%%%Invistigation of diagonally domenance of the inverted TF
gershband(H, 'V')
%%%to Find InvQ %%%%%%%%%and invistigate diagonally dominance with
%%%gersbands%%%
%%%by selecting pre compensator K=k1*k2%%%%%%%%

k1=[1 -0.03;-0.03 1];%first compensator%%
k2=[2 0;0 2];%%second compensator%%
K=invk1*invk2;
K
invQ=K*inv(G);
invQ
gershband(invQ, 'v');% creates Figures 4.17 to 4.21
%%%to find the overall K(S)%%%%%%%%
%%%K(s)=Dynamic controller*precompensator%%%%%%%%
%%% find the Dynamic controller from dealing with q11 as SISO and using
PID procedure %%
k3=[tf([1 50],[1 0]) 0;0 tf([1 50],[1 0])];
k3
Ks=inv(k2*k1)*k3;
Ks

%%%to find the final inverted Q
Q=G*Ks;
Q
function gershband(a,b,c,d,e)
%GERSHBAND - Finds the Gershgorin Bands of a nxn LTI MIMO SYS model
% The use of the Gershgorin Bands along the Nyquist plot is helpful for
% finding the coupling grade of a MIMO system.
%
% Syntax: gershband(SYS) - computes the Gershgorin bands of SYS
% gershband(SYS,'v') - computes the Gershgorin bands and the
% Nyquist array of SYS
% Inputs:
```

```

% SYS - LTI MIMO system, either in State Space or Transfer Function
% representation.
%
% Example:
% g11=tf(2,[1 3 2]);
% g12=tf(0.1,[1 1]);
% g21=tf(0.1,[1 2 1]);
% g22=tf(6,[1 5 6]);
% G=[g11 g12; g21 g22];
% gershband(G);
%
% Other m-files required: sym2tf, ss2sym
% Subfunctions: center, radio
% See also: rga
%
% Author: Oskar Vivero Osornio
% email: oskar.vivero@gmail.com% Created: February 2006;
% Last revision: 11-May-2006;
% May be distributed freely for non-commercial use,
% but please leave the above info unchanged, for
% credit and feedback purposes
%----- BEGIN CODE -----
%----- Determines Syntax -----
ni=nargin;
switch ni
case 1
%Transfer Function Syntax
switch class(a)
case 'tf'
%Numeric Transfer Function Syntax
Q=a;
case 'sym'
%Symbolic Transfer Function Syntax
Q=sym2tf(a);
end
e=0;
case 2
%Transfer Function Syntax with Nyquist Array
switch class(a)
case 'tf'
%Numeric Transfer Function Syntax
Q=a;
case 'sym'
%Symbolic Transfer Function Syntax
Q=sym2tf(a);
end
e=1;
case 4
%State Space Syntax
Q=ss2sym(a,b,c,d);
Q=sym2tf(Q);
e=0;
case 5
%State Space Syntax
Q=ss2sym(a,b,c,d);
Q=sym2tf(Q);
e=1;
end
%-----
[n,m]=size(Q);
w=logspace(-1,6,200);

```

```

q=0:(pi/50):(2*pi);
for i=1:n
for j=1:m
if i==j
figure(i)
nyquist(Q(i,i));
grid on
title(['Nyquist Diagram of G(',num2str(i),',',num2str(j),')'])
for iest=1:n
for jest=1:m
if iest~=jest
hold on
C=center(Q(i,j),w);
R=radio(Q(iest,jest),w);
for k=1:length(C)
plot((R(k)*cos(q))+real(C(k)),(R(k)*sin(q))+imag(C(k)),'g-')
end
hold off
end
end
end
end
end
end
if e==1
figure(n+1)
nyquist(Q);
grid on
end
%----- Subfunction -----
function C = center(g,w)
Q=tf2sym(Q);
C=subs(Q,complex(0,w));
end
function R = radio(g,w)
Q=tf2sym(Q);
R=abs(subs(Q,complex(0,w)));
end
%----- END OF CODE -----

```

H-infinity m-file

```
a=68271.3;
b=a*40.15;
c=553.29;
d=c*3285;

a = 6.8271e+04
b = 2.7411e+06
c = 553.2900
d = 1.8176e+06
%%%%%%%%%%%%%%%%%%%%%%%%%%%%%%%%%%%%%%%%%%%%%%%%%%%%%%%%%%%%%%%%%%%%%%%%
den=[1 1245 125850 1135000];
%%%%%%%%%%%%%%%%%%%%%%%%%%%%%%%%%%%%%%%%%%%%%%%%%%%%%%%%%%%%%%%%%%%%%%%%
g11=[6.8271e+04 2.7411e+06];
g12=[553.2900 -1.8176e+06];
g21=[553.2900 -1.8176e+06];
g22=[6.8271e+04 2.7411e+06];
%%%%%%%%%%%%%%%%%%%%%%%%%%%%%%%%%%%%%%%%%%%%%%%%%%%%%%%%%%%%%%%%%%%%%%%%
sys11=tf(g11,den);
sys12=tf(g12,den);
g21=tf(g21,den);
sys22=tf(g22,den);
%%%%%%%%%%%%%%%%%%%%%%%%%%%%%%%%%%%%%%%%%%%%%%%%%%%%%%%%%%%%%%%%%%%%%%%%

I=[1 0;0 1];

%%%%%%%%%%%%%%%%%%%%%%%%%%%%%%%%%%%%%%%%%%%%%%%%%%%%%%%%%%%%%%%%%%%%%%%%H-Infinity code%%%%%%%%%%%%%%%%%%%%%%%%%%%%%%%%%%%%%%%%%%%%%%%%%%%%%%%%%%%%%%%%%%%%%%%%
%%%%%%%%%%%%%%%%%%%%%%%%%%%%%%%%%%%%%%%%%%%%%%%%%%%%%%%%%%%%%%%%%%%%%%%%
sys11=tf([6.8271e+04 2.7411e+06],[1 1245 125850 1135000]); s=tf('s');
sys12=tf([553.2900 -1.8176e+06],[1 1245 125850 1135000]);
sys21=tf([553.2900 -1.8176e+06],[1 1245 125850 1135000]);
sys22=tf([6.8271e+04 2.7411e+06],[1 1245 125850 1135000]);
G=[sys11, sys12; sys21, sys22];
W1=[100/(s+0.5),0; 0,100/(s+1)];
W2=[tf(1),0;0,tf(1)];
W3=[s/1000,0; 0,s/200];
Tss=augtf(G,W1,W2,W3);
[g,Gc]=hinftopt(Tss);
zpk(Gc(1,1))
step(feedback(G*Gc,eye(2)),0.1)
zpk(Gc(1,2))
step(feedback(G*Gc,eye(2)),0.1)
zpk(Gc(2,1))
step(feedback(G*Gc,eye(2)),0.1)
zpk(Gc(2,2))
step(feedback(G*Gc,eye(2)),0.1)
```